THERMODYNAMICS OF ION INTERACTION IN SOLVENT EXTRACTION

By

DEBASMITA DASH
Enrolment No: CHEM 02200804003
Indira Gandhi Centre for Atomic Research, Kalpakkam, India

A thesis submitted to the
Board of Studies in Chemical Sciences

In partial fulfillment of requirements
for the Degree of

DOCTOR OF PHILOSOPHY
of
HOMI BHABHA NATIONAL INSTITUTE

August, 2013

Homi Bhabha National Institute

Recommendations of the Viva Voce Board

As members of the Viva Voce board, we certify that we have read the dissertation prepared by Debasmita Dash entitled "Thermodynamics of Ion Interaction in Solvent Extraction" and recommend that it may be accepted as fulfilling the dissertation requirement for the Degree of Doctor of Philosophy.

Chairman- Dr. T.G. Srinivasan **Date:** 21.2.14

CMallika
Guide/Convener- Dr. C. Mallika **Date:** 21.02.2014

Mahendra Nath Roy
External Examiner- Dr. M. N. Roy **Date:** 21-02-2014

Member 1- Dr. M. SaiBaba **Date:** 21-2-14

Member 2- Dr. K. Ananthasivan **Date:** 21/02/2014

Technology Advisor- Shri Shekhar Kumar **Date:** 21.02.14

Final approval and acceptance of this dissertation is contingent upon the candidate's submission of the final copies of the dissertation to HBNI.

I hereby certify that I have read this dissertation prepared under our direction and recommend that it may be accepted as fulfilling the dissertation requirement.

Date: 21/02/14
Place: Kalpakkam

STATEMENT BY AUTHOR

This dissertation has been submitted in partial fulfillment of requirements for an advanced degree at Homi Bhabha National Institute (HBNI) and is deposited in the library to be made to borrowers under rules of the HBNI.

Brief quotations from this dissertation are allowable without special permission, provided that accurate acknowledgement of source is made. Requests for permission for extended quotation from or reproduction of this manuscript in whole or in part may be granted by the Competent Authority of HBNI when in his or her judgment the proposed use of the material is in the interest of scholarship. In all other instances, however, permission must be obtained from the author.

Debasmita Dash

Debasmita Dash

DECLARATION

I, hereby declare that the investigation presented in the thesis has been carried out by me. The work is original and has not been submitted earlier as a whole or in part for a degree / diploma at this or any other Institution / University.

Debasmitā Dash

Debasmita Dash

“In Scientific Research the Most
Beautiful Hypotheses Always Proves
To Be the Right One

But:

The Most Beautiful Hypothesis Can
Be Murdered By an Ugly Fact”

-Thomas H. Huxley-

DEDICATION

Dedicated to

My Dear Parents

&

My Beloved Husband

ACKNOWLEDGEMENT

Completing the PhD degree has been one of the most cherished dreams of my life right from the early days of my graduation. At the juncture of this milestone achievement, I would like to express my sincere gratitude to number of people to whom I am really indebted to for their help, support and motivation in all my endeavors. At the outset I wish to record my heartfelt gratitude and indebtness to **Prof. Raghavendra Rao** whose magical and inspiring teaching deeply motivated me to choose research in Chemistry as my scientific career.

I would like to express my deep and sincere gratitude to my guide, **Dr. C. Mallika** for her invaluable guidance, constant encouragement, unstinted inspiration, keen interest and good wishes. I am also grateful to her for being patient while critically reviewing this thesis.

This thesis would not have been possible without the help, support, and valuable suggestions from **Shri Shekhar Kumar** who has been truly invaluable to me for which I am extremely grateful.

It is an honour for me to thank **Dr. U. Kamachi Mudali**, Head, Reprocessing Research and Development Division and for his constant support and encouragement throughout my work.

It is my great privilege to acknowledge **Dr. P.R. Vasudeva Rao**, Director, IGCAR, **Shri. S.C. Chetal** and **Dr. Baldev Raj**, Former Director, IGCAR for giving me permission to work in this institute and allowing me to stay in Kalpakkam with nice facilities during this period.

I am grateful to **Dr. T.G. Srinivasan**, Chairman, Doctoral Committee and Raja Ramanna Fellow, Doctoral Committee members, **Dr. M. Sai Baba,** Associate Director,

Resource Management Group and **Dr. K. Ananthasivan,** Head, Advanced Fuels Studies Section, Fuel Chemistry Division for their constructive suggestions and time to time evaluation of the research work.

I would like to thank **Mr. S. Balasubramonian** for his generous involvement, fruitful scientific discussion and support in writing programme for data analysis. I wish to express my sincere thanks to **Mr. S. Sundaramurthy, Ms. N. Priyadarshini, Mr. Pranay Kumar Sinha**, **Mr. Sanat Karmakar**, **Mr. M. Balamurugan**, **Mr. D. Siva Kumar**, **Mr. Bijendra Kumar**, **Mr. Abhishek Singh**, **Mr. P. Vishnu Anand**, **Mr. Satyabrata Mishra**, **Mr. S. Singaravel** and all my colleagues of RRDD for their diversified help and moral support offered to me from time to time throughout the course of the work.

This is my pleasure to express my affectionateness thanks to **Maneesha**, **Prasana** and **Bishnu** who have given me a family like environment in Kalpakkam. I would like to thank **Pravati**, **Sudhansu**, **Subhra**, **Madhu**, **Alok**, **Asit**, **Pradeep**, **SrimahaVishnu**, **Ilaiyaraja**, **Sharath** and all members of our enclave for their numerous help, support and enjoyable company for making my research life more cheerful.

I would like to express my heartiest gratitude and honor to my husband, **Mr. Satya Narayan Das**, my parents, **Mrs. Jyotshna Dash** and **Mr. Nirod Kumar Dash**, my brother and sister, **Mr. Debashrit Dash**, **Ms. Krishna Dash** and all other family members for their love, compassion, caring nature, and patience in the walkway of my life.

Finally, I thank almighty for providing me the opportunity to step into the exciting world of science and enabling me to write the thesis.

Debasmita Dash

Debasmita Dash

CONTENTS

CHAPTER I
Introduction

CHAPTER II

Experimental Techniques

CHAPTER III

Measurement of Single Ion Activity Coefficient of Electrolytes in Binary Systems

CHAPTER IV

Structural Interactions Leading to Volumetric Changes in Aqueous Nitrate Solutions at 298.15 K

CHAPTER V

Temperature Dependence Studies on Volumetric Change and Structural Interaction in Aqueous Nitrate solutions

CHAPTER VI

Volumetric and Viscometric Study of Aqueous PEG-200, PEG-400 and [HMIm] Br system

CHAPTER VII

Brief Summary of the Thesis work and Future Prospective

SYNOPSIS

When an electrolyte is dissolved in water, it dissociates into cations and anions, which will be surrounded by water molecules as well as the counter ions and the electrolyte solution will no longer behave as an ideal solution. The nonideality in the electrolyte solutions is attributed mainly to the interactions of water–ion and ion–ion. Thermodynamic properties, including activity coefficients at infinite dilution and other thermophysical and volumetric properties, find application in the development of reliable predictive models for systems containing aqueous solutions.

Thermodynamic properties, including activity coefficients at infinite dilution and excess molal volumes, find application in the development of reliable predictive models for systems containing aqueous solutions. Excess molal volumes and partial molal volumes can be considered as a basis for understanding some of the molecular interactions (such as dispersion forces and hydrogen-bonding interactions) in binary mixtures. Excess volume is one of the useful parameters in the development of technological processes of a reactive system, and to predict vapour-liquid equilibria by incorporating into appropriate equation of state (EoS) models. Partial molal volume at infinite dilution data provide useful information about the interactions occurring in infinitely dilute solutions and are of great importance in characterizing the structure and properties of solutions. All these thermodynamics of aqueous solutions and the instruments used for their measurement are the content of Chapter 1and 2 respectively.

The knowledge of individual ionic activity coefficients is important for the design of equilibrium processes involving electrolyte solutions as well as for processes involving ion-exchange, and pollution control. Activity coefficients can also be used for the prediction of rate constant, equilibrium constant, chemical potential value, solubility product and for the separation of a species from a mixture of substances on the basis of their high or low activity coefficient. In this work, we have studied the single ion activity coefficients of chloride, nitrate, potassium and sodium ions. The emf values have been measured for aqueous solutions of nitrates and chlorides of sodium and potassium by pH/ISE meter and they were substituted in Nernst equation to calculate the single ion activity coefficient. Mean ionic activity coefficient was calculated by taking the geometric mean of the calculated values and compared with the literature which constitutes Chapter 3.

The fission products obtained from nuclear fission such as rare earth and some other nitrate salts are very important from a socioeconomic perspective. A complete thermodynamic investigation of the rare earths in aqueous solution is essential in order to understand how these ions behave in solvent such as water. The thermophysical studies reported in this thesis have provided precise volumetric and structural behaviour data for aqueous solutions of $RbNO_3$, $CsNO_3$, $Sr(NO_3)_2$, $Y(NO_3)_3$, $Ga(NO_3)_3$, $La(NO_3)_3$, $Ce(NO_3)_3$, $Pr(NO_3)_3$, $Sm(NO_3)_3$, $Eu(NO_3)_3$ at 298.15 k and 0.1 MPa which constitute Chapter 4.

In addition to the thermophysical and volumetric studies at 298.15 K and 0.1 MPa reported in Chapter 4, volumetric studies have been performed at higher temperatures and reported in Chapter 5. The density measurements were done by Anton Paar DMA 5000 vibrating tube densimeter (described in Chapter 2). Chapter 5 reported density data for aqueous solutions of $RbNO_3$, $CsNO_3$, $Sr(NO_3)_2$, $Y(NO_3)_3$, $Ga(NO_3)_3$, $La(NO_3)_3$, $Ce(NO_3)_3$, $Pr(NO_3)_3$, $Sm(NO_3)_3$ and $Eu(NO_3)_3$ over the temperature range T=(293.15-343.15) K in 5K interval. These measurements provided apparent molal volume at infinite dilution, cubic expansion coefficient and prediction of structural behaviour for different temperatures.

PEG solutions and ionic liquids which are acting as new solvents are also important according to extraction point of view. This thesis also provides volumetric and viscometric study on the aqueous solutions of PEG-200, PEG-400, 1-hexyl-3-methyl imidazolium bromide [HMIm]Br reported in Chapter 6. Such studies were conducted in order to provide detailed thermophysical and volumetric information regarding these solvents. The study of volumetric property has been extended for Poly ethylene glycol-200 and Poly ethylene glycol-400 in the temperature range 293.15 - 343.15 K in 5 K interval and 1-hexyl-3-methyl imidazolium bromide ([HMIm]Br) at 298.15 K. The densities, refractive indices and viscosities are measured for PEG-200 and PEG-400. Apparent molal volume, partial molal volume, cubic expansion coefficient, structural behaviour and excess properties are studied for different temperatures. The density, refractive index and water activity are measured for [HMIm]Br. The volumetric property, excess property and vapour pressure have been calculated. The excess properties are correlated to Redlich-Kister equation.

Chapter 7 represents the summary, conclusion and the future perspectives. The various studies presented within this thesis have indicated how more detailed and precise thermodynamic data can improve our understanding of the equilibrium properties of solutions beyond 298.15 K and 0.1 MPa.

LIST OF FIGURES

LIST OF TABLES

CHAPTER 1

INTRODUCTION

CHAPTER 1

INTRODUCTION

1.1 GENERAL

Electrolyte solutions are mixtures where the components are the solute and the solvent. At infinity dilution, when the concentration of the solute tends to zero, the solution is regarded as ideal. When the concentration of solute is finite, the solution is regarded as non-ideal. In electrolyte solutions, the solute is partly or wholly in the form of ions. The ion-solvent and solvent-solvent interactions are dominated by the electrostatic forces between ions and permanent dipoles which also can be treated as short range forces in nature. The ion-ion interactions are dominated by the long range forces. The thermodynamic and physical properties of aqueous electrolyte solutions depend on both types of forces. The relative importance of each type of forces depends on the concentration of the salt (solute). In concentrated solutions short range forces dominate while in the dilute solutions long-range forces control the thermodynamic behaviour of the solution.

The most important aspects of aqueous electrolytes are the structure of water (solvent) and the interaction of ions of the solute with water molecules. In an ideal electrolyte, solvent-solvent interactions are insignificant. Solute-solvent interactions exist, but considered to be less significant than solvent-solvent interactions, as the ratio of solute to solvent is very low. Solute-solute interactions are present; however, to a very small extent because of the low concentration of solute.

Non-ideality comprises all ion-ion, ion-solvent and solvent-solvent interactions. The ion-ion interactions are of three types:

- cation and anion interaction
- cation and cation interaction
- anion and anion interaction

There could be some modified interactions also, contributing to the non-ideality of the solution. Ion-solvent interactions come into existence when an ion interacts with the solvent and modifies the solvent around it or two ions could modify the solvent in between them. These ion-solvent interactions are different from those exist in ideal solution and they increase with the increase in concentration. Solvent-solvent interactions are also present in aqueous electrolyte system, but they are not as significant as those of the other two interactions.

1.2 IMPORTANCE OF THERMOPHYSICAL PROPERTIES

Thermophysical properties of electrolyte solutions, expressed as apparent or partial molal quantities are useful in characterizing solute-solvent and solute-solute interactions [1-5]. The thermophysical properties of dilute aqueous electrolytes are extensively used in designing the process equipments in industries and also in various separation processes like extraction, distillation etc. These properties include activity coefficient, density, volumetric, viscometric and excess properties. The volumetric property of a component in a solution can be obtained from measurement of the density of the solution as a function of its concentration. The density of liquid systems provides information about the weak molecular interactions in the liquid state. The volumetric effects observed in aqueous solutions of electrolytes are due to interactions of the ions with the solvent water, i.e. the solvation effects, known as electrostriction of water.

Thermodynamic properties, including activity coefficients at infinite dilution and excess molal volumes find application in the development of reliable predictive models for systems containing aqueous solutions. Excess molal volumes and partial molal volumes can be considered as a basis for understanding some of the molecular interactions (such as dispersion forces and hydrogen-bonding interactions) in binary mixtures. Excess molal volume is one of the useful parameters in the development of technological processes involving a reactive system, and to predict vapour-liquid equilibria by incorporating into appropriate Eq. of state models.

1.3 PARTIAL MOLAL AND APPARENT MOLAL PROPERTIES

In complex multi-component systems such as solutions, it is easier to describe a system in terms of the intrinsic or molal properties rather than the extensive properties. The partial molal Gibbs energy of any species, ‘i’ (known as chemical potential, μ_i, and defined in Eq. (1.1)) can be used to describe the properties of individual component of macroscopic systems such as the properties of solvent and solute [6].

$$\mu_i = \left(\frac{\partial G}{\partial n_i}\right)_{n_{j\neq i},T,p} \tag{1.1}$$

In general, any partial molal property can be defined as

$$\overline{Y}_i = \left(\frac{\partial Y}{\partial n_i}\right)_{n_{j\neq i},T,p} \tag{1. 2}$$

Further, partial molal properties can be described by equations similar to those of the extensive properties; therefore partial molal volumes and heat capacities in a binary system are defined as

$$V = \left(\frac{\partial G}{\partial P}\right)_T \Rightarrow \overline{V}_i = \left(\frac{\partial \mu_i}{\partial P}\right)_T \tag{1. 3}$$

$$C_P = \left(\frac{\partial H}{\partial T}\right)_P \Rightarrow \overline{C}_{P,i} = \left(\frac{\partial \overline{H}_i}{\partial T}\right)_P \tag{1. 4}$$

Any extensive property of a system can be calculated as the sum of the respective partial molal properties if all components have a known concentration. Although the additive definition of partial molal properties is convenient, direct measurement of these solution properties are difficult, because interactions with other species contribute to partial molal properties. When dealing with solutions it is more common to measure the apparent molal quantities, Y_{φ}, which can be defined as the change in property Y due to a known amount of solute in a known amount of solvent, assuming the contribution by the solvent is the same as that of the pure species. In other words, all changes in the state properties can be attributed to the presence of the solute, even if these changes contribute to a change in partial molal property of the solvent. The apparent molal property of any solute, $Y_{2,\varphi}$, can be defined as

$$Y_{2,\varphi} = \frac{Y - n_1 \overline{Y}_1^0}{n_2} \tag{1. 5}$$

Where, n_1 and n_2 represent the mole of the solvent and solute respectively, in the system. $\overline{Y}_1^0$ denotes the partial molal property of the pure solvent.

Because the solvent is assumed to contribute a definite, constant quantity for all solute concentrations at fixed temperature and pressure, the partial derivative of the extensive property with respect to the number of moles of solute can be defined in terms of the apparent molal quantity:

$$\left(\frac{\partial Y}{\partial n_2}\right)_{n_1,T,P} = \left(\frac{\partial Y_{2,\varphi}}{\partial n_2}\right)_{n_1} + Y_{2,\varphi} \tag{1. 6}$$

Eqs. (1.5) and (1.6) shows that if the apparent molal property and its derivative with respect to moles of solute is known, the partial molal property can be calculated. In other words, if any appropriate Eq. for the apparent molal property with respect to any concentration scale, which is in good agreement with experimental data is known, the apparent molal property at infinite dilution can also be found out. Theoretically, as the concentration approaches zero, the apparent molal property approaches the partial molal property of the solute at infinite dilution, because by definition the solvent is already assumed to be in its pure form. If the apparent molal property is assumed to reflect the apparent molal property of the solute only and not the solute-solvent complex, then the apparent molal property at infinite dilution, $Y_{2,\varphi}^{\infty}$, would be equal to the standard state molal property of the solute, as defined by Henry's law. Ignoring the previous equality, equation of state developed for standard state partial molal variables have been used successfully to describe partial molal quantities at infinite dilution.

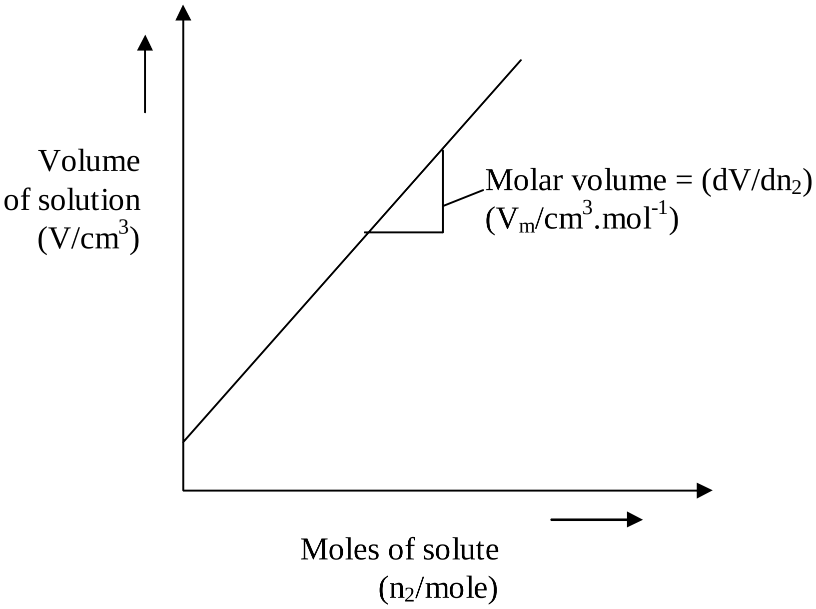

Fig. 1.1: A diagram for the explanation of molal volume [7]

The easiest way to explain this is in terms of the molal volume, V_m, shown in the Fig. 1.1, where the volume increases with respect to the amount of solute added [7]. A dissolved solute has its own property, referred to as partial molal property. Fig. 1.2 shows an extremely large tank containing 1 mol.L^{-1} solution of a solute with a certain volume, shown at position (1). If 1mole of solute is added to the solution in the tank, the volume will increase to (2); however the concentration of the other species of the solution will not change by any detectable amount.

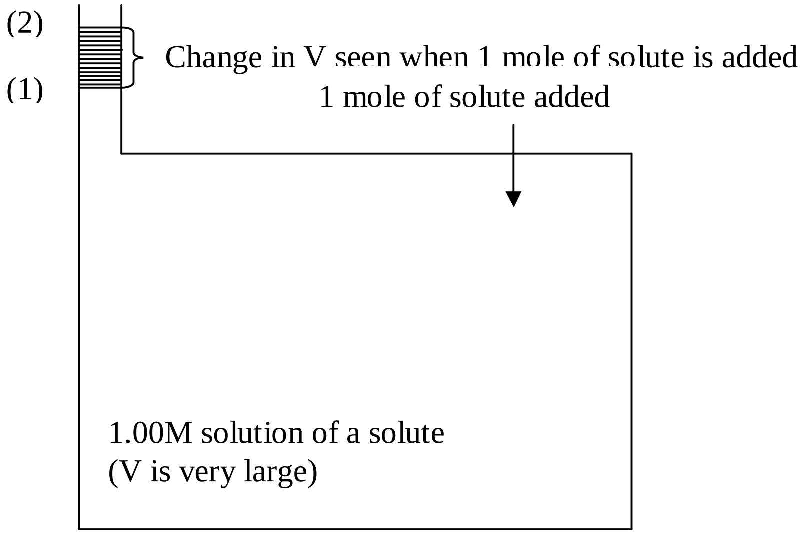

Fig. 1.2: A diagram to assist in the explanation of a partial molal volume [7]

Therefore for a two component system, where one component is the solvent and the other is solute, the total volume of the system can be represented as the sum of the partial molal volumes of the solvent, $\overline{V}_1$, and the solute, $\overline{V}_2$:

$$V = n_1\overline{V}_1 + n_2\overline{V}_2 \tag{1. 7}$$

Dividing Eq. (1.7) by $n_1 + n_2$, the molal volume of the solution is obtained as:

$$V_m = X_1\overline{V}_1 + X_2\overline{V}_2 \tag{1. 8}$$

where, x_1 and x_2 represent the mole fraction of the solvent and the solute, respectively. The partial molal property of a solute is defined as the change in the total property of the system with respect to the change in the number of moles of solute added, with all other variables (T, P, and the amount of the solvent) are held constant. An alternative, widely used property of the solute is the apparent molal property. The apparent molal volume is the volume that should be attributed to the solute in solution if it is assumed that the solvent contributes the exact volume it would if it was in its pure state.

Under this assumption, the apparent molal volume of the solute, $V_{2,\varphi}$, as defined by Harned and Owen [8] is the difference between the total volume (or the total molal volume) and the partial molal volume of the pure solvent ($\overline{V}_1^0$) divided by the number of moles (or the mole fraction) of the solute present:

$$V_{2,\varphi} = \frac{V - n_1\overline{V}_1^0}{n_2} \tag{1. 9}$$

$$V_{2,\varphi} = \frac{V_m - x_1\overline{V}_1^0}{x_2} \tag{1.10}$$

In experimentation, $\overline{V}_1^0$ is generally considered to be constant over the range of solute concentration at constant temperature and pressure [9]. Hence, $V_{2,\varphi}$ can be easily calculated using Eq. (1.9) or (1.10) when the total volume or molal volume is known.

Eq. (1.9) can be modified in order to find out the apparent molal volume of a solute using density of the solution containing the solute and the density of the pure solvent, ρ and ρ^0, respectively. Assuming there is 1 kilogram (Kg) of solvent:

$$n_1 = \frac{1}{M_1}\text{, therefore } V = \frac{\overline{V}_1^{\,0}}{M_1} + m_2.V_{2,\varphi} \tag{1.11}$$

where, M_1 is the molal mass of the solvent.

Since $\rho_1 = \frac{M_1}{\overline{V}_1^{\,0}}$, Eq. (1.11) becomes:

$$V = \frac{1}{\rho_1} + m_2.V_{2,\varphi} \tag{1.12}$$

where, m_2 is the molality of the solute (which is equivalent to n_1 if 1kg of solvent is present). The entire mass of the solution will be composed of the mass of the solvent (1 kg) and the mass of the solute ($m_2.M_2$). Since volume is the ratio of mass to density, the equation for V becomes:

$$\frac{1 + m_2.M_2}{\rho_2} = \frac{1}{\rho_1} + m_2.V_{2,\varphi} \tag{1.13}$$

By rearranging this Eq. (1.13) and solving for $V_{2,\varphi}$, an equation for apparent molal volume of the solute is obtained:

$$V_{2,\varphi} = \frac{\rho_2 - \rho_1}{m_2.\rho_2.\rho_1} + \frac{M_2}{\rho_2} \tag{1.14}$$

The apparent molal volume was found to vary linearly with square root of the concentration and could be expressed by the Masson equation [10] as

$$V_{2,\phi} = V_{2,\phi}{}^{0} + a_v\sqrt{m} \tag{1.15}$$

where, $V_{2,\phi}{}^{0}$ is the partial molal volume, a_v is the experimental slope, m is the concentration in mol.kg^{-1}.

The apparent molal property of a solute can be related to its partial molal property by Eq. (1.16) given below:

$$\bar{Y}_2 = Y_{2,\varphi} + \left(\frac{\partial Y_{2,\varphi}}{\partial n_2}\right)_{n_1} .n_2 \tag{1.16}$$

As n_1 approaches 0, $\left(\frac{\partial Y_{2,\varphi}}{\partial n_2}\right)_{n_1}$ also approaches 0. Therefore, at infinite dilution (a theoretical point at which only 1 mole of solute exists in an extremely large volume of solvent, and where only solute-solvent interactions are present within the aqueous solution), this apparent molal property, known as Y_2^0, of the solute equals the partial molal property of the solute (V_2^0 is the standard term used for apparent molal volume at infinite dilution [7, 9]). This assumption becomes important in obtaining a value for the partial molal volume of a system (which normally cannot be calculated directly from experimental results) that represents solute-solvent interactions within a solution [3-5, 11].

1.4 EXCESS PROPERTIES

Mixing of different elements and compounds gives rise to solutions that generally do not behave ideally. The deviation from ideality is expressed by many thermodynamic properties, particularly activity coefficient and excess properties. The excess thermodynamic properties find applications in the study of molecular interaction and arrangements. In particular, the excess properties can be used for understanding the interactions that take place between solute-solute, solute-solvent, and solvent-solvent species. There is a vast literature on the thermodynamic properties of mixtures of liquids where the nonideality is represented as excess quantities, Y^{EX}. The excess thermodynamic functions give a measure of the deviation from Raoult's law and are calculated from the expression:

$$Y^{EX} = Y - X_1Y_1^* - X_2Y_2^* \tag{1.17}$$

where, Y is the total property of the solution or mixture per total number of moles of components 1 and 2, Y_i^* is the molal property of pure component 1 or 2. This quantity gives an overall view of the magnitude of the nonideality in the solution and it is often used in conjunction with Redlich-Kister equation [12] to represent thermodynamic data for mixtures of liquids. Redlich-Kister equation is an expanded Margules equation and has the form:

$$Y^{EX} = X_2(1 - X_2)\sum_{i=0}^{p} A_i(2X_2 - 1)^i \tag{1.18}$$

where, A_i's are least square parameters. Redlich-Kister equation is a flexible polynomial expression in mole fraction and it provides a convenient method for representing the excess properties of a liquid mixture and classifying different types of liquid solutions [13]. In proposing this equation, the authors stated that the relation must contain the factor X_2 (1-X_2), while it is desirable to develope a series with respect to the mole fraction which is symmetrical with respect to the two components. The first term in the expression is symmetric in X_1 and gives a parabola when the excess property is plotted against X_1. The odd powered correction terms [first (A_1), third (A_3) …] are asymmetric in X_2 and therefore, skew the parabola either to the left or right. The even powered correction terms [second (A_2), fourth (A_4) …] which are symmetric in X_1, flatten or sharpen the parabola. For an equimolal mixture (X_1 = X_2 = 0.5), this expression gives Y^{EX} = A_0. Thus, regardless of the number of terms in the series, just from A_0, one can determine the correlated equimolal value of the scaled excess property [14]. In principle, many subtleties can be accommodated by including an adequate number of terms in a polynomial representation. However, so many terms may be needed in certain cases as to render the correction meaningless. A general guideline is that if more than four terms are required, an alternative method for representing the data should be considered since the goal is always to represent data to within their precision by using as few empirical parameters as possible.

Although thermodynamic data on mixtures of liquids are usually expressed as excess quantities, Y^{EX}, this approach can in some cases be misleading because it can hide strong interactions at low concentrations. So properties of solutes in dilute aqueous solutions are conveniently represented by apparent molal properties [15, 16].

1.5 OVERVIEW OF EARLIER WORK

Determination of apparent and partial molal volume from precise density measurements continues to attract considerable attention. In 1770, Watson [16] made the first accurate measurements on the volume change of adding electrolytes to water; in 1887, Arrhenius [17] presented his theory on the dissociation of electrolytes into ions; in 1913, Debye and Huckel [18] presented their theory of interionic attraction; and in 1957, various workers, e.g., Achermann [19], Buckingham [20], Eigen [21], Frank and Wen [22], Kaminsky [23], Samilov [24], Young, Wu, and Krawetz [25], etc., presented a number of papers on structural hydration interactions in the Discussions of the Faraday Society.

In 1891, Traube [26] had determined the apparent molal volume of about 50 salts in solution and correlated the change of $V_{2,\varphi}$ with valence state. He considered $V_{2,\varphi}$ values as the actual volume of the salt in solution. Dunn [27-29] reported the densities of sodium chloride, potassium chloride, bromide, and iodide and also tetra-n-butyl ammonium bromide at 298 K in the range 0.001-1.0M using a precise dilatometric technique. In a later work [29], he had measured the density values at seven temperatures 273-338 K and confirmed the Debye-Huckel slope for volumes at these temperatures for barium and calcium chloride in addition to the alkali halide salts investigated by him previously. Dunn observed that $V_{2,\varphi}^{0}$ (apparent molal volume at zero concentration) increases with temperature, reaching maximum values at 333K for the 1:1 electrolytes, 308K for calcium chloride and 318K for barium chloride. The effect of increase in $V_{2,\varphi}^{0}$ with increase in temperature was attributed to changes in the water structure. Desnoyers et al. [30], and Millero and Drost- Hansen [31] reported the precise determination of density by float methods for 1:1 electrolytes in water. Values of density were measured with 0.1 molal solutions at 1K intervals in the range 293-313 K. A cubic fit of these density data was differentiated by Millero and Drost- Hansen [31] to yield apparent molal expansibilities. These authors with Korson [32] found no evidence for reported anomalies in the temperature dependence of the apparent molal volume (or viscosity) of sodium sulphate near 305.5 K. Ellis [33] determined the densities of electrolyte solutions at high temperatures (up to 473K).

Apparent molal volumes of aqueous solutions of sodium alkyl sulphates (C_{10}-C_{14}) had been reported by Franks et al. [34] exhibited negative deviations from the limiting law in $V_{2,\varphi}^{0}$, both above and below the critical micelle concentration (c.m.c) at which there was a large positive volume change. Franks and smith [35] attributed that the negative deviation from the limiting law was due to the ‘co-operative hydrophobic hydration effects’.

Thermodynamic properties of aqueous solutions of inorganic salts were extensively studied, taking into account their importance in natural and industrial processes. These properties were determined as a function of concentration and temperature. The volumetric properties of 0.1, 0.5 and 1.0 M aqueous solutions of electrolytes have been determined at closely spaced 1 K temperature intervals [36-40]. The densities of aqueous solutions of sodium carbonate (m ≤1.0 M) were determined by Hershey et al. [41] from 273.15 to 318.15 K in 5 K intervals and at 298.15 K by Millero et al. [42]. The densities of sodium sulphate aqueous solutions were measured by the following researchers, considering its importance in geological and desalination processes. Millero and Knox [43] determined the densities at 273.15 and 323.15 K, Chen et al. [44] from 273.15 to 308.15 K, Isono [45] from 288.15 to 328.15 K, Fabuss et al. [46] from 298.15 to 448.15 K, Korosi and Fabuss [47] from 298.15 to 413.15 K, Phutela and Pitzer [48] from 273.15 to 473.15 K, Sharygin and Wood [49] from 298.15 to 613.15 K and Lo Surdo et al. [50] from 273.15 to 323.15 K.

The volume changes accompanying the addition of an electrolyte to water are only incompletely understood. Detailed molecular configuration of the ion-water aggregates must be considered for a successful understanding of the molal volume of electrolytes. The theory of molal volumes was reviewed by Redlich [51], Harned and Owen [52] and Redlich and Meyer [53]. Millero [54, 55] had reviewed the literature data and discussed in detail the partial molal volumes at infinite dilution.

1.6 ELECTROLYTE SOLUTION

Aqueous electrolyte solutions are important in various chemical, biological and environmental systems. The presence of both ionic and molecular species is one of the most important criteria to differentiate electrolyte solutions from non-electrolyte solutions. Prior to 1887, dissolved salts were considered to occupy voids in the solvent lattice; therefore, could be treated as ideal solution [54]. According to Arrhenius [56-58], the degree of dissociation of partially dissociated electrolytes depends upon the dielectric properties of the solvent. Based on the dissociation constant, the electrolytes were classified as strong, complex and weak electrolytes. As a consequence of the presence of ionic and molecular species in electrolyte systems, both chemical and physical equilibria exist simultaneously. A wide variety of chemical reactions could be possible leading to complex solution chemistry. Arrhenius theory [57] of complete ion dissociation prompted interest in explaining the phenomenon of solvation, as it was already found out that the addition of certain salts would decrease the volume of the solution.

The important aspect of electrolyte systems, which prompted to carry out the present thesis work, is the thermodynamic non-ideality of the liquid phases, mainly due to the different interionic and intermolecular interactions among various ionic and molecular species. The presence of long range interionic forces in aqueous electrolyte solutions results in the deviation from the normal thermodynamic behaviour of ideal solutions. A study revealed that the deviation from ideality is mainly due to two effects, one related to long range coulombic forces between ions and the other is attributed to the short range Vander Waals type forces between the species. The short range forces become prominent at high concentrations.

Tammann [59] developed the theory of internal pressure, caused by a dissolved salt and make the solvent to behave as if it were under an external pressure. He applied his theory to solution volumes and discussed apparent molal volumes in terms of change in volume of the solute, solvent, and mixture of the two, when the pressure was changed from 1 atm to an internal pressure, π.

Drude and Nernst [60] treated ions as hard sphere charges and developed an electrostatic theory, where hard sphere charges were placed in a continous dielectric medium, such as any solvent. Born [61] later developed calculation procedures which gave the size of the solvated ions and Webb [62] calculated the magnitude of the effect, charged ions have on water. Most of the theories are still used for describing standard state molal properties for ions; however, they do not address solute-solute or solute-solvent interactions.

Debye and Huckel [63, 64] proposed that long range coulombic effects cause a partially structured ionic atmosphere to be formed within a solution. The present widely accepted Debye- Huckel theory describes the work involved in bringing a unit charge from infinity to the surface of a hard sphere. This work is made up of the energy required to charge the sphere in a dielectric medium and the interaction energy or long-range coulombic effects.

1.6.1CHEMICAL POTENTIAL AND ACTIVITY OF ELECTROLYTES

For an open system in which matter is able to enter or leave, and where surface and force

field effects are negligible, differential Gibbs energy can be written as

$$dG = -SdT + VdP + \sum_j \mu_j dn_j \tag{1.19}$$

where, S and V are the entropy and volume of the system and n_j denotes the number of moles of species ‘j’ present in the phase. At constant temperature and pressure, the chemical potential of the species ‘i’ is given in Eq. (1.1) as,

$$\mu_i = \left(\frac{\partial G}{\partial n_i}\right)_{n_{j\neq i},T,p}$$

The right hand side of the above equation shows that the chemical potential is the partial molal property of the Gibbs free energy with respect to species i. Partial molal Gibbs energy cannot be measured directly. Thus, the activity 'a_i' of species i in a solution provide a convenient way to express its chemical potential:

$$\mu_i = \mu_i^0 + RT \ln\left(\frac{a_i}{a_i^0}\right) \tag{1.20}$$

Following the nomenclature of Stokes [65], superscript 0 denotes an arbitrarily chosen standard state for the component i at the temperature of the system T and μ_i^0 is the standard chemical potential of i at T. it is conventional to choose the standard state so that the corresponding standard activity a_i^0 becomes unity and a simpler relation is obtained:

$$\mu_i = \mu_i^0 + RT \ln a_i \tag{1.21}$$

The activity a_i of a species can also be expressed in terms of its fugacity as

$$a_i = \frac{f_i}{f_i^0} \tag{1.22}$$

where, f_i^0 is the standard fugacity for the component i at the given temperature.

For aqueous solutions the activity of a salt can be expressed in terms of different concentration scales such as molality (m), molarity (M), and mole fractions (x). The most commonly used concentration scale in the thermodynamics of aqueous electrolytes is the molality, i.e., moles per 1000 g of solvent. The molality of a stable mixture does not change with temperature and pressure unless a phase change occurs. For ions, the arbitrarily chosen standard state for the activity of the species 'i' is the hypothetical ideal solution of unit molality of the ion 'i'. The ideal solution is chosen such that the ratio $\frac{a_i}{m_i}$ tends to become unity as the molality approaches zero. This ratio is known as the molal activity coefficient γ_i:

$$\gamma_i = \frac{a_i}{m_i}\left(a_i = m_i \gamma_i\right) \; ; \; \gamma_i \to 1 \text{ when } m_i \to 0 \tag{1.23}$$

Using Eq. (1.23), Eq. (1.21) takes the form

$$\mu_i = \mu_i^0 + RT \ln\left(m_i \gamma_i\right) \tag{1.24}$$

Combining Eqs. (1.22) and (1.23), fugacity of the species 'i' becomes

$$f_i = \gamma_i m_i f_i^0 \tag{1.25}$$

However Eq. (1.25) is not conventional because the fugacity is usually expressed using a mole fraction scale. One can also define the chemical potential in terms of the mole fraction scale,

$$\mu_i = \mu_i^* + RT \ln\left(x_i \gamma_i^{(x)}\right) \tag{1.26}$$

Where $\gamma_i^{(x)}$ denotes the rational or mole fraction activity coefficient of species 'i'. The fugacity of species 'i' is then expressed as:

$$f_i = \gamma_i^{(x)} x_i f_i^* \tag{1.27}$$

Where f_i^* is the fugacity standard state of the species i. In this case, the ideal solution is chosen such that the ratio (a_i/x_i) tends to unity as the mole fraction approaches zero. Thus $\gamma_i^{(x)} \to 1$ when $x_i \to 0$. The standard state fugacity corresponds to unit mole fraction of the ideal solution.

1.6.2 SINGLE ION ACTIVITY COEFFICIENT

Two methods widely used to measure the activity coefficients of non-volatile electrolytes in solution are

- Solvent activity method
- Electrochemical cell technique

In solvent activity method, the activity coefficient of the solvent is first calculated by measuring the equilibrium pressure of the pure solvent vapour phase with the binary mixture and using Gibbs-Duhem equation the mean ionic activity coefficient of the electrolyte is calculated. The second method allows a direct calculation of the activity of an electrolyte by measuring the electrochemical potential of the ions in an electrochemical cell.

1.6.2.1 SOLVENT ACTIVITY METHOD

Solvent activity or vapour pressure method has been traditionally used in vapour-liquid equilibria studies of aqueous electrolytes. Different techniques have been proposed [65-69] depending upon the way of measuring the activity of the solvent. The most widely used ones are the static and the isopiestic method.

1.6.2.2 ELECTROCHEMICAL METHODS

Electrochemical cell is an essential tool for experimental studies of electrolyte solutions and has been used widely in electrochemistry for the measurement of thermodynamic properties of electrolyte solutions. In contrast to vapour pressure measurements, this technique is very useful in the measurement of the chemical potential or activity of electrolytes in very dilute binary electrolyte mixtures. Thus, this technique provides an independent check on the validity of the thermodynamics relations used to calculate the electrolyte activity from solvent activity methods. To set up an electrochemical cell for determining the activity of an electrolyte in an aqueous solution, at least two half cell electrodes required to be inserted into the solution. One of these electrodes, which respond directly to analyte, is called indicator electrode. The other electrode, against which the potential of analyte should be compared, is called the reference electrode. One of the most advanced types of indicator electrodes are the Ion-Selective Electrodes (ISE).

1.7 VISCOSITY

Viscosity is a fundamental characteristic property of all liquids. When a liquid flows, it has an internal resistance to flow. Viscosity is a measure of this resistance to flow or shear. Viscosity can also be termed as a drag force and is a measure of the frictional properties of the fluid. Viscosity is a function of temperature and pressure. The viscosities of both liquids and gases change with temperature and pressure. Viscosity is expressed in two distinct forms,

- Dynamic viscosity
- Kinematic viscosity

Dynamic viscosity is also termed as absolute viscosity. When dynamic viscosity is divided by the density, kinematic viscosity is obtained. One of the applications of kinematic viscosity is in the calculation of Reynolds number, used for flow characterization.

Viscosity can be estimated using time of efflux for the given liquid through a capillary and the same is compared with the time of efflux of water under similar condition. The instrument used to measure viscosity is known as viscometer. Under the conditions of kinetic similarity for fluid flow, the viscometer performance equation may be written as:

$$\eta = At - Bt^2 \tag{1.28}$$

Where η is the kinematic viscosity**,** A is the viscometer constant, t is the time of efflux and B is the kinetic correction. As per ASTM-D445/446 [70] standards, the correction B is negligible if time of efflux is more than 100 second. If this condition is met, experiments can be performed with water and experimental liquid and the time of efflux under identical conditions can be recorded. If Eq. (1.28) is written twice (one time for water and one time for experimental liquid) and these two expressions are mutually divided, the following equation results:

$$\frac{v}{v_0} = \frac{t}{t_0} \tag{1.29}$$

Equation (1.29) transforms into following form for dynamic viscosities-

$$\frac{\eta}{\eta_0} = \frac{t}{t_0}\frac{\rho}{\rho_0} \tag{1.30}$$

Where, η_0 is the viscosity of standard water

ρ_0 is the density of standard water

t_0 is the efflux time of standard (or water).

η is the viscosity of the sample.

ρ is the density of the sample.

t is the flow time of the sample.

Thus, by knowing the values for the standard and the density of the experimental liquid, the viscosity of the experimental liquid can be estimated.

1.8 GOALS AND OBJECTIVES

As discussed in the Section 1.1, the thermophysical properties of dilute aqueous electrolytes are extensively used in designing the process equipment in industries and also in various separation processes like extraction, distillation etc. They can also be used for developing predictive models for the behaviour of aqueous electrolytes at different temperatures. Although volumetric data have been reported for some of the nitrate salts for a limited range of temperature, experimental data are not available for the salts over a wide range of temperature. Information regarding cubic expansion coefficient of the nitrate salts are seldom known in the literature.

The goals of the work are (i) to obtain single ion activity coefficients of some alkali nitrate and chloride salts using ion selective electrodes for which the reported information is very scarce (ii) to obtain accurate thermophysical data for dilute aqueous solutions of nitrates of Rb, Cs, Sr, Y, Ga, La, Ce, Pr, Sm and Eu nitrates over a range of temperature (293.15 - 343.15) K and (iii) to obtain thermophysical data of the room temperature ionic liquid [HMIm]Br at 298.15 K and other non-aqueous solvents like PEG-200, PEG-400 over a temperature range of (293.15 - 343.15) K.

The objectives of this work are:

1. Determination of single ion activity coefficient of nitrate and chloride salts of sodium and potassium using ion selective electrodes
2. Measurement of apparent molal volume $V_{2,\varphi}$, standard partial molal volume $V_{2,\varphi}^{0}$, cubic expansion coefficient α and prediction of structure making and breaking characteristic of aqueous solutions of some ionic solutes.

3. Calculation of the water activity, vapour pressure, excess volume, excess refractive index and excess viscosity of aqueous solution of PEG-200, PEG-400 and [HMIm]Br and fitting the data in appropriate model equations such as the Redlich-Kister equation.
4. Prediction of the effect of temperature on all the thermophysical properties studied.
5. Fitting of the density model and Masson model to the experimentally determined data and comparison of the model predicted results with that of the experimental values.

REFERENCES

1. C.W. Zhao, P.S. Ma, J.D. Li, J. Chem. Thermodyn., 37 (2005) 37.
2. M.L. Parmer, D.S. Banyal, Indian J. Chem., 44A (2005) 1582
3. W.J. Crooks, J.D. Christian, Indian J. Chem., 43A (2004) 1872
4. E.G. Paneda, P. Guardado, A. Mastre, J. Soln. Chem., 33 (2004) 1277
5. Man Singh, J. Chem. Sci, 118 (2006) 269
6. Pitzer K. S. ed., “Activity Coefficients in Electrolyte Solutions”, Vol. 2. CRC Press, Boca Raton (1991)
7. G. M. Anderson, D. A. Crerar, “Thermodynamics in Geochemistry: The Equilibrium Model”, Oxford university press, New York (1993)
8. H. S. Harned, B. B. Owen, “The Physical Chemistry of Electrolytes Solution”, Reinhold, New York, 3rd ed., section 8.7 (1958)
9. M. Klotz, R. M. Rosenberg, “Chemical Thermodynamics: Basic Theory and Methods”, W. A. Benjamin Inc, Menlo Park, California (1972)
10. Masson D.O., Philos. Mag., 79 (1929) 218.
11. R. D. Barbosa, PhD thesis, University of Florida (2003)
12. O. Redlich, A. T. Kister, Ind. Eng. Chem. 40 (1948) 345
13. J. M. Prausnitz, R. N. Lichtenthder, E. G. de Azevedo, “Molecular Thermodynamics of Fluid-Phase Equilibria”, 2nd Edn. Prentice-Hall Inc. New Jersey, 193 (1986)

14. S. I. Sandler, “Models for Thermodynamic and Phase Equilibria Calculations”.Marcel Dekker, Inc. New York (1994)
15. M. Davis, Chem. Soc. Rev., 22 (1993) 127
16. R. Watson, Phil. Trans. Roy. SOC. London, 60 (1770) 325
17. S. Arrhenius, Phys. Chem., 1,631 (1887).
18. P. Debye, E. Huckel, Physik. Z., 24 (1923) 185
19. T. Ackermann, Discuss. Faraday Soc., 24 (1957) 180
20. A.D. Buckingham, Ibid., 24 (1957) 151
21. M. Eigen, Ibid., 24 (1957) 25
22. H. S. Frank, W.-Y. Wen, Ibid., 24 (1957) 133
23. M. Kaminsky, Ibid., 24 (1957) 171
24. O. Ya. Samoilov, Ibid., 24 (1957) 141
25. T. F. Young, Y. C. Wu, A. A. Krawetz, Discuss. Faraday Soc., 24 (1957) 78
26. J. Traube, Ann. Phys. Chem., 22 (1907) 519
27. L.A. Dunn, trans. Faraday Soc., 62 (1966) 2348
28. L.A. Dunn, trans. Faraday Soc., 64 (1968) 1898
29. L.A. Dunn, trans. Faraday Soc., 64 (1968) 2951
30. J.E. Desnoyers, M. Arel, G. Perron, C. Jolicoeur, J. Phys. Chem., 73 (1969) 3346

31. F.J. Millero, W. Drost-Hansen, J. Chem. Eng. Data, 13 (1968) 330
32. F.J. Millero, W. Drost-Hansen, L. Korson, J. Phys. Chem., 72 (1968) 2251
33. A.J. Ellis, J. Chem. Soc. (A), 1138 (1968)
34. F. Franks, M. J. Quickenden, J.R. Ravenhill, H.T. Smith, J. Phys. Chem., 72 (1968) 2668
35. F. Franks, H.T. Smith, Trans. Faraday Soc, 63 (1967) 2586
36. A. Apelblat, E. Manzurola, J. Chem. Thermodyn., 31 (1999) 869
37. P. R. Tremaine, P. G. Hill, D. E. Irish, P. V. Balakrishnan, Eds.; NRC Research Press: Ottawa, Canada, pp. 183 (2000)
38. A. Apelblat, E. Manzurola, J. Chem. Thermodyn., 33 (2001) 581
39. A. Apelblat, E. Manzurola, J. Chem. Thermodyn., 33 (2001) 1133
40. A. Apelblat, E. Manzurola, J. Mol. Liq., 118 (2005) 77
41. J. P. Hershey, S. Sotolongo, F. J. Millero, J. Soln. Chem., 12 (1983) 233
42. F. J. Millero, G. K. Ward, P. V. Chetirkin, J. Acoust. Soc. Am., 61 (1977) 1492
43. F. J. Millero, J. H. Knox, J. Chem. Eng. Data, 18 (1973) 407
44. T. A. Chen, J. H. Chen, F. J. Millero, J. Chem. Eng. Data, 25 (1980) 307
45. T. Isono, J. Chem. Eng. Data,29 (1984) 32
46. B. M. Fabuss, A. Korosi, A. K. M. Shamsul Hug, J. Chem. Eng. Data, 11 (1966) 325

47. A. Korosi, B. M. Fabuss, J. Chem. Eng. Data, 13 (1968) 548
48. R. C. Phutela, K. S. Pitzer, J. Chem. Eng. Data, 31 (1986) 320
49. A. V. Sharygin, R. H. Wood, J. Chem. Thermodyn., 30 (1998) 1555
50. Lo Surdo, E. M. Alzola, F. J. Millero, J. Chem. Thermodyn., 14 (1982) 649
51. O. Redlich, J. Phys. Chem., 44 (1960) 619
52. H.S. Harned, B.B. Owen, "The physical chemistry of electrolytic solutions", 2nd ed., Reinhold, New York (1958)
53. O. Redlich, D. Meyer, Chem Rev, 64 (1964) 221
54. F.J. Millero, Chem. Rev., 71 (1971) 147
55. F. J. Millero, In "Water and aqueous solutions", R.A. Horne ed., Wiley Interscience, New York, N.Y, Chap 13, 14 (1972)
56. S. Arrhenius, J. Phys. Chem., 1 (1888) 481
57. S. Arrhenius, J. Phys. Chem., 1 (1887) 631
58. S. Arrhenius, Philos. Mag., 26 (1887) 81
59. G. Tammann, J. Phys. Chem., 16 (1895) 91
60. P. Drude, W. Nernst, J. Phys. Chem.,15 (1894) 79
61. M. Born, J. Phys. 1 (1920) 45
62. T.J. Webb, J. Am. Chem. Soc., 48 (1926) 2589
63. P. Debye, E. Huckel, J. Phys. , 24 (1923) 185

64. P. Debye, E. Huckel, J. Phys., 25 (1924) 49

65. R.H. Stokes, “Activity Coefficients in Electrolyte Solutions”, Vol. 1, edited by Pyikowicz, R. M., CRC Press (1979)

66. G. N. Lewis, M. Randall, “Thermodynamics”, revised by Pitzer, K.S., Brewer, L., McGraw-Hill, New York (1961)

67. R. A. Robinson, R. H. Stokes, “Electrolyte Solutions”, Butterworths Scientific, London (1959)

68. Z.F. Zemaitis, D.M. Clarke, M. Rafal, N.C. Scrinver, “Handbook of aqueous electrolyte thermodynamics, Design Institute for Physical Property Data”, New York (1986)

69. K. S. Pitzer, “Theory: ion interaction approach”, in Pytkowicz (1979)

70. ASTM D445-11a, “Standard Test Method for Kinematic Viscosity of Transparent and Opaque Liquids (and Calculation of Dynamic Viscosity)” (2006)

CHAPTER 2

EXPERIMENTAL TECHNIQUES

CHAPTER 2

EXPERIMENTAL TECHNIQUES

2.1 INTRODUCTION

The study of thermodynamics of ion interaction in solvent extraction encompasses the measurement of single ion activity coefficient of some aqueous ionic solutes, density, viscosity, refractive index, volumetric and excess properties of these ionic solutes as well as molecular liquids. In the present Chapter, the details of the experimental techniques employed for the determination of the above mentioned properties have been discussed. The methodologies for analysis of data and details of the instruments used in the present work along with the calibration of the instruments have also been described.

2.2 MATERIALS AND SOLUTION PREPARATION

Aqueous solutions of alkali metal nitrates and chlorides were used in the experiments carried out for single ion activity coefficient measurement. The salts were oven dried for 48 h and cooled in vacuum desiccator for 24 h prior to use. All the nitrate salts used for volumetric study were AR grade and obtained from M/s. Alfa Aesar. The salts were vacuum dried and used. In some cases, the bottles were under dry nitrogen seals. Analytical grade PEG-200 (approx. molecular weight range: 190-210) and PEG-400 (approx. molecular weight range: 380-420) were purchased from M/s. BDH (Mumbai) and M/s. Aldrich (Germany) respectively and were used without further purification. The compound [HMIm]Br (M/s. *io-li-tec*, Germany) was subjected to IR spectral study and used without further purification.

ASTM Grade-1 water as per ASTM D-1193 [1] with a resistivity of 18.2 MΩ·cm at 298.15 K and TOC < 15 ppb from a MILLIPORE Simplicity system was used in the experiments for reagent/solution preparation and as water standard. Water for density standard was drawn from the water-purifier immediately before the experiments and it was degassed in an ultrasonic bath (TEC-110H) at 35 kHz for 60s. Solutes were weighed in a precision Shimadzu AUW220D balance (220 g, 0.01 mg resolution). When not in use, the solutions were kept in air-tight closed condition in a JULABO SW-22 Shaker Bath at 298.15 ± 0.1 K. JULABO SW-22 Shaker Bath was coupled with JULABO FP-40 chiller for cooling. To ensure ripple-free power supply to all the equipment, AC supply was regulated with an uninterrupted power supply (APC), set at high sensitivity. The ambient conditions were monitored with a Cole-Parmer hygrometer (0.1 %) comprising a thermometer and pressure sensor with accuracies 0.1 K and 0.1 kPa respectively.

2.3 ION-SELECTIVE ELECTRODES

Ion-Selective Electrodes (ISEs) are electrochemical sensors that allow the potentiometric determination of the activity of an ionic species in the presence of other kinds of ions [2].

About 35 years ago, the pH glass membrane electrode was the only potentiometric sensor commonly available [3]. The growth in the use of potentiometric methods started when attention was turned from glass membrane to polyvalent membrane systems such as pellets of insoluble salts [4], ion exchange liquids [5, 6] and polymeric membranes [7]. The investigations have led to the development of a variety of electrodes selective to inorganic ions such as halides [8], nitrates [9], potassium [10] and calcium [11]. Further development has resulted in the availability of ion-selective electrodes for the monitoring of organic species like quaternary ammonium ions [12] and drugs [13].

A unique feature of ISE is that its response to an ion occurs in a heterogeneous mixture of ions. Ion-selective electrodes therefore, facilitate the development of a simple and rapid response analytical method requiring minimal sample preparation. ISEs can be used in the direct determination of activities and as sensors for titrations [3]. Measurements with ISEs do not affect the composition of the test solution [14]. Further ISEs exhibit wide response ranges and are portable and inexpensive [3, 14].

The sensing part of an ISE is a membrane which is in contact with the sample solution. The membranes are semi-permeable so that only one kind of ions (ions of the same sign) may be selected. The most common and oldest ISEs are the glass electrodes. The pH glass electrode is one of the most widely used glass electrode in any laboratory. Other glass electrodes like sodium and ammonium are used in the determination of the activity of Na^+ and NH_4^+ ions. Solid-state electrodes are based on inorganic salt crystals. The membrane of these ISEs comprises a non-porous layer of a sparingly soluble salt in contact with a solution containing a single kind of ion. Another kind of ion then constitutes the charge carrier within the membrane. The well known examples are the membranes made of silver halides. The membrane potential depends on the anion activity in the solution and Ag^+ is the charge carrier in the membrane [15-17]. Examples of this type of electrodes include chloride, fluoride, bromide and iodide ion selective electrodes.

Liquid membrane electrodes are based on hydrophobic membranes saturated with a hydrophobic liquid ion exchanger [18, 19]. The ion exchange material is supported by a solid plastic membrane. The sensed ion is exchanged across the membrane creating a potential which contributes to the total potential of the ISE. While solid state electrodes respond to monovalent anions and glass electrodes respond to certain monovalent cations, only liquid membrane electrodes respond to some of the important ions such as NO_3^-, Ca^{2+} and K^+. Gas electrodes are used in the estimation of the solubility of CO_2 and NH_3 in solutions.

Ion-selective electrodes find wide ranging applications in many industrial processes. In fact, in many cases ISEs have replaced spectrophotometric methods [14]. For example, over the past 20 years, the number of clinical assays of sodium and potassium ions performed with ISE has surpassed those done by flame photometry [14]. This is mainly attributed to the low cost and simplicity of the instrumentation required for potentiometric analysis.

2.4 REFERENCE ELECTRODE

The signal of an ion-selective electrode needs to be measured against a reference electrode. In other words, a reference electrode is a half cell electrode which provides the second terminal of an electrochemical cell. The reference electrode should maintain a constant potential relative to the sample solution, regardless of its composition and should not cause chemical changes in the solution. Two types of reference electrodes are single junction and double junction electrodes. The three most common single junction reference electrodes are (i) silver chloride, (ii) mercury chloride (calomel), (iii) mercury sulphate. The simplest single junction reference is Ag/AgCl electrode. It can be represented by

KCl (satd), AgCl (satd) / Ag(s) (2.I)

It consists of a silver wire coated with AgCl in contact with an internal filling solution of saturated KCl. This solution contains Cl^- ions of a fixed activity which keeps the potential of the reference electrode constant. The internal solution is in contact with the sample solution through a porous plug or a flow restriction which permits the filling solution to flow very slowly into the sample. This kind of reference electrode is called as single junction reference electrode. The half cell reaction and the half cell potential are as follows:

$$\mathrm{AgCl(s)} + \mathrm{e} \Leftrightarrow \mathrm{Ag(s)} + \mathrm{Cl^-} \tag{2.1}$$

$$E_{ref} = E^0{}_{AgCl/Ag} - \frac{RT}{F}\ln a(Cl^-) \tag{2.2}$$

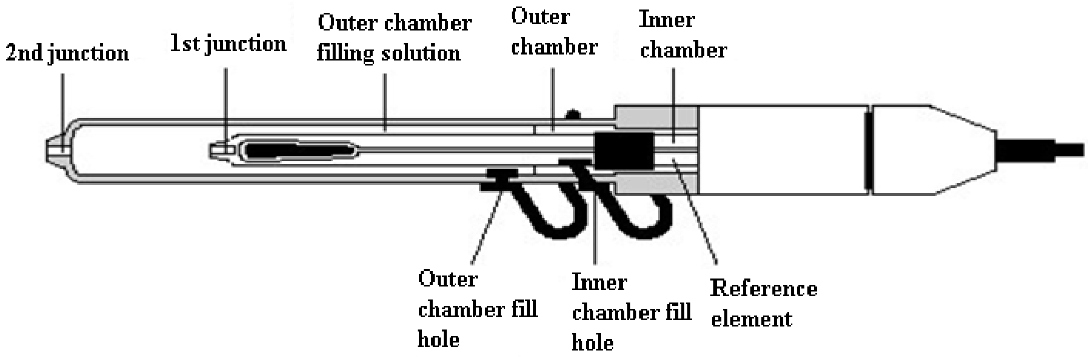

Fig. 2.1: Configuration of a simple double junction reference electrode [20]

The problem with single junction reference electrode is that in order to maintain a stable voltage, a steady flow of electrolyte requires to be provided. While doing it, some interfering species may diffuse across the porous plug from the solution under investigation into the internal solution [16, 17]. The general standard half cells have KCl based electrolyte filling solutions which will interfere in potassium and chloride measurements. To overcome this practical difficulty, a double junction reference electrode (shown in Fig. 2.1) is used in which the escaping KCl is retained in a second chamber containing non-interfering electrolytes, which in turn escapes into the test solution at the second junction. In double junction reference electrode, the inner element is itself a single junction reference electrode. This electrode is inserted in an outer tube containing a different electrolyte which is then allowed to contact with the outer test solution through a second porous frit. The outer filling solution forms a "salt bridge" between the inner reference system and the test solution [15]. By doing this, the contamination of the test solution by any other ions which would affect the analysis is prevented.

Salt bridge solutions should be compatible with sample solutions. It is desirable that salt bridge solutions are equitransferent, i.e., the transport numbers of its anions and cations should be nearly equal. This condition minimises the liquid junction potential, which can otherwise drift and cause instability.

2.5 POTENTIAL OF AN ION-SELECTIVE ELECTRODE

As shown in Fig. 2.2, the Ion-Selective Electrode usually consists of a secondary type electrode (Ag/AgCl) immersed in a standard filling solution which is in contact with the sample solution through a semi-permeable membrane. Two processes control the membrane potential of an ISE [16, 17]. The first is the diffusion of ions through the membrane in a liquid membrane electrode and the second is the ion exchange reactions at the membrane boundary in the solid state and glass electrodes.

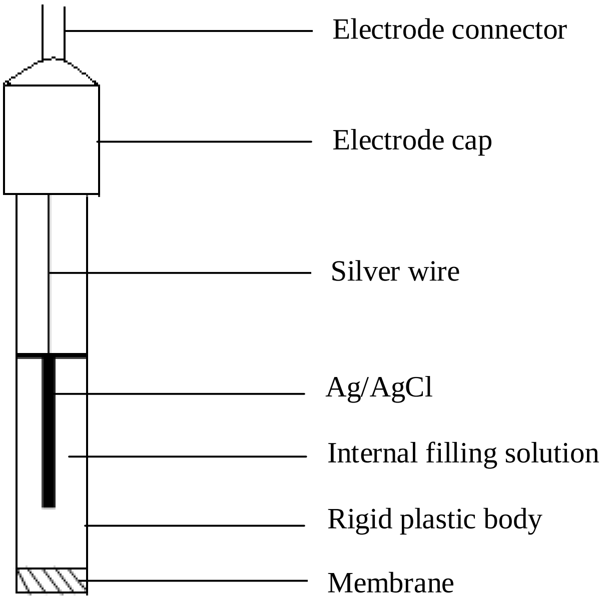

Fig. 2.2: Schematic view of a chloride Ion Selective Electrode

As shown in Fig. 2.3, the membrane is in contact with two electrolyte solutions, the sample solution and the standard solution. The potential of an Ion-Selective Electrode for a specific ion may be obtained from the following relation [18, 17, 21].

$$E_{ISE} = E_R + \Delta E + E_{ASY} \tag{2.3}$$

where, E_R is the potential of the internal reference electrode (Ag/AgCl), ΔE is the membrane potential and E_{ASY} is the asymmetric potential of the electrode. The potential of the internal reference, Ag/AgCl electrode is given in Eq. (2.2).

Solution (2)	Membrane	Solution (1)
E_2		E_1

Fig. 2.3: Membrane of an Ion Selective Electrode

The activity of Cl^- in the internal solution of a reference electrode and in the standard internal solution of an ISE are different, thus E_{ref} and E_R are usually different. The major contribution to the potential of an ISE is the membrane potential (ΔE) which depends on the type of ISE. Most of the membranes are made from solid crystals or organic liquids embedded on a solid support. They have fixed active sites or mobile active sites on both sides, in contact with both inner and outer electrolyte solutions.

The way in which the membrane works depends upon the type of ISE. However, the phenomena occurring at the interface between two electrolytes are diffusion process and Donnan equilibria [17, 22]. The membrane potential is the result of the diffusion potential and the Donnan potential. The diffusion potential, which is reflected in the liquid junction potential, results from different mobilities and concentrations of the ions in the electrolytes in contact while the Donnan potential is due to the transfer of one or more kinds of ions across the interface between two electrolytes. Thus, as shown in Fig. 2.3, ΔE is the difference in the potential of a specific ion in the inner solution (2) and the outer solution (1).

$$\Delta E = E_1 - E_2 \tag{2.4}$$

The terms E_1 and E_2 are called the inner-potential of the phases (1) and (2) respectively.

As a first approximation, one can assume that the ISE is selective only to one specific ion so that no interference from other ions is observed. In addition, one can assume that the membrane has the same number of fixed sites on both boundary surfaces. Following these assumptions and using the relations for the electrochemical potential of ions and the boundary ion exchange relations, one can obtain the membrane potential for a specific ion ‘i' as [16, 23]

$$\Delta E = E_1 - E_2 = \pm \frac{RT}{Z_i F} \ln \frac{a_i(1)}{a_i(2)} \tag{2.5}$$

However, the membrane potential of an actual ISE is not as simple as given in Eq. (2.5). In fact, ISEs have selectivity towards other ions of the same sign as the ion of interest in the solution. Based on more realistic assumptions, the membrane potential of an ISE can be written as [16, 17, 23]:

$$\Delta E = E_1 - E_2 = \pm \frac{RT}{Z_i F} \ln \frac{a_i(1) + \Sigma_j K_{ij}^{pot} a_j^{z_i/z_j}(1)}{a_i(2)} \tag{2.6}$$

where, K_{ij}^{pot} is the selectivity coefficient of the ISE, which is selective to ion 'i', towards ion 'j'.

$$K_{ij}^{pot} = \frac{\text{response to j}}{\text{response to i}} \tag{2.7}$$

K_{ij}^{pot} is not an empirical coefficient, but arises from the consideration of the diffusion process and of the Donnan equilibria. Equation (2.6) for a binary aqueous electrolyte solution can be written as:

$$\Delta E = E_1 - E_2 = \pm \frac{RT}{Z_1 F} \ln \frac{a_1(1) + K_{12}^{pot} a_2^{z_1/z_2}(1)}{a_1(2)} \tag{2.8}$$

Substituting Eq. (2.8) in Eq. (2.3) gives

$$E_{ISE} = E' \pm \frac{RT}{Z_1 F} \ln \left[a_1(1) + K_{12}^{pot} a_2^{z_1/z_2}(1) \right] \tag{2.9}$$

where,

$$E' = E_R + E_{ASY} \mp \frac{RT}{Z_1 F} \ln a_1(2) \tag{2.10}$$

The asymmetric potential E_{ASY} of the ISE depends on the crystal structure of the electrode body, particularly in glass ISEs.

Equation (2.9) is called Nikolsky-Eisenman equation and was proposed to approximate the effect of the interfering ions. As is evident from Eq. (2.10), E' is the electromotive force (emf) of the measuring circuit with a standard internal solution and depends on the activity of ions in the inner solution and the type of internal reference electrode. The theoretical value of RT/F at 298.15 K is 25.692 mV. This is the slope of an ISE if Nernstian behaviour is followed and when natural logarithm of the activity of the ions is considered. The potential of the ISE against a reference electrode is measured by a pH/ISE meter. The photo of the ISE meter along with the ISE and the reference electrode is shown in Fig. 2.4.

Fig. 2.4: A view of the ISE meter along with ISE and reference electrode

One of the best methods to predict the structural interactions, in addition to the measurement of single ion activity coefficient is based on the study of volumetric properties which can be calculated from density measurement.

2.6 VIBRATING TUBE DENSITOMETER (ANTON PAAR DMA 5000)

Among the modern instruments for measuring densities, a more sensitive and precise type is the vibrating tube density meter. The first vibrating tube used to measure the density of blood was improved upon by Picker et al. [24]. Henceforth, vibrating tube density meters have been the standard instrument for measuring densities of gases and fluids. A high precision density meter, DMA 5000 [25] was used to measure the density for this thesis work. The mode of operation and principle of working of the vibrating tube density meter is given below.

The density determination is based on the measurement of the oscillations of a vibrating sample tube. This tube is filled with the liquid sample mixture. The relationship between the period τ and the density ρ of the mixture is given by

$$P = A + B\tau^2 \tag{2.11}$$

A and B are instrument constants for each individual oscillator and can be determined by two calibration measurements with samples of known density (e.g.) dry air and millipore water. The photo of the density measuring apparatus used in this work is shown in Fig. 2.5.

Fig. 2.5: Density measurement system

2.6.1 MODE OF OPERATION

The density measurements are based on the electromagnetically induced oscillation of the glass U tube. One complete back and forth movement of a vibration is a period; its duration is the period of oscillation τ. The number of periods per second is the frequency υ. Each glass tube vibrates at a characteristic or natural frequency, which changes when the tube is filled with the substance. As the frequency is a function of mass, when the mass increases the frequency decreases. In other words, the period of oscillation τ increases.

$$\upsilon = \frac{1}{\tau} \tag{2.12}$$

A magnet is fixed to the measurement tube which is made to oscillate by a transmitter. A sensor measures the period of oscillation τ. The period of oscillation is obtained from the equation:

$$\tau = 2\pi\sqrt{\frac{\rho(V_c + m_c)}{K}} \tag{2.13}$$

where ρ is the density of the test sample, V_c is the volume of sample (capacity of the tube), m_c is the mass of the measured tube and K is the measurement tube constant.

It is followed from Eq. (2.13) that

$$\rho = \frac{K\tau^2}{4\pi^2 V_c} - \frac{m_c}{V_c} \tag{2.14}$$

The density and the period of oscillation τ are related as follows:

$$\rho = A\tau^2 + B \tag{2.15}$$

where $A = K\tau^2/4\ \pi^2 V_c$ and $B = -m_c/V_c$

A and B are constants which are determined from the elasticity, structure and mass of the measurement tube. In this work, the density values were obtained as the output from the DMA 5000 density meter.

2.6.2 EXPERIMENTAL PROCEDURE

The Anton Paar DMA5000 vibrating tube density meter consists of a built-in thermostat controller capable of maintaining temperature precisely up to ±0.001 K and measuring density up to ±0.00001 $g.cm^{-3}$. Prior to each experimental run, the cell was first flushed with ethanol. After flushing with acetone, dry air was blown through it for drying. ASTM Grade-1 water as per ASTM D-1193 [1] with a resistivity of 18.2 MΩ.cm at 298.15 K and TOC < 15 ppb from a MILLIPORE Simplicity system was used for calibration. The density of air and water was set for the calibration and the density of solution mixtures was then measured. Density values of water and air were determined between each experiment, to permit a continous check on both sample purity and densitometer operation. All the density measurements were done as per ASTM-D-4052 procedure [26].

2.6.3 SPECIFICATION

Accuracy	: 1×10^{-6} g.cm^{-3}
Minimum Sample Volume	: Approx. 1 ml
Measuring Range	: 0- 3 g.cm^{-3}
Temperature Range	: 273.15 – 363 K
Pressure Range	: 0-10 bar

2.7 REFRACTOMETER (ANTON-PAAR ABBEMAT RXA 156)

Refractive index is one of the physical properties that can be used for the characterization and identification of a material. Measurement of refractive index is easy, fast and non-destructive which is independent of viscosity. Quality control of multi-component mixtures of a given mixing ratio can be undertaken by means of a refractive index measurement. Therefore, a wide range of scales and quality control applications can be derived from this measuring technology. The instrument used in the present study for the accurate measurement of refractive index was Anton-Paar ABBEMAT RXA 156 [27], the picture of which is given in Fig. 2.9.

Fig. 2.9: A view of Refractive index measurement system

2.7.1 MEASURING PRINCIPLE

The working principle of the refractometer is as follows:

- The sample is kept in contact with the measuring prism and is irradiated by an LED
- The critical angle of the total reflection at 589.3 nm sodium D wavelength is measured with a high resolution sensor array
- The refractive index (nD) is calculated from the value of critical angle
- The sample and the measuring prism are thermostated precisely via Peltier technology to get highly accurate results

The block diagram of the refractive index measuring system is shown in Fig. 2.10:

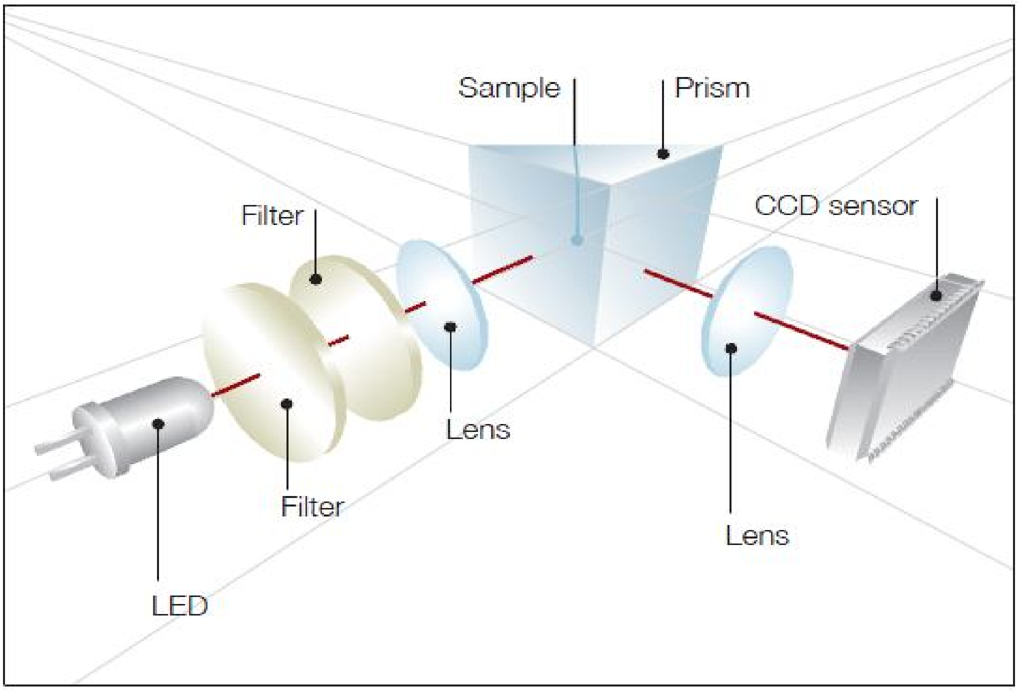

Fig. 2.10: Working principle of refractometer [27]

2.7.2 SPECIFICATION

Measuring range	: 1.32-1.56 nD
Accuracy	: 2×10^{-5} nD
Prism	: YAG (Yttrium Aluminium Garnet)
Sample mold	: Stainless steel
Seal	: FFKM (Perfluoroelastomer)
Measuring principle	: Critical angle of total reflection measured by shadow line detection with 2048- element linear CCD array and digital data
Light source	: High performance LED lamp, average life > 100,000 h
Wavelength	: 589.3 ± 0.1 nm (sodium D) by wavelength-adjuster interference filter
Sample/prism temperature control	: Built-in solid state thermostat (Peltier), range 283-343 K

2.8 WATER ACTIVITY METER

Water activity (a_w) is described qualitatively as the equilibrium amount of water available for hydration of materials. Water activity is defined as the effective mole fraction of water, given as $a_w = P/P_0$, where P is the partial pressure of water above the material and P_0 is the partial pressure of pure water at the same temperature i.e., water activity is equal to the equilibrium relative humidity expressed as a fraction. Water activity has been measured by a thermodynamic water activity meter (NOVASINA AW-Master) [28] with a built-in thermoelectric Peltier element module for maintaining the temperature of sample. The schematic of the instrument is shown in the Fig. 2.6.

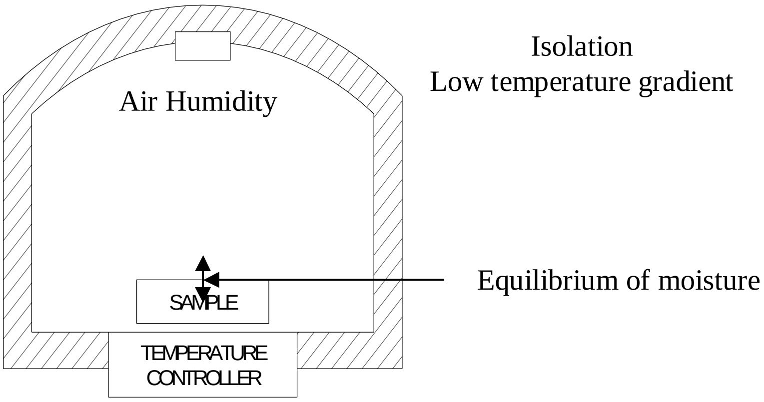

Fig. 2.6: A schematic view of water activity meter

Samples were loaded in polystyrene cups and placed into the activity meter. The activity meter was standardized using a two-step procedure. In the first step, purified and degassed millipore water was used as the standard ($a_w = 1.000$). In the second step, five immobilized electrolyte solutions, in sealed tablets supplied by M/s. Novasina [28] were used as standards. These solutions were ~25 % LiCl ($a_W = 0.113$), ~25 % $MgCl_2.6H_2O$ ($a_W = 0.328$), ~25 % NaCl ($a_W = 0.753$), 25 % $BaCl_2.2H_2O$ ($a_W = 0.901$) and ~20 % K_2SO_4 ($a_W = 0.973$). Humidity standards are based on saturated salt solutions in plastic tablets with humidity permeable membrane for multi-use. The salts generate a defined air humidity in the temperature range 288 – 303 K which flows out of the tablet through the permeable membrane inside the measuring chamber and generate a defined and stable humidity environment. This method of humidity generation is very precise and has an excellent repeatability. The humidity values for the standards LiCl, $MgCl_2.6H_2O$, NaCl, $BaCl_2.2H_2O$ and K_2SO_4 are 11.3%, 32.8%, 75.3%, 90.1% and 97.3% respectively. A photo of the NOVASINA water activity meter is shown in Fig. 2.7.

Fig. 2.7: Setup for thermodynamic water activity measurement

2.8.1 SPECIFICATION

Range : 0.03-1.00 aw (3-100% RH) from 32-122 °F (273.15 K-323.15 K)

Resolution : 0.001 aw

Accuracy : ± 0.003 aw (from 0.1-0.98 aw) at 77°F (298.15 K)

Repeatability : ±0.002 aw

Sensor type : resistive, electrolytic

2.9 VISCOMETER

A number of devices are available to measure the viscosity of a Newtonian fluid. However, the accurate determination of viscosity depends on the careful selection of the experimental technique to be employed. A Cannon-Fenske viscometer was used in this study to measure the viscosity of transparent liquids. The viscosity measurements conform to ASTM D445-11a [29]. The Cannon-Fenske viscometer with its main components is shown in Fig. 2.8. The viscometer is of capillary type and is designed to measure the kinematic viscosity of Newtonian fluid. It can also be used to study the shear stress versus shear rate relations applicable to the study of non-Newtonian liquids, wax crystallization and oil flow characteristics at low temperatures.

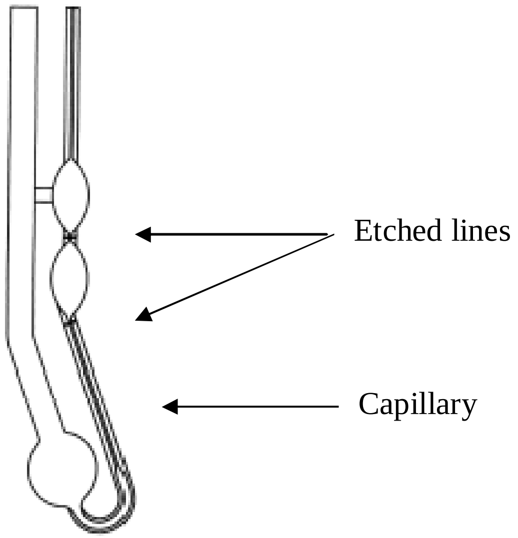

Fig. 2.10: Cannon-Fenske routine viscometer

2.9.1 EXPERIMENTAL PROCEDURE

1. The viscometer was fixed on the holder and was inserted into the constant temperature bath. It was aligned vertically in the bath and was allowed to reach equilibrium for 10 minutes at 313 K or for 15 minutes at 373 K, depending on the time required for temperature equilibration.

2. The sample solution was drawn above the mark by applying suction.
3. The efflux time was measured by allowing the liquid sample to flow freely down past mark, measuring the time for the meniscus to pass between two marks.
4. A check run was made by repeating steps 3 and 4 by minimum five times.
5. The efflux time for millipore water was measured by repeating the steps 1 to 5.

2.9.2 SPECIFICATION

Universal size number	: 75
Accuracy	: ± 0.2%
Approximate constant	: 0.008 cSt /sec
Sample volume needed	: 7 ml
Range	: 1.6 to 8 cSt

REFERENCES

1. ASTM Standard D-1193, Specification for Reagent Water (2006).
2. W. E. Morf, “ The principles of ion-selective electrodes and of membrane transport”, Elsevier, New York (1981)
3. A. K. Covington, Ed., “Ion selective electrode methodology”, Vol. I, CRC press, Boca Ralton (Florida) (1979)
4. M. S. Frant, J. W. Ross, Science, 154 (1966) 1553
5. K. Sollner , G. M. Shean, J. Am. Chem. Soc., 86 (1964) 1901
6. O. D. Bonner, D. C. Lunney, J. Phys. Chem., 70 (1966) 1140
7. A. Shatkay, Anal. Chem., 39 (1967) 1056
8. H. Adametzova, R. Vadura, J. Electroanal. Chem., 55 (1974) 53
9. B. M. Kneebone, H. Freiser, Anal. Chem., 45 (1973) 449
10. L. A. R. Pioda, V. Stankova, W. Simon, Anal. Lett., 2 (1969) 665
11. J. W. Ross, Science, 156 (1967) 1378
12. C. R. Martin, H. Freiser, Anal. Chem., 52 (1980) 562
13. H. Freiser, J. Chem. Soc., Faraday Trans. 1, 82 (1986) 1217
14. J. Koryta, Ann. Rev. Matter. Sci., 16 (1986) 13
15. K. Camman, “Working with ion-selective electrodes”, Springer-Verlag, Berlin Heidelberg, New York (1979)
16. H. Freiser, “Ion-selective electrodes in analytical chemistry”, Vol. 1, Plenum Press, New York (1978)
17. J. Koryta, “Ion-selective electrodes”, Cambridge university Press, London (1975)
18. R. A. Robinson, R. H. Stokes, “Electrolyte solutions”, Butterworths scientific, London (1959)

19. D. C. Harris, “Quantitative Chemical Anlysis”, W. H. Frieman and Company, New York (1987)
20. D. C. Harris, “Quantitative Chemical Anlysis”, W. H. Frieman and Company, New York, (2007)
21. R. H. Stokes and R. A. Robinson, J. Am. Chem. Soc., 70 (1948) 1870
22. A. J. Bard, L. R. Faulkner, "Electrochemical Methods", John Wiley & Sons, New York (1980)
23. D. A. Skoog, “Principles of Instrumental Analysis”, Saunders College Pub., Philadelphia (1985)
24. P. Picker, E. Tremblay and C. Jolicoeur, J. Soln. Chem., 3 (1974) 377
25. DMA-5000 operation manual, Anton Paar, Austria (2006)
26. ASTM Standard D-4052, Standard Test Method for Density and Relative Density of Liquids by Digital Density Meter (2002).
27. Abbemat high performance automatic refractometer operation manual, Anton Paar, Austria
28. Lab-Master operation manual, M/S NOVASINA, Switzerland (2009)
29. ASTM D445-11a, Standard Test Method for Kinematic Viscosity of Transparent and Opaque Liquids (and Calculation of Dynamic Viscosity) (2006)

CHAPTER 3

MEASUREMENT OF SINGLE ION ACTIVITY COEFFICIENT OF ELECTROLYTES IN BINARY SYSTEMS

CHAPTER 3

MEASUREMENT OF SINGLE ION ACTIVITY COEFFICIENT OF ELECTROLYTES IN BINARY SYSTEMS

3.1 INTRODUCTION

In Chapter 2 potentiometric methods were reviewed and the application of ion-selective electrodes to perform electromotive force (EMF) measurement of electrochemical cells was discussed. In this Chapter, the different techniques for EMF measurements and the calculation of single ion activity coefficient of electrolytes in binary systems will be briefly discussed.

Activity of a species in a solution is referred to as its effective concentration in that solution. In a very dilute solution, as interactions are insignificant, concentration and effective concentration are the same. But as the concentration increases, the electrostatic interaction increases and deviations from ideality are accommodated by modifying the concentration with activity coefficient. The non-ideality in aqueous solution can be attributed to ionic activity coefficient and it corresponds to interaction between different species in solution, both ionic and molecular. When the solute undergoes ionic dissociation in solution, the activities of cations and anions (a_+, a_-) can be defined; so also activity coefficients (γ_+, γ_-). The knowledge of individual ionic activity coefficient is important for the design of equilibrium processes involving electrolyte solutions as well as for processes involving ion-exchange and pollution control [1]. Activity coefficients can also be used for the prediction of rate constant, equilibrium constant, chemical potential values, solubility product and for the separation of a species from a mixture of substances on the basis of the magnitude of activity coefficient.

Single ion activity coefficients are traditionally termed as not measurable by simple thermodynamic methods due to space charge interactions. Information regarding mean ionic activity coefficient is available in literature [2-7], but the absence of reliable methods for the measurement of individual ion activity coefficients is a major barrier for the study of the systems which are really complex in nature. Attempts were made to measure single ion activity coefficient of non volatile electrolytes in solution by two methods: (1) solvent activity method involving vapour pressure and Gibbs-Duhem equation; (2) electrochemical cell technique involving direct calculation of the activity of an electrolyte by measuring the EMF of the electrochemical cell. Vera and co-workers [8-12] and other researchers [13-16] demonstrated the application of ISE (Ion Selective Electrode) technique for the measurement of single ion activity coefficients. The same approach has been utilized to determine the single ion activity coefficient in this work. Measurement of the activity coefficients of both anion and cation in aqueous solutions of single electrolytes using ISE method has been demonstrated. The activity coefficients are used to find out mean ionic activity coefficient for different salts. The calculated mean ionic activity coefficients are in good agreement with the values reported by Hamer and Wu [3].

3.2 OVERVIEW OF EARLIER WORK

The problem of measurement of the activity coefficient of individual ions has been a topic of discussion for over 85 years. Lewis and Randall [17] in their classical text book

‘*Thermodynamics’* stated that: “This is a problem of difficulty, and indeed we are far from any complete solution”. Some standard text books have declared that such measurements are impossible to make [18, 19]. In spite of all the discrepancies, there has been continuous effort from various research groups through the years to measure individual ionic activity coefficients by diverse techniques [10, 11, 20-29].

Bates et al. [13, 20] extended the Robinson and Stokes [4] hydration model for the mean activity coefficient of salts and proposed a model for the calculation of activity coefficients of individual ions in unassociated chlorides. Assuming that chloride ion is not hydrated, Bates et al. prepared tables for the activities of different ions in non-associating chlorides by using hydration numbers reported in the literature for cations and considering the experimental data for $\gamma_{\pm}$. The results obtained with this model, predicted that the activity coefficients of monovalent cations in non-associating chlorides are either equal or higher than those of the chloride anion. For CsCl, the model predicted the same values for the activity coefficients of cation and anion, but for all other chlorides it predicted higher value for monovalent cations. Komar and Kaftanov [21] estimated the activity coefficients of the chloride ion in a potassium chloride solution at high (11-12) and low (2-2.7) pH.

Shatkay and Lerman [22] obtained activity coefficients of sodium and chloride ions in a sodium chloride solution using Ion selective electrode (ISE) and AgCl/Ag electrode, each against a calomel reference electrode and used a modified Henderson equation to calculate the liquid junction potential. Although they used a Nernstian slope for the electrode potential, they determined the conditions under which this assumption was valid. The values of the standard potential were chosen arbitrarily. Their direct measurements of the mean ionic activity coefficients of sodium chloride agreed well with literature data.

Milazzo [23, 24] suggested a procedure for determining the activity coefficient of individual ions from the variation of the EMF of electrodes with temperature. Further studies [25, 26] made by him indicated some shortcomings of this method. As the method proposed was unsuccessful, Millazo et al. [27] discussed the conditions that would be required to obtain reliable data. The values of activity coefficients of sodium and chloride ions in sodium chloride solution at different temperatures reported by Mokhov et al. [28] gave a poor reproduction of $\gamma_{\pm}$ for sodium chloride.

3.2.1 USE OF ION SELECTIVE ELECTRODES TO MEASURE THE IONIC ACTIVITY

The major breakthrough towards the measurement of the activity of individual ions was achieved with the use of ion selective electrodes. One of the advantages of ISEs is their “ability to measure the activity of ions” [30]. The ISEs have also been used for the measurement of $\gamma_{\pm}$ of an electrolyte in mixed electrolyte solutions [31, 32] and to measure the activities of amino acids in aqueous electrolyte solutions [10, 33-38]

An important step toward the measurement of the activity of ions was based on the finding of Kakabadse [39] that for a single electrolyte in an aqueous solution, the resultant EMF value was obtained from the direct measurement of the EMF of the ISE for the cation against the ISE for the anion, as the difference of the two EMF values of the individual ISEs with respect to a common reference electrode. Haghtalab [40] verified this finding and used the difference of the EMF readings to measure $\gamma_{\pm}$ for electrolytes up to high molalities [31, 32]. These experimental results made it evident that the EMF measured with a single ISE against a reference electrode contained the information on the activity of the individual ion.

Haghtalab [32] determined the mean ionic activity coefficients of NaBr in aqueous mixtures of NaBr and $Ca(NO_3)_2$ at 298 K at a total ionic strength of 3, 4.5 and 6 mole. The measurements were made using an electrochemical cell with the ion selective electrodes, Na-ISE against Br-ISE as a reference electrode. The mean activity coefficients of $Ca(NO_3)_2$ were calculated using the cross differentiation of the mean activity coefficients. He also investigated the thermodynamics of aqueous solutions of strong electrolytes for both binary and multi-component systems. Electrochemical data generated from electrochemical cells using ion-selective electrodes were used to derive activity coefficient values.

In 1996, Khoshkbarchi and Vera [10, 11] measured the activity of ions using two ISEs against a single junction reference electrode (SJRE). They used ISEs to measure the activity coefficients of individual ions in aqueous solutions of NaCl and NaBr at 298.2 K, up to of 5 mole and of KCl up to 4 mole. The mean ionic activity coefficients of NaCl, NaBr and KCl obtained from the values of the activity coefficients of the individual ions showed good agreement with values reported in the literature. The experimental results revealed that the activity coefficients are different for the anion and the cation in an aqueous solution of a single electrolyte and that, as expected from the ion-ion and ion-solvent interactions, the activity coefficient of an ion depends on the nature of its counter ion. A modified form of Pitzer's model, which distinguishes between the activity coefficients of the anion and the cation, was used to correlate the experimental results. A novel method was developed for the measurement of the activity coefficients of an amino acid and the mean ionic activity coefficient of an electrolyte in water-electrolyte-amino acid systems using electrochemical cell.

From 1996 till today, Vera and Co-workers [8, 12, 41-43] generated lot of results on single ion activity coefficient, both in single and mixed solvents. They observed that the change of filling solution of reference electrode did not have much effect on the ionic activity coefficient and the individual activities of the ions were measured by them using ISEs. The available commercial electrodes could be used in a wide range of concentrations of the respective ion. In the systems chosen for measurements, there was no interference to the response of an ISE due to the presence of other ions in the solution because of the precautions taken during the measurement.

3.3 EXPERIMENTAL

Electrochemical cells with ion-selective electrodes and an AgCl/Ag double junction reference electrode (DJ), have been used to measure the activity coefficients of sodium, potassium, chloride and nitrate ions in aqueous solutions of sodium nitrate, potassium nitrate, sodium chloride and potassium chloride. The values of potential difference of the following cell configuration were measured and were then converted to the ionic activity coefficients.

ISE | electrolyte (s) | KCl, AgCl/ Ag (DJ) (3.I)

AR grade $NaNO_3$, NaCl, KNO_3 and KCl of 99.9 and 99.5 % purity were obtained from M/s. Loba Chemie (Mumbai) and M/s. Merck (Mumbai) respectively. The salts were oven dried for 48 h and cooled in vacuum desiccator for 24 h prior to use. A sodium ion selective electrode glass body, a potassium ion selective electrode polymer body, a nitrate ion selective electrode polymer body, a chloride ISE, solid state and a double junction reference electrode were obtained from M/s. Orion, USA. An Orion pH / ISE meter (EA $920A^+$) with a resolution of ± 0.1 mV was used to monitor the electrochemical potentials. The ISE meter had two BNC connectors for ISEs and two pin-tip connectors for the reference electrode. During the experiments, the solutions were stirred continuously and the temperature was kept constant at 298.15 ± 2 K using a thermostatic bath.

The electrodes were conditioned according to the manufacturer’s procedure prior to the experiment. The main features of the apparatus, designed to conduct the experiment include a double wall jacketed vessel, ion selective electrode, a double junction reference electrode, a thermostatic bath, a high impedance millivolt meter, a temperature probe, and a magnetic stirrer. Fig. 3.1 shows the schematic diagram of the experimental setup. The temperature in the double wall jacketed vessel was controlled by water from a thermostatic bath. The temperature of water in the thermostatic bath was stabilized by using an additional cooling bath.

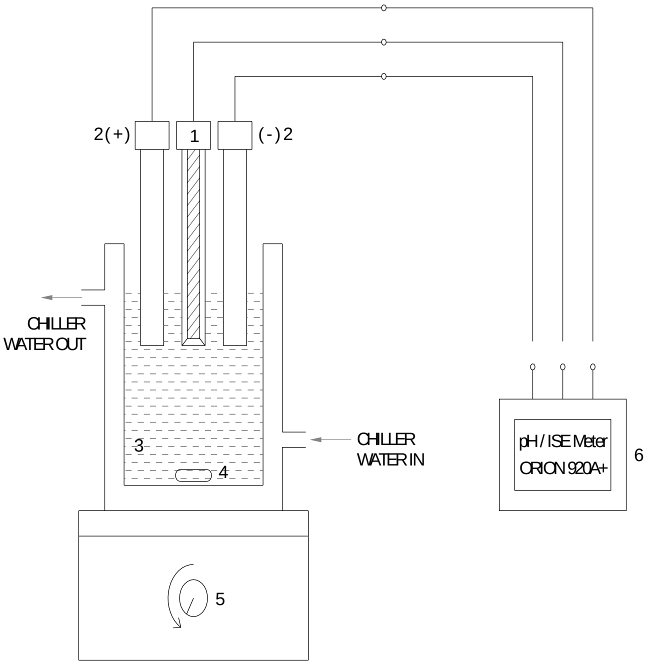

Fig. 3.1: Schematic diagram of the experimental system

1. Reference electrode; 2. ISE, (+) cation, (-) anion; 3. Thermostated cell,
4. Stirring bar; 5. Magnetic stirrer, 6. PH/ISE meter

ASTM Grade-1 water as per ASTM D-1193 [44] with a resistivity of 18.2 MΩ·cm at 298.15 K and TOC < 15 ppb from a MILLIPORE Simplicity system was used in the experiments for reagent/solution preparation and as water standard. All the solutions were prepared based on molality and the water was also weighed. Solutes were accurately weighed in a precision Shimadzu AUW220D balance (220 g, 0.01 mg resolution). When not in use, the solutions were kept in air-tight closed condition in a JULABO SW-22 Shaker Bath at 298.15 ± 0.1 K. JULABO SW-22 Shaker Bath was coupled with JULABO FP-40 chiller for cooling. To ensure ripple-free power supply to all the equipment, AC supply was regulated with an uninterrupted power supply (APC), set at high sensitivity. The ambient conditions were monitored with a Cole-Parmer hygrometer (0.1%) comprising a thermometer (0.1 K) and pressure sensor (0.1 kPa).

The experiments were initiated with the lowest concentration of electrolyte and the concentration was increased by addition of electrolyte. The EMF of both the cation and anion ISE were measured against a double junction reference electrode. The readings of the potentiometer were recorded only when the drift was less than 0.1 mV. To avoid the bias potential between different reference electrodes, in each experiment, the response of both cation and anion ISEs were measured simultaneously against the same reference electrode. In order to minimize the risk of concentration gradient in the beaker, the solutions were stirred continuously during the experiment with a magnetic stirrer and the temperature was kept constant using thermostatic bath.

3.4 CALIBRATION OF ION SELECTIVE ELECTRODES

For the electrodes to exhibit Nernstian behaviour, they were calibrated using the standard solutions supplied along with the electrodes. Three buffer solutions were prepared from the standard solutions differing 10 times each in concentration.

For a 1:1 electrolyte, the EMF (E) values of the cells obtained from these solutions could be represented by an equation given by Butler and Roy [45]

$$E = E^0 + S \ln a = E^0 + 2S \ln (m\gamma_\pm) \qquad (3.1)$$

where, E is the potential of the cell, E^0 is the standard EMF of the cell, S is the slope of the electrode's response to the ionic activities, $\gamma_\pm$ is the mean activity coefficient and m is the molality.

When ISEs were used for determining the activity coefficients of electrolytes in binary systems, it was reported that the use of the theoretical value of the reversible Nernstian slope as S in Eq. (3.1) could not be justified [13]. In the present study, both E^0 and S were treated as adjustable parameters and could be obtained by optimization method. The variation of ln m with E (mV) for the calibration of different ISEs with their respective salts is shown in Figs. 3.2 to 3.5 respectively. The slope and intercept of Eq. (3.1) were calculated from these plots in very dilute region.

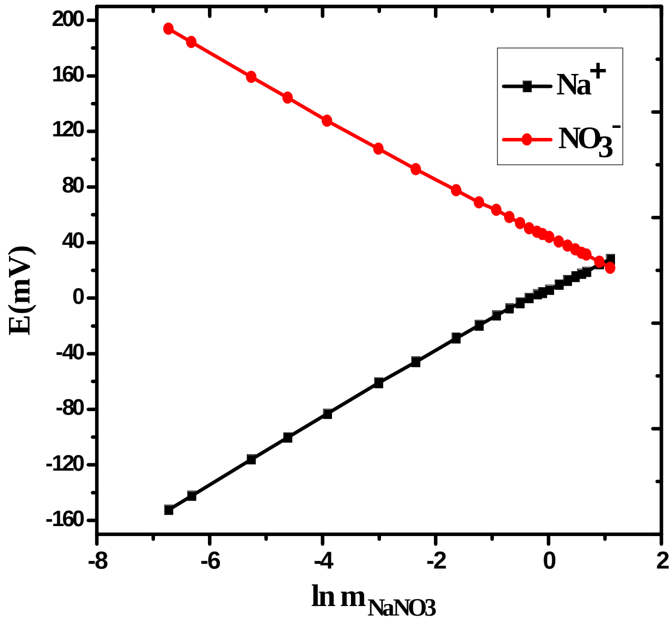

Fig. 3.2: Variation of the potential of NaNO$_3$ (E) with concentration

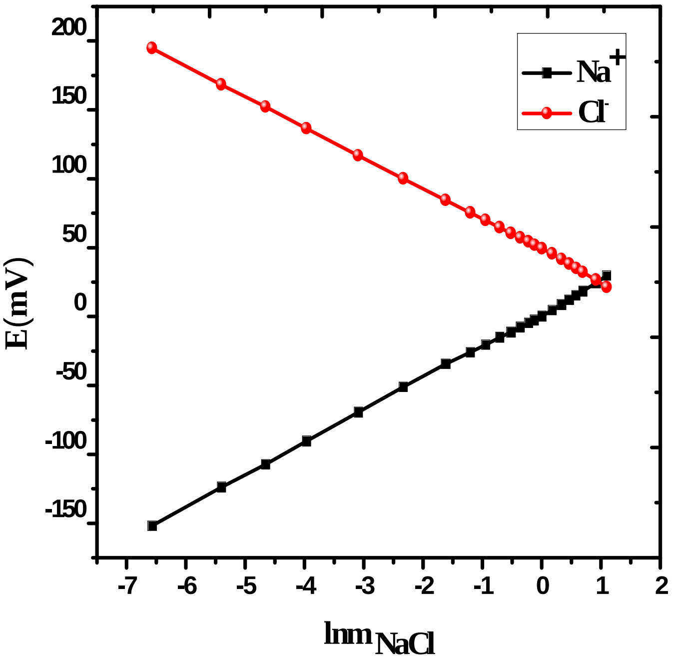

Fig. 3.3: Variation of the potential of NaCl (E) with concentration

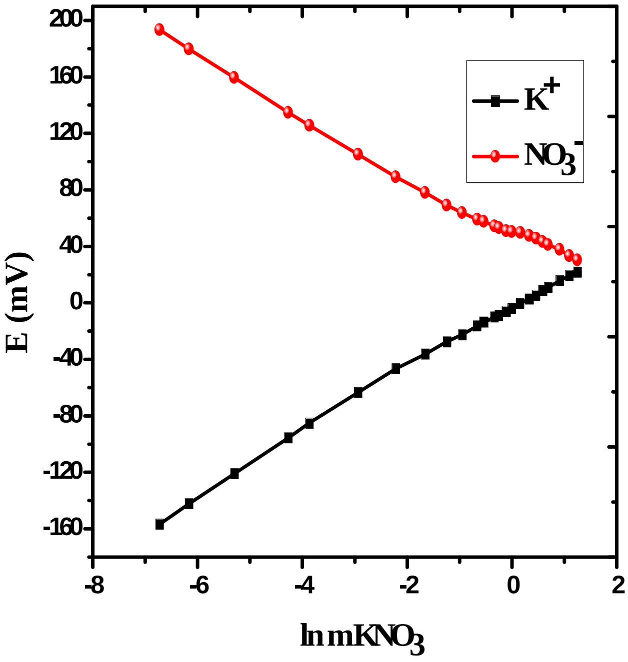

Fig. 3.4: Variation of the potential of KNO_3 (E) with concentration

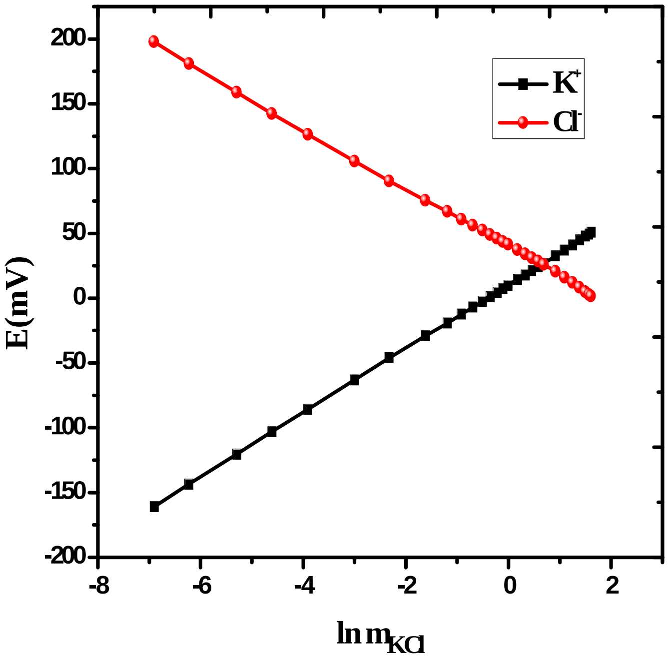

Fig. 3.5: Variation of the potential of KCl (E) with concentration

3.5 RESULTS AND DISCUSSION

The ISEs used in this work were calibrated prior to the experiment. The cell arrangement for the experiments were

Na glass body ISE | $NaNO_3$ (m_1) | NO_3 polymer body ISE (3.II)

Na glass body ISE| NaCl (m_2)| Cl solid-state ISE (3.III)

K polymer body ISE | KNO_3 (m_1) | NO_3 polymer body ISE and (3.IV)

K polymer body ISE| KCl (m_2)| Cl solid-state ISE (3.V)

The potential of the respective ISE was measured against a double junction reference electrode and is related to the ionic activity coefficient of the corresponding ion by Nernst equation. For a solution containing an electrolyte of molality m_1, the Nernst equations for the potentials of a cation and an anion ISE, E_+ and E_- in the electrochemical cell of type 3.II, ISE| $NaNO_3$| reference electrode, can be written as

$$E_+ = E_+{}^0 + \frac{RT}{z_+F}\ln(m_+\gamma_+) \tag{3.2}$$

$$E_- = E_-{}^0 + \frac{RT}{z_-F}\ln(m_-\gamma_-) \tag{3.3}$$

where γ is the activity coefficient, R is the universal gas constant, T is absolute temperature, F is Faraday's constant, z is the charge number, and subscripts plus and minus sign denote the cation and the anion respectively. The terms $E_+{}^0$ and $E_-{}^0$ in Eqs. (3.2) and (3.3) are linear combinations of the junction potential, reference electrode potential and ISE potentials:

$$E_+{}^0 = E^{ref} + E^J + E_+{}^{ISE} \tag{3.4}$$

$$E_-{}^0 = E^{ref} + E^J + E_-{}^{ISE} \tag{3.5}$$

where, superscripts 'ref' and 'J' denote the potential of the reference electrode and junction potential and the terms $E_+{}^{ISE}$ and $E_-{}^{ISE}$ include all asymmetry, internal solution and reference potential of the cation and anion ISE respectively. Subtracting Eq. (3.3) from Eq. (3.2) and substituting Eqs. (3.4) and (3.5), a relation between the difference in the potential of a cation and an anion ISE is obtained with the mean ionic activity coefficient of the electrolyte, $\gamma^{(1)}_{\pm}$, in cell type (1) as

$$E_+ - E_- = (E_+{}^{ISE} - E_-{}^{ISE}) + \frac{RT}{F}\left(\frac{z_+ + z_-}{z_+z_-}\right)\ln\left(\upsilon_+{}^{\upsilon_+}\upsilon_-{}^{\upsilon_-}\right)^{1/(\upsilon_+ + \upsilon_-)} m_1\gamma_{\pm}{}^{(1)} \tag{3.6}$$

For a 1:1 electrolyte, equation (3.6) simplifies to

$$E_+ - E_- = (E_+^{ISE} - E_-^{ISE}) + \frac{2RT}{F}\ln(m_1\gamma_\pm^{(1)}) \tag{3.7}$$

Equation (3.7) is valid only when the reference electrode is same both for cation and anion ISEs. The more general form of Eq. (3.7) for $NaNO_3$, NaCl, KNO_3 and KCl solutions is

$$\Delta E_{NaNO_3} = E^0{}_{NaNO_3} + 2S\ln(m_1\gamma_\pm^{(1)}) \tag{3.8}$$

$$\Delta E_{NaCl} = E^0{}_{NaCl} + 2S\ln(m_2\gamma_\pm^{(2)}) \tag{3.9}$$

$$\Delta E_{KNO_3} = E^0{}_{KNO_3} + 2S\ln(m_3\gamma_\pm^{(3)}) \tag{3.10}$$

$$\Delta E_{KCl} = E^0{}_{KCl} + 2S\ln(m_4\gamma_\pm^{(4)}) \tag{3.11}$$

Determination of activity coefficients of electrolytes by ISEs is a rapid method. However, some interference from other ions will be there at high concentrations. To avoid the interferences, the experiments were performed with dilute solutions, by measuring the EMF of both the cation and the anion ISEs against a double junction reference electrode. The sample and the standard solutions were maintained at the same ionic strength. Figs 3.6 and 3.7 depict the ion activity coefficients of sodium, chloride and nitrate ions at various molalities in aqueous solutions of $NaNO_3$ and NaCl.

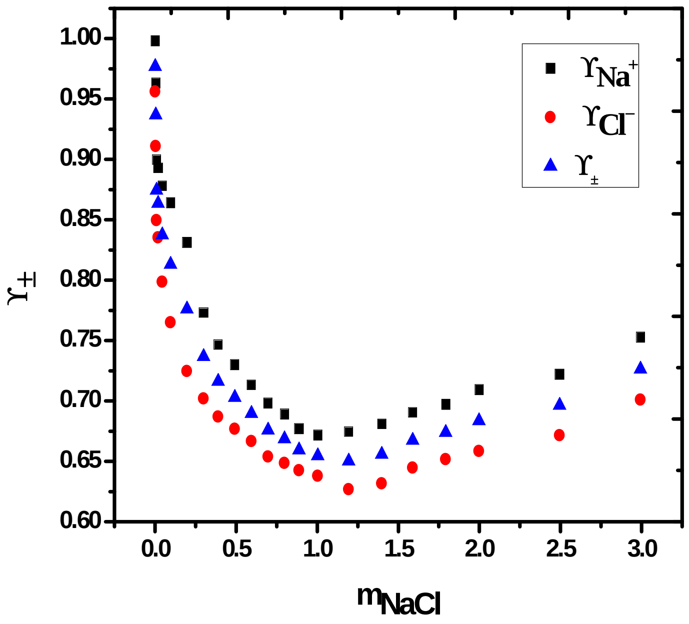

Fig. 3.6: Variation of activity coefficient values of NaCl with concentration

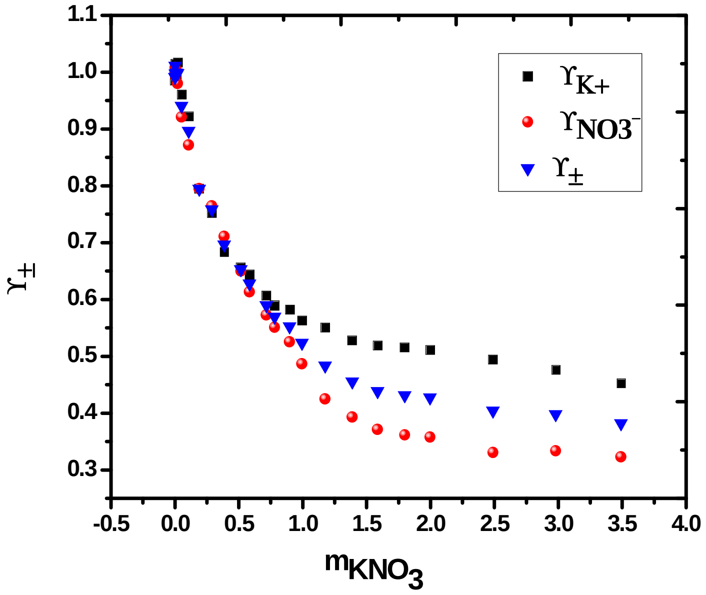

Fig. 3.7: Variation of activity coefficient values of KNO_3 with concentration

The numerical data for the ionic activity coefficients in the aqueous solutions of KCl and $NaNO_3$ are presented in Tables 3.1 and 3.2 respectively along with the literature value for the sake of comparison.

Table 3.1: Single ion activity coefficient and mean activity coefficient values for aqueous solution of KCl

Conc. (mol.kg^{-1})	γ_{K^+}	γ_{Cl^-}	$\gamma_\pm$(Expt.)	$\gamma_\pm$ (Ref. [3])
0.001	0.998	0.962	0.980	0.965
0.002	1.006	0.957	0.981	0.951
0.005	0.998	0.926	0.961	0.927
0.010	1.000	0.902	0.950	0.901
0.020	0.985	0.858	0.919	0.869
0.050	0.972	0.795	0.879	0.816
0.098	0.970	0.747	0.851	0.768
0.198	0.938	0.674	0.795	0.717
0.305	0.901	0.620	0.747	0.687
0.400	0.904	0.602	0.738	0.665
0.500	0.896	0.582	0.722	0.649
0.603	0.885	0.563	0.706	0.636
0.700	0.884	0.554	0.700	0.626
0.800	0.880	0.544	0.692	0.617
0.897	0.879	0.537	0.687	0.610
0.993	0.880	0.532	0.684	0.604
1.190	0.875	0.521	0.675	0.594
1.384	0.874	0.513	0.669	0.586
1.582	0.871	0.506	0.664	0.580
1.792	0.863	0.498	0.656	0.576
1.989	0.863	0.495	0.654	0.573
2.504	0.857	0.487	0.646	0.568
2.984	0.865	0.492	0.653	0.568
3.498	0.865	0.495	0.654	0.571
3.994	0.871	0.503	0.662	0.576
4.490	0.880	0.515	0.673	0.584
4.791	0.884	0.523	0.680	0.589
4.991	0.888	0.528	0.685	0.593

Table 3.2: Individual activity coefficient and mean activity coefficient values for $NaNO_3$ solution

Conc. (mol.kg^{-1})	γ_{Na^+}	$\gamma_{NO_3^-}$	$\gamma_{\pm}$(Expt.)	$\gamma_{\pm}$(Ref. [3])
0.001	0.979	0.957	0.968	0.965
0.002	0.969	0.944	0.956	0.951
0.005	0.945	0.900	0.922	0.926
0.010	0.931	0.867	0.898	0.900
0.020	0.907	0.843	0.874	0.867
0.049	0.877	0.763	0.818	0.811
0.096	0.824	0.718	0.769	0.760
0.196	0.788	0.643	0.712	0.702
0.294	0.762	0.609	0.681	0.666
0.399	0.746	0.560	0.647	0.639
0.504	0.720	0.547	0.627	0.618
0.609	0.691	0.540	0.611	0.600
0.713	0.681	0.534	0.603	0.585
0.820	0.657	0.516	0.582	0.571
0.904	0.629	0.501	0.562	0.559
1.019	0.604	0.484	0.540	0.549
1.208	0.585	0.466	0.522	0.530
1.408	0.568	0.450	0.505	0.515
1.619	0.551	0.436	0.490	0.501
1.807	0.535	0.430	0.480	0.489
1.965	0.522	0.417	0.466	0.478
2.481	0.516	0.406	0.458	0.456
2.996	0.487	0.402	0.442	0.437

The mean activity coefficient of each salt was obtained from the relation:

$$\gamma_{\pm} = \left(\gamma_{+}^{\nu^{+}} \gamma_{-}^{\nu^{-}}\right)^{\frac{1}{\nu^{+}+\nu^{-}}} \tag{3.12}$$

From the Tables 3.1 and 3.2 and Figs. 3.6 and 3.7, it is evident that the activity coefficients of the cation and anion are nearly equal in very dilute solutions, but with increase in concentration they deviate from each other i.e., their contribution to non-ideal behaviour increases. The mean ionic activity coefficient obtained from the experimental measurements is generally larger than the literature reported values [3]. The mean ionic activity coefficients derived from the present study are compared with literature data in Figs. 3.8 to 3.11.

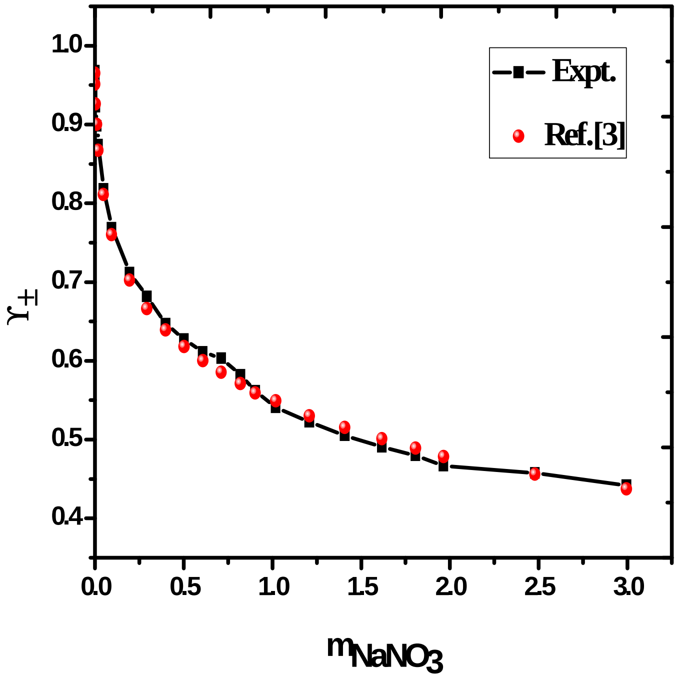

Fig. 3.8: Comparison of experimental activity coefficient values for $NaNO_3$ with literature

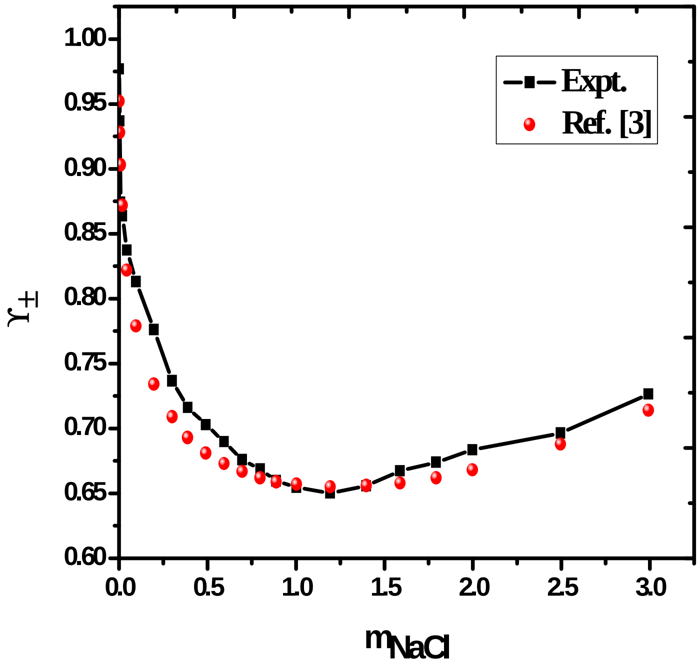

Fig. 3.9: Plot of comparison of experimental mean ionic activity coefficients of NaCl with literature

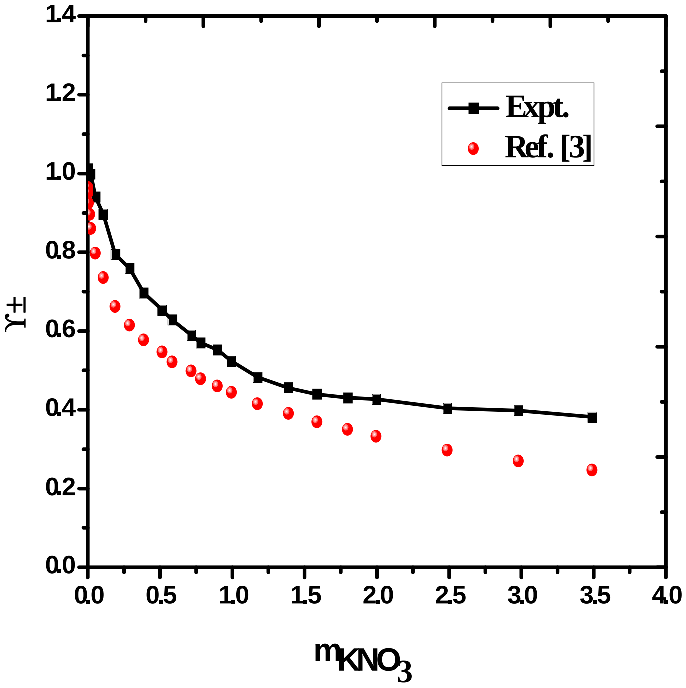

Fig. 3.10: Comparison of experimental mean ionic activity coefficients of KNO_3 with literature

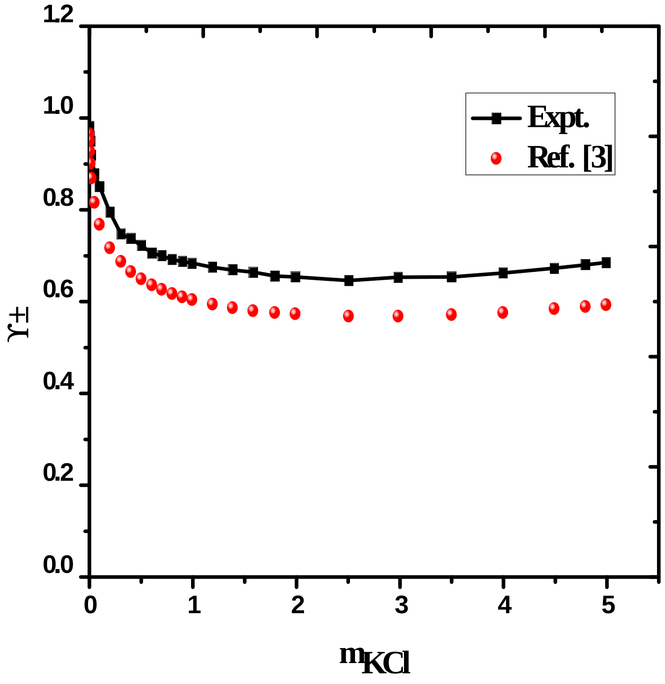

Fig. 3.11: Plot of comparison of experimental mean ionic activity coefficients of KCl with literature

As the concentration of the solution is increased, the activity coefficient of the electrolyte falls to a minimum and then rises to values which may be considerably greater than unity. The main cause for these high values is considered to be due to the hydration of ions. Hydration increases the activity coefficient of the electrolyte in aqueous solutions by two ways:

1. By weakening the electrostatic interaction between ions due to their greater separation
2. By removing water from the role of solvent to become a part of the hydrated ion

Figures 3.8 to 3.11 reveal that the agreement between the literature and the experimental values for $NaNO_3$ and NaCl electrolytes is good, but for potassium salts deviation from literature value is found, which could be because of the impurities present in the potassium salts.

The thermodynamic properties of electrolyte solutions depend not only on hydration but also on the ion-ion and ion-solvent interactions. Ions in solution interact with each other as well as with water molecules. At low concentrations, these interactions can be ignored, but at higher concentrations ions behave as if they are less concentrated than they really are. Therefore, the ionic activity coefficients can be interpreted in terms of the combination of Debye-Huckel equation, hydration effect and interionic interactions. In very dilute region, Debye-Huckel equation alone is applicable, but with increasing concentration the other two effects dominate and should be considered.

SUMMARY

In very dilute solutions of electrolytes, the ions are surrounded by only water molecules. Interionic and ion-solvent interactions are negligible and the solution behaves ideally. When the concentration of ions in the solution is greater than approximately 0.01 m, a shielding effect arises around the ions i.e., the cations tend to surround the nearby anions and anions tend to surround the nearby cations. These interactions make the solution non-ideal and one can define activities for cations and anions (a_+ and a_-) separately. The difference between activity and other measures of composition arises because molecules in non-ideal solutions interact with each other which give rise to activity coefficients (γ_+ and γ_-). When there is ion-ion interaction, effective concentration decreases, i.e., activity will decrease. Similarly, when ion-solvent interaction exists, some of the solvent molecules become separated from the bulk solution and effective concentration and also activity will increase. For the aqueous solutions of $NaNO_3$, NaCl, KNO_3 and KCl systems under investigation, electrochemical cells were assembled using suitable ISEs and EMFs were measured using a double junction reference electrode to calculate the single ion activity coefficient of K^+, Na^+, Cl^- and NO_3^-. The experimental results confirmed that the activity coefficients of cation and anion in aqueous single electrolyte solutions of KNO_3, $NaNO_3$, NaCl and KCl were different from each other over the whole range of concentration studied which is attributed to the ion-ion and ion-solvent interactions. The activities of both ions were measured independently and the data were found to be reliable.

REFERENCES

1. G. Eisenman, Glass electrodes for hydrogen and other cations, Marcel Dekker, New York (1967)
2. R.N. Goldberg, J. Phys. Chem. Ref. Data, 10 (1981) 671
3. W.J. Hamer, Y.C. Wu, J. Phys. Chem. Ref. Data, 1 (1972) 1047
4. R.A. Robinson, R.H. Stokes, Electrolyte solutions, Butterworths Scientific, London (1959).
5. B.R. Staples, J. Phys. Chem. Ref. Data, 10 (1981) 765
6. X. Ji, X. Lu, W. Lin, L. Zhang, Y. Wang, J. Shi, B. C.Y. Lu, J. Chem. Thermodyn., 33 (2001) 1107
7. A. Lopes, J. Santos, F. Farelo, M.I.A. Ferra, Portugaliae Electrochim. Acta, 17 (1999) 201
8. G.W. Vera, E. Rodil, J.H. Vera, Fluid Phase Equil., 241 (2006) 59
9. G.W. Arce, J.H. Vera, Chem. Eng. Sci., 62 (2007) 3849
10. M.K. Khoshkbarchi, J.H. Vera, AIChE J., 42 (1996) 249
11. M.K. Khoshkbarchi, J.H. Vera, Fluid Phase Equil., 121 (1996) 253
12. E. Rodil, J.H. Vera, Can. J. Chem. Eng., 79 (2001) 771
13. R.G. Bates, A.G. Dickson, M. Gratzl, A. Hrabeczy-Pall, E. Lindner, E. Pungor, Anal. Chem., 55 (1983) 1275

14. G.N. Lewis, M. Randall, Thermodynamics (Revised by K.S. Pitzer, L. Brewer) McGraw-Hill, New York (1961)

15. K. Zhuo, W. Dong, W. Wang, J. Wang, Fluid Phase Equil., 274 (2008) 80

16. D. Dash, S. Kumar, C. Mallika, U.K. Mudali, ISRN Chem. Eng., .2012 (2012) doi:10.5402/2012/730154

17. G.N. Lewis, M. Randall, Thermodynamics, 1st Ed., McGraw Hill, New York (1923)

18. J.O' M. Bockris, A.K.N. Reddy, Modern Electrochemistry, 3rd Ed., Plenum, New York (1977)

19. K.S. Pitzer, Thermodynamics, 3rd Ed., McGraw Hill, New York (1995)

20. R.G. Bates, B.R. Staples, R.A. Robinson, Anal. Chem., 42 (1970) 867

21. N.P. Komar, A.Z. Kaftanov, Russ. J. Phys. Chem., 48 (1974) 246

22. A. Shatkay, A. Lerman, Anal. Chem., 41 (1969) 514

23. G. Millazo, Z. Phys. Chem., 54 (1967) 27

24. G. Millazo, Z. Phys. Chem., 62 (1968) 47

25. G. Millazo, K. V. Sharma, Z. Phys. Chem., 73 (1970) 223

26. G. Millazo, G. Schenk, Z. Phys. Chem., 76 (1971) 127

27. G. Millazo, N. Bonciocat, M. Borda, Electrochim. Acta, 21 (1976) 349

28. V.M. Mokhov, I.P. Bagdasarova, A.G. Kekeliya, L.V. Lavrelashvilig, Russ. J. Phys. Chem., 51 (1977) 1406

29. M.M. Marcos-Arroyo, M.K. Khoshkbarchi, J.H. Vera, J. Soln. Chem., 25 (1996) 983
30. J. Ruzicka, J. Chem. Ed., 74 (1997) 167
31. A. Haghtalab, J.H. Vera, J. Chem. Eng. Data, 36 (1991) 332
32. A. Haghtalab, J.H. Vera, J. Soln. Chem., 20 (1991) 479
33. A.M. Soto-Campos, M.K. Khoshkbarchi, J.H. Vera, J. Chem. Thermodyn., 29 (1997) 609
34. M.K. Khoshkbarchi, J.H. Vera, J. Soln. Chem., 25 (1996) 865
35. M.K. Khoshkbarchi, J.H. Vera, Ind. Eng. Chem. Res., 35 (1996) 2735
36. A.M. Soto-Campos, M.K. Khoshkbarchi, J.H. Vera, Biophys. Chem., 67 (1997) 95
37. M.K. Khoshkbarchi, A.M. Soto-Campos, J.H. Vera, J. Soln. Chem., 26 (1997) 941
38. A.M. Soto-Campos, M.K. Khoshkbarchi, J.H. Vera, Fluid Phase Equil., 142 (1998) 193
39. G. Kakabadse, Ion-Selective Electrodes Rev., 3 (1981) 127
40. A. Haghtalab, Ph. D. Thesis, McGill University (1990)
41. G. Wilczek-Vera, E. Rodil, J.H. Vera, AIChE J., 50 (2004) 445
42. G. Wilczek-Vera, J.H. Vera, Fluid Phase Equil., 236 (2005) 96
43. G. Wilczek-Vera, E. Rodil, J.H. Vera, Fluid Phase Equil., 244 (2006) 33

44. ASTM standard D-1193, Specification for reagent water (2006)

45. J.N. Butler, R.N. Roy, Activity coefficients in electrolyte solutions, 2nd Ed., CRC Press, Boca Raton, FL, Chapter 4 (1991)

CHAPTER 4

STRUCTURAL INTERACTIONS LEADING TO VOLUMETRIC CHANGES IN AQUEOUS NITRATE SOLUTIONS AT 298.15 K

CHAPTER 4

STRUCTURAL INTERACTIONS LEADING TO VOLUMETRIC CHANGES IN AQUEOUS NITRATE SOLUTIONS AT 298.15 K

4.1 INTRODUCTION

Thermophysical properties of electrolyte solutions expressed as apparent or partial molal quantities aid in characterizing solute-solvent and solute-solute interactions [1-5]. These properties are employed in designing the process equipment in industries and also in various separation processes like extraction and distillation. The volumetric property of a component in a solution can be obtained from the measurement of density of the solution as a function of concentration. The density of liquid systems provides information about the weak molecular interactions in the liquid state. The volumetric effects observed in aqueous solutions of electrolytes are due to the interactions of the ions with solvent water, i.e., the solvation effects known as electrostriction of water. The density and volumetric properties of water [6-14] have been extensively measured and discussed in the literature but the properties of aqueous solutions of nitrates of metals have been rarely investigated. In the aqueous reprocessing of spent nuclear fuel, the aqueous nitrates of U, Pu and fission products are treated with the solvent, Tributyl phosphate (TBP) to separate U and Pu from the fission products. The volumetric properties of aqueous nitrates of fission products and the solvation effects play an important role in the retention of fission products in the aqueous phase. Hence, the volumetric properties of some of the major fission products, cesium and strontium (heat emitters), rubidium, yttrium and an important nuclear material, gallium have been measured and reported in this Chapter. This study was carried out with natural non-radioactive solutes. As most of the volumetric investigations of aqueous solutions reported in the literature focus on estimating the volume of solutes at infinite dilution, the present study aims at the measurement of concentration and temperature dependence on the volume of aqueous nitrate solutions of simulated fission product elements, which will help us to understand the interactions in complex aqueous systems. The variation of the cubic expansion coefficient with concentration and the structure making and structure breaking behaviour of the solutes have also been discussed.

4.2 OVERVIEW OF EARLIER WORK

Spedding et al. [15] measured specific gravity and apparent molal volumes of aqueous solutions of 14 rare earth salts over the concentration range of about 0.002 to 0.2 m. They had prepared chloride and nitrate salt solutions by dissolving the oxides in pure acids. The apparent molal volumes showed significant deviation from the simple limiting law at low concentrations. They did not observe a smooth variation of partial molal volumes at infinite dilution with ionic radius of the cations for either of the anion series. They found out that the values for partial molal volume at infinity dilution decreased with decreasing ionic radius from La to Nd and from Tb to Yb, but from Nd to Tb the values increased with decreasing ionic radius.

Spedding et al. [16] prepared aqueous solutions of La, Nd, Gd and Lu perchlorate, Pr, Sm, Eu, Gd, Tb, Dy, Ho, Tm and Lu nitrate and Eu, Tm and Lu chloride in the concentration range 0.0015 to about 0.15 m at 298 K. They had measured specific gravities using a magnetically controlled float and calculated apparent molal volumes.

The concentration dependence of the apparent molal volumes showed significant deviation from the simple limiting law at the lowest concentrations measured. The behaviour exhibited in the plot of apparent molal volume at infinity dilution of a rare earth anion series against rare earth ionic radius upheld their observation in their earlier work [15]. In a later work Spedding et al. [17] measured the densities of aqueous solutions of La, Pr, Nd, Sm, Gd, Tb, Dy, Ho, Er, Yb and Lu nitrates from approximately 0.03 m to saturation at 298 K with an accuracy of ± 3×10^{-5} $g.cm^{-3}$ by pycnometric method. They had fitted the densities into empirical equations and apparent molal volumes in semi-empirical equations. The partial molal volumes were calculated and compared with that of the rare earth chloride and perchlorate data. The results were interpreted in terms of inner-sphere nitrate complex formation. The apparent molal volumes calculated from the densities of aqueous solutions of lanthanide perchlorates and chlorides, measured by Spedding et al. [18, 19] by pycnometric method from approximately 0.02 m to saturation at 298 K were fitted to semi-empirical equations. They had interpreted the partial molal volumes of the salt and water in terms of ion-water and ion- ion interactions.

Robert Marriott [20] carried out heat capacity and density measurements, the properties that provide insight into the mechanism by which chemical equilibria respond to changes in their environment, and also indicated how solutes interact with other solutes and solvent molecules. Partial and apparent molar properties and certain electrostatic theories useful in modelling were reported by him.

Rard [21] prepared $Eu(NO_3)_3$ stock solution from AR grade HNO_3 and Eu_2O_3 and measured the density values at 298 ± 0.05 K using a matched pair of 30.87 cm^3 single-stem pycnometers. Water density was assumed to be 0.997045 $g.cm^{-3}$. He had determined the apparent molal volumes in the concentration range 0.039961-1.1014 mol.kg^{-1}.

Atkins et al. [22] determined the apparent molar volumes of seven electrolytes by vibrating tube densitometer in non-aqueous solvent mixtures of propylene carbonate with acetonitrile, dimethoxymethane and tetrahydrofuran. Aminabhavi et al. [23] measured the densities and viscosities of ten binary and four ternary mixtures containing bromoform, bromobenzene, chlorobenzene, toluene, mesitylene and dimethylformamide at 298 K over the whole range of mixture compositions. Excess molar volumes, apparent values of excess molar viscosities and Gibbs energy of activation of flow have been calculated for these mixtures. The calculated results were fitted into a linear regression equation to estimate the parameters and the standard deviation between the calculated and the experimental data.

Bijan Das [24] reported the apparent molar volumes of six symmetrical tetra alkyl ammonium bromides, determined in (methanol + acetonitrile) binary mixtures (containing 0.2, 0.4, 0.6 and 0.8 mole fraction of acetonitrile) over the concentration range 0.005 – 0.065 mol.kg^{-1} at 298.15 K from precise density measurements. He used the non-thermodynamic, so-called extrapolation method to split the limiting apparent molar volumes into ionic contributions. The results were interpreted in terms of ion-ion and ion-solvent interactions. Further, Pitzer ion interaction approach was applied to describe the thermodynamic properties of electrolytic solutions. A comprehensive equation was generated for the thermodynamic properties of hydrochloric acid in dioxane-water mixtures over a wide temperature range. This model is claimed to reproduce the EMF values obtained experimentally. The results and implications on the Pitzer's parameters were discussed by him in the light of interionic forces.

4.3 EXPERIMENTAL

All the nitrate salts used for volumetric study were AR grade and obtained from M/s Alfa Aesar. The salts were vacuum dried and then used. In some cases the bottles were under dry nitrogen seals. They were dried in a vacuum desiccator for several days and used directly. All the solutions were freshly prepared in ASTM Grade-1 water as per ASTM D-1193 [25]. The binary electrolyte solutions were prepared on a molality basis (~0.0005 to ~ 1.5 m). All weighing were made with a precision Shimadzu AUW220D balance (220 g, 0.01 mg resolution). Water for density standard was drawn from the water-purifier immediately before the experiments and it was degassed in an ultrasonic bath (TEC-110H) at 35 KHz for 60 s. When not in use, the solutions were kept in air-tight closed condition in a JULABO SW-22 Shaker Bath at 298.15 K. JULABO SW-22 Shaker Bath was coupled to JULABO FP-40 chiller for cooling. The ambient conditions were monitored with a Cole-Parmer hygrometer (0.1%) consisting of thermometer (0.1 K) and pressure sensor (0.1 kPa).

For density and refractive index measurements, a precise vibrating-tube densitometer (Anton Paar DMA-5000) coupled with Anton Paar ABBEMAT RXA-156 refractometer and a 30-station autosampler SP-3m was used. Densitometer and refractometer were attached to Peltier thermostats for maintaining the desired sample temperature with an accuracy of ± 0.001 K. The accuracy of all density measurements was found to be $\pm1\times10^{-6}$ $g.cm^{-3}$. Density measurements were made in complete conformation to ASTM-D4052 [26].

4.4 RESULTS AND DISCUSSION

The measured values of densities and refractive indices for aqueous solutions of $La(NO_3)_3$, $Sm(NO_3)_3$, $Ce(NO_3)_3$, $Eu(NO_3)_3$, $Pr(NO_3)_3$, $RbNO_3$, $CsNO_3$, $Sr(NO_3)_2$,

$Y(NO_3)_3$ and $Ga(NO_3)_3$ have been listed in Tables 4.1 and 4.2 respectively. The experimental value of density measured for $Eu(NO_3)_3$ was compared with the values reported by Rard [21]. Similarly the experimental density of $La(NO_3)_3$, $Pr(NO_3)_3$ and $Sm(NO_3)_3$ were compared with those values reported by Spedding et al. [15, 17]. The comparison plots are shown in Figs. 4.1 to 4.4. The experimental data are found to be in good agreement with literature values.

Table 4.1: Refractive indices and densities of aqueous solutions of La, Ce, Pr, Sm and Eu nitrates

	$La(NO_3)_3$			$Sm(NO_3)_3$			$Ce(NO_3)_3$	
m	$^{n}D_{25}$	ρ(g/cm^3)	m	$^{n}D_{25}$	ρ(g/cm^3)	m	$^{n}D_{25}$	ρ(g/cm^3)
0.0002	1.332449	0.997119	0.0002	1.332468	0.997102	0.0002	1.332588	0.997135
0.0007	1.332496	0.997293	0.0005	1.332486	0.997207	0.0009	1.332619	0.997312
0.0012	1.332497	0.997418	0.0009	1.332509	0.997293	0.0025	1.332687	0.997766
0.0043	1.332671	0.998265	0.0044	1.332662	0.998313	0.0063	1.332862	0.998814
0.0093	1.332896	0.999608	0.0091	1.332897	0.999653	0.0138	1.333199	1.000844
0.0497	1.334711	1.010413	0.0470	1.334551	1.010263	0.0562	1.335085	1.012159
0.0979	1.336758	1.023011	0.0980	1.336732	1.024475	0.0984	1.336848	1.023213
0.2449	1.342758	1.059761	0.2497	1.342847	1.064504	0.2024	1.341191	1.049458
0.5045	1.352446	1.120089	0.4972	1.352041	1.125630	0.4811	1.351600	1.114278
1.0045	1.367915	1.218730	0.9989	1.367830	1.232759	0.8941	1.364917	1.198953

	$Eu(NO_3)_3$			$Pr(NO_3)_3$	
m	$^{n}D_{25}$	ρ(g/cm^3)	m	$^{n}D_{25}$	ρ(g/cm^3)
0.0002	1.332463	0.997113	0.0003	1.332456	0.997147
0.0007	1.332490	0.997248	0.0064	1.332488	0.997265
0.0014	1.332510	0.997451	0.0018	1.332531	0.997573
0.0046	1.332680	0.998367	0.0052	1.332685	0.989121
0.0099	1.332912	0.999799	0.0111	1.332989	1.000106
0.0478	1.334521	1.010358	0.0441	1.33442	1.008915
0.0981	1.336614	1.024092	0.0965	1.336673	1.022774
0.2421	1.342327	1.062149	0.2724	1.343611	1.065519
0.4187	1.348688	1.104823	0.5142	1.352305	1.120299
			1.0311	1.368010	1.221009

Table 4.2: Refractive indices and densities of aqueous solutions of Rb, Cs, Sr, Y and Ga nitrates

RbNO$_3$			CsNO$_3$			Sr(NO$_3$)$_2$		
m	$^nD_{25}$	ρ(g/cm^3)	m	$^nD_{25}$	ρ(g/cm^3)	m	$^nD_{25}$	ρ(g/cm^3)
0.0002	1.332445	0.997082	0.0001	1.332519	0.997096	0.0001	1.332469	0.997296
0.0007	1.332442	0.997123	0.0005	1.332527	0.997155	0.0003	1.332469	0.997345
0.0014	1.332474	0.997213	0.0010	1.332527	0.997236	0.0009	1.332491	0.997441
0.0049	1.332509	0.997548	0.0055	1.332594	0.997883	0.0035	1.332561	0.997875
0.0104	1.332556	0.998139	0.0425	1.333151	1.003424	0.0091	1.332726	0.998825
0.0495	1.333001	1.002183	0.0890	1.333624	1.009773	0.0547	1.333937	1.006284
0.1019	1.333506	1.007555	0.0983	1.333766	1.011037	0.1008	1.335130	1.013930
0.2582	1.335022	1.023347	0.2552	1.335672	1.033013	0.2471	1.338811	1.037638
			0.4987	1.338458	1.066292			
			1.0012	1.343945	1.131977			

Y(NO$_3$)$_3$			Ga(NO$_3$)$_3$		
m	$^nD_{25}$	ρ(g/cm^3)	m	$^nD_{25}$	ρ(g/cm^3)
0.0001	1.332460	0.99729	0.0001	1.332461	0.997075
0.0005	1.332487	0.997396	0.0005	1.332479	0.997176
0.0009	1.332490	0.997478	0.0009	1.332545	0.997099
0.0047	1.332693	0.998349	0.0046	1.332614	0.998023
0.0098	1.332936	0.999576	0.0099	1.332849	0.999123
0.0467	1.334484	1.007924	0.0492	1.334279	1.006913
0.0996	1.336695	1.019595	0.0990	1.336212	1.016663
0.2472	1.342510	1.050939	0.2493	1.341440	1.045167
			0.4995	1.349400	1.088122
			0.9899	1.362283	1.158242

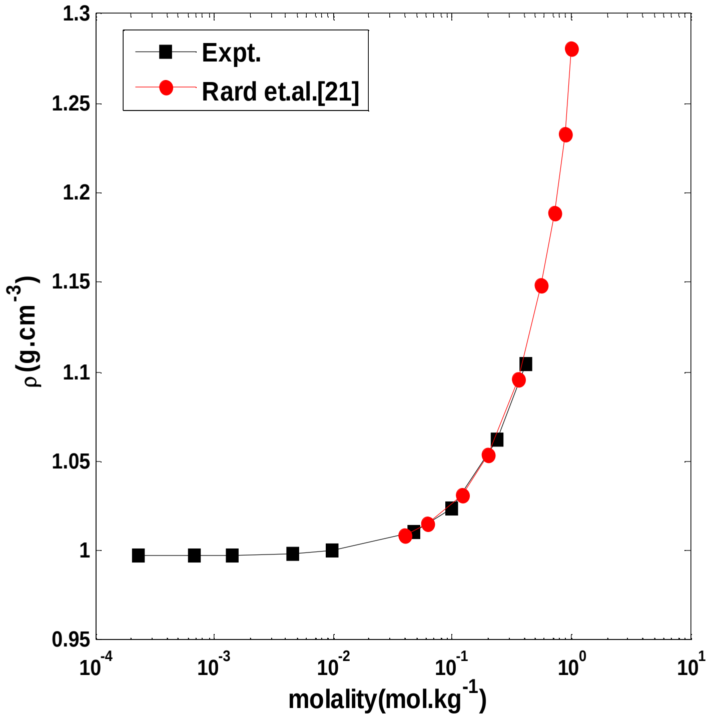

Fig. 4.1: Experimental density of $Eu(NO_3)_3$ compared with Rard et al. [21]

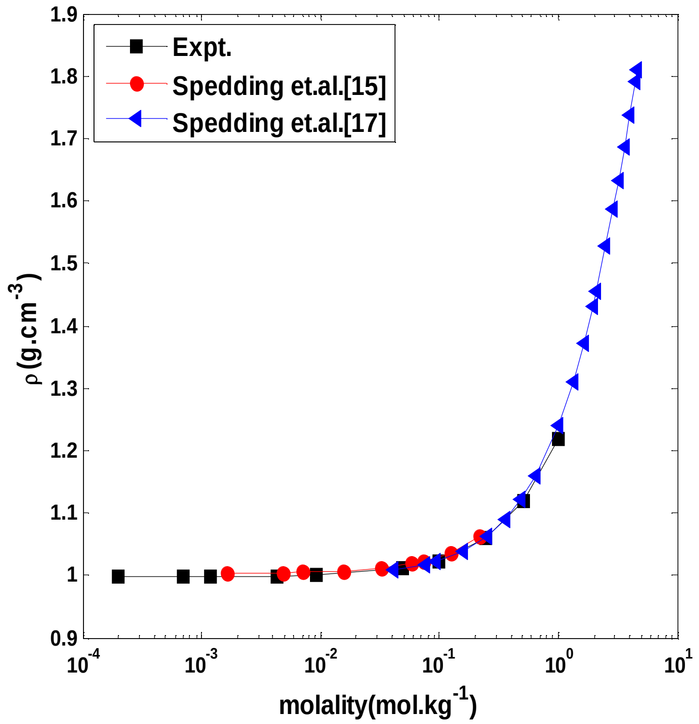

Fig. 4.2: Plot showing comparison of experimental density of $La(NO_3)_3$ with Spedding et al .[15, 17]

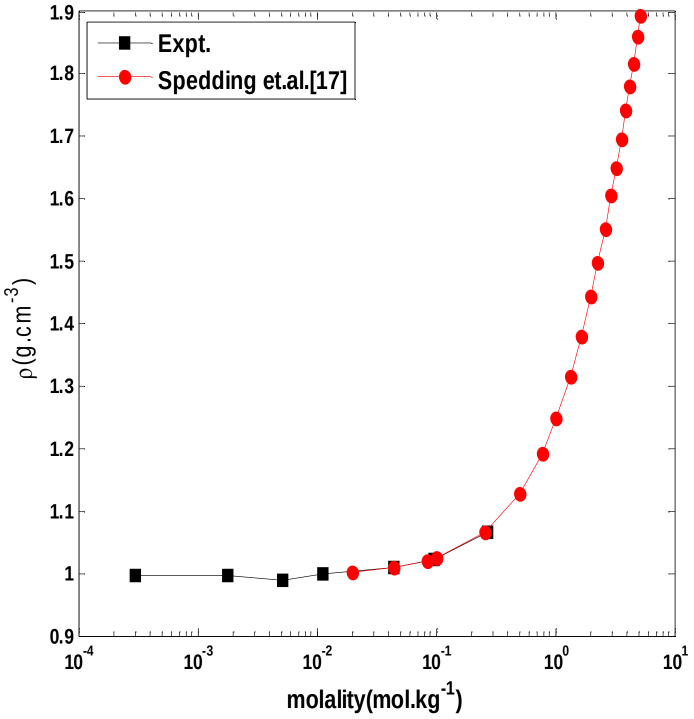

Fig. 4.3: Graph of experimental density of $Pr(NO_3)_3$ compared with Spedding et al.[17]

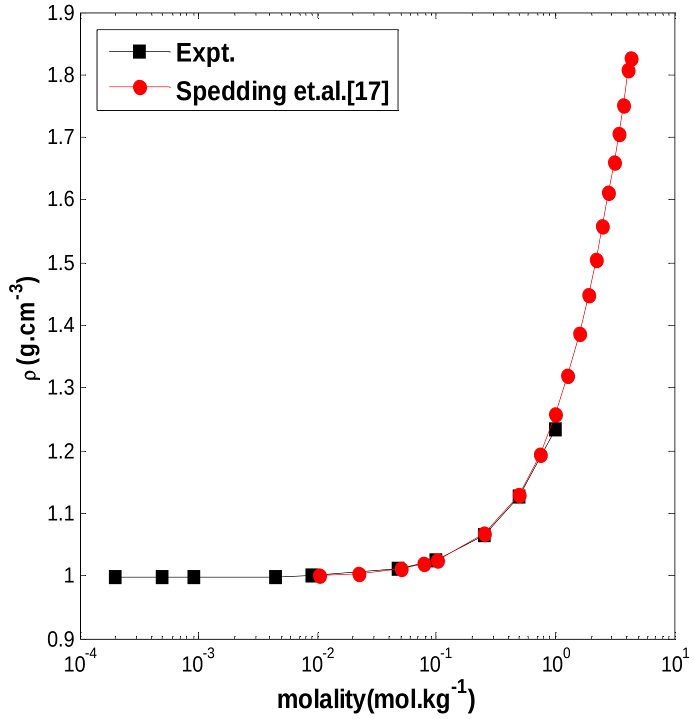

Fig. 4.4: Comparison of experimental density of $Sm(NO_3)_3$ with Spedding et al.[17]

In complex multi-component systems such as solutions, it becomes easy to describe the system in terms of the intrinsic or molal properties rather than the extrinsic properties. In general, any partial molal property, $\overline{Y}_i$, can be defined as

$$\overline{Y}_i = \left(\frac{\partial Y}{\partial n_i}\right)_{n_{j\neq i},T,p} \tag{4.1}$$

Interactions with other species contribute to partial molal properties. Hence, when dealing with solutions, it is more common to measure the apparent molal quantities, $Y_{2,\varphi}$, which can be defined as the change in property Y due to a known amount of solute in a known amount of solvent, assuming the solvent contributes the same as it would if it exists in its pure form. The apparent molal property of any solute, $Y_{2,\varphi}$, can be defined as

$$Y_{2,\varphi} = \frac{Y - n_1\overline{Y}_1^0}{n_2} \tag{4.2}$$

The apparent molal volume of solutes (designated as 2) in solutions at T = 298.15 K was calculated using the following equation:

$$\mathrm{V}_{2,\phi} = \frac{1000}{m\rho\rho^0}(\rho^0 - \rho) + \frac{M_2}{\rho} \tag{4.3}$$

where, $V_{2,\phi}$ is the apparent molal volume, m is the molality, M_2 is the molecular weight of the solute and ρ^0 and ρ are the densities of water and the solution, respectively.

The calculated apparent molal volume was correlated with Masson equation [27] as follows:

$$V_{2,\phi} = V_{2,\phi}{}^{0} + a_v\sqrt{m} \tag{4.4}$$

where, $V_{2,\phi}{}^{0}$ is the limiting apparent molal volume, also known as partial molal volume of the solvent, m is the molality and a_v is an empirical constant determined from experimental results. The slope of the plot between $V_{2,\phi}$ and $\sqrt{m}$ gives the value of a_v, which represents solute-solute interaction and the intercept gives the value of $V_{2,\phi}{}^{0}$, which represents solute-solvent interaction.

The $V_{2,\phi}{}^{0}$ values thus, obtained for rare earth nitrates were compared in Table 4.3 with literature values [16, 17, 28-30] and those of Rb, Cs, Sr, Y and Ga nitrate were compared with the data reported by Millero [28] at 298.15 K in Table 4.4. A good agreement was found between the experimental and literature values.

Table 4.3: Comparison of experimental $V_{2,\varphi}{}^{0}$ ($cm^3.mol^{-1}$) values of rare earth nitrates with literature

Solute	$V_{2,\phi}{}^{0}$ Expt.	$V_{2,\phi}{}^{0}$ Spedding et al. [16]*	$V_{2,\phi}{}^{0}$ Spedding et al. [17]	$V_{2,\phi}{}^{0}$ Millero [28]	$V_{2,\phi}{}^{0}$ Marriott et al. [29]	$V_{2,\phi}{}^{0}$ Hakin et al. [30]
$Ce(NO_3)_3$	45.76	-	-	-	-	-
$La(NO_3)_3$	48.69	-	49.49	47.90	49.16	-
$Pr(NO_3)_3$	44.15	45.46	45.52	44.47	46.03	46.97
$Sm(NO_3)_3$	45.65	45.86	45.99	44.67	46.57	-
$Eu(NO_3)_3$	45.18	46.87	-	-	46.85	-

*calculated using the Owen-Brinkley equation

Table 4.4: Comparison of experimental $V_{2,\varphi}^{0}$ ($cm^3.mol^{-1}$) values of nitrates of Rb, Cs, Sr, Y and Ga with literature

Electrolyte	$V_{2,\phi}^{0}$ This work	$V_{2,\phi}^{0}$ Millero [28]
$RbNO_3$	42.90	43.07
$CsNO_3$	50.53	50.34
$Sr(NO_3)_2$	39.89	39.84
$Y(NO_3)_3$	33.61	-
$Ga(NO_3)_3$	40.89	-

The variation of $V_{2,\phi}$ with concentration for different electrolytes is shown in Figs. 4.5 to 4.14. Positive value of $V_{2,\phi}^{0}$ indicates the existence of solute-solvent interactions which increase with increase in concentration.

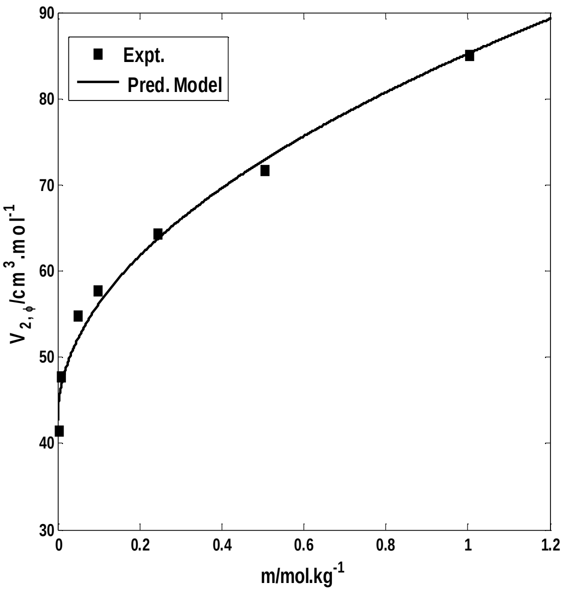

Fig. 4.5: Variation of apparent molal volume of $La(NO_3)_3$ with concentration at 298.15 K

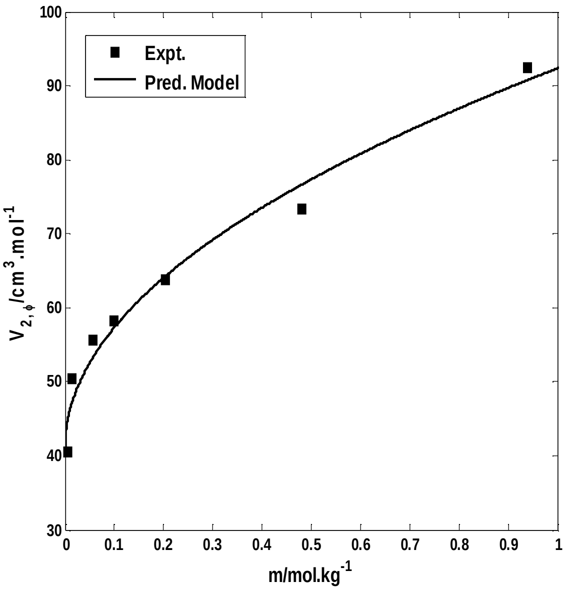

Fig. 4.6: Apparent molal volume of $Ce(NO_3)_3$ as a function of concentration at 298.15 K

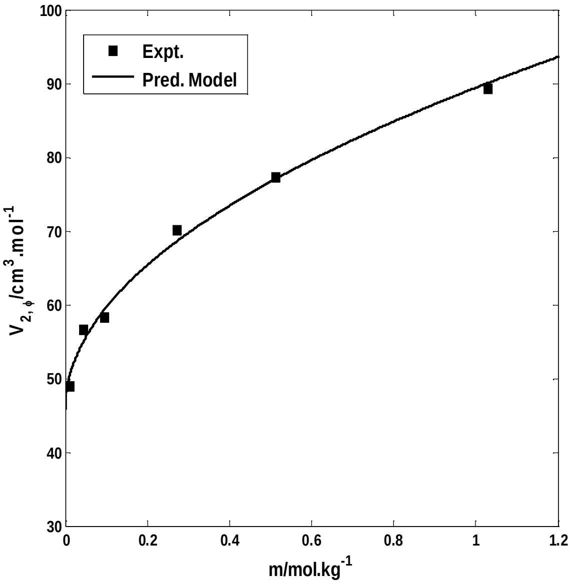

Fig. 4.7: Plot of apparent molal volume of $Pr(NO_3)_3$ vs. concentration at 298.15 K

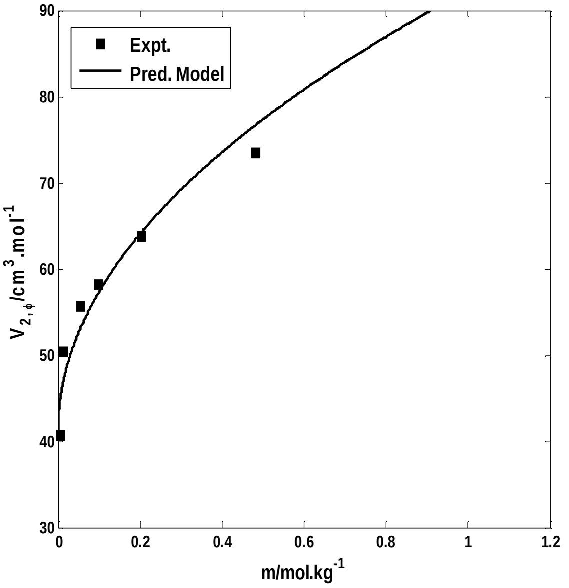

Fig. 4.8: Variation of apparent molal volume of $Sm(NO_3)_3$ with concentration at 298.15 K

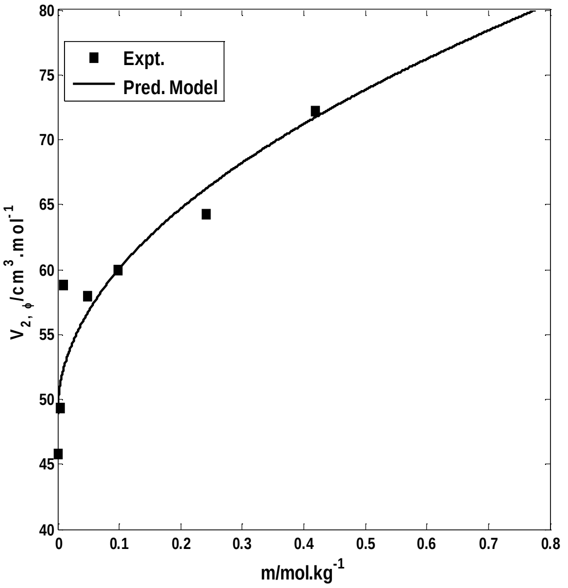

Fig. 4.9: Concentration dependence of apparent molal volume of $Pr(NO_3)_3$ at 298.15 K

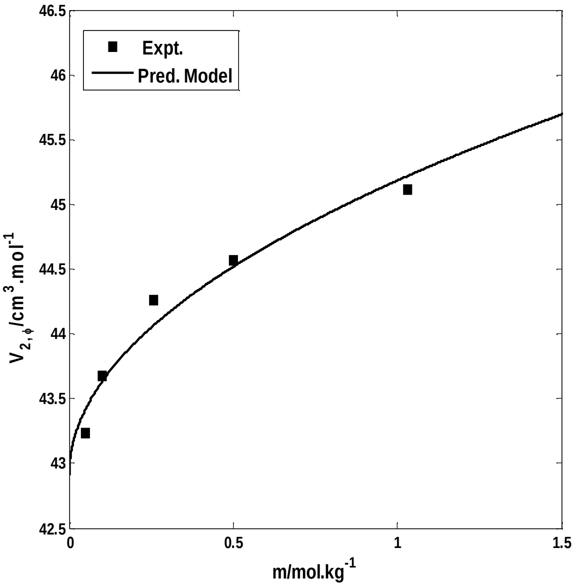

Fig. 4.10: Effect of concentration on apparent molal volume of $RbNO_3$ at 298.15 K

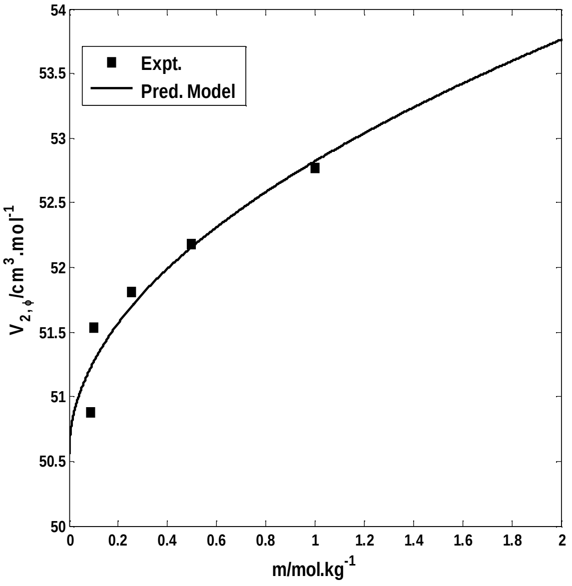

Fig. 4.11: Plot of variation of apparent molal volume of $CsNO_3$ with concentration at 298.15K

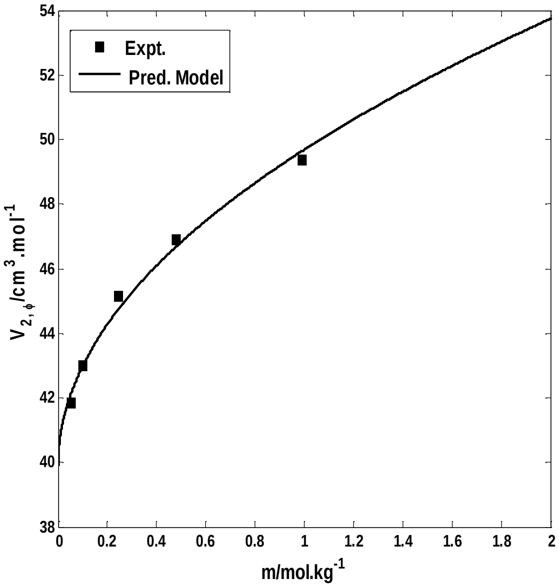

Fig. 4.12: Apparent molal volume of $Sr(NO_3)_2$ as a function of concentration at 298.15 K

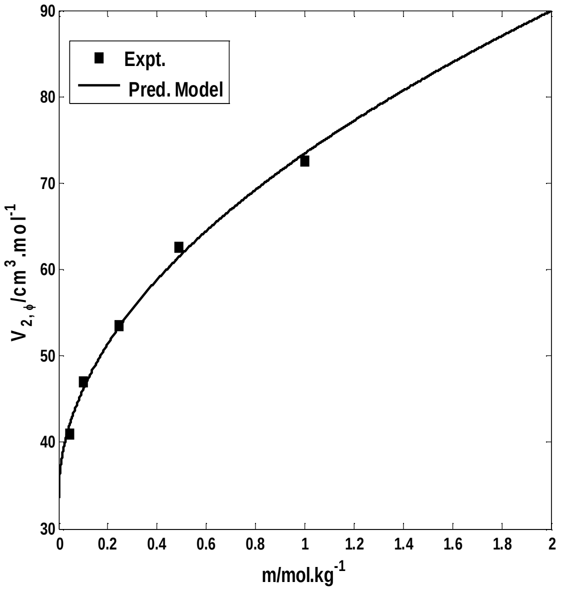

Fig. 4.13: Variation of apparent molal volume of $Y(NO_3)_3$ with concentration at 298.15 K

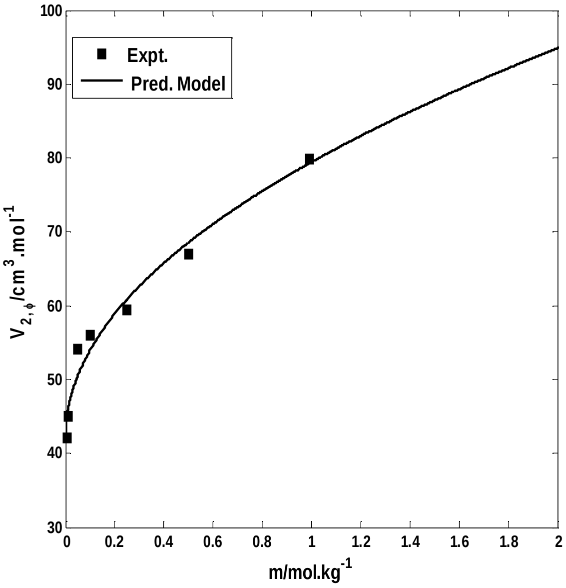

Fig. 4.14: Concentration dependence of apparent molal volume of $Ga(NO_3)_3$ at 298.15 K

The density was correlated by the following equation [31]

$$\frac{\rho}{\rho^0} = 1.00 + a_0 m + b_0 m^{1.5} \tag{4.5}$$

where $a_0 = \dfrac{M_2 - \rho^0 \times V_{2,\phi}{}^0}{10^3}$ (4.6)

and $b_0 = -\dfrac{a_0}{10^3}$ (4.7)

The density of ASTM Grade-I water at 298.15 K was taken as 0.997043 g.cm^{-3}. The regressed coefficients of density for the electrolytes under study are shown in Table 4.5.

Table 4.5: Regressed coefficients of density for different electrolytes at 298.15 K

Electrolyte	a_0	b_0	Std.dev.
$Ce(NO_3)_3$	0.2818	-0.0412	0.0024
$La(NO_3)_3$	0.2854	-0.0462	0.0188
$Pr(NO_3)_3$	0.2798	-0.0424	0.2856
$Sm(NO_3)_3$	0.2983	-0.0435	0.0148
$Eu(NO_3)_3$	0.2946	-0.0434	0.0141
$RbNO_3$	0.1046	-0.0018	0.0014
$CSNO_3$	0.1450	-0.0024	0.0090
$Sr(NO_3)_2$	0.1716	-0.0090	0.0125
$Y(NO_3)_3$	0.2403	-0.0386	0.0145
$Ga(NO_3)_3$	0.2196	-0.0447	0.0232

The refractive index and apparent molar refraction of some aqueous rare earth nitrates were reported for selected wave lengths of the helium and mercury spectra [32], but the values for sodium D-line have not been reported. In the present work the refractive indices related to sodium D-line were measured for different aqueous nitrate salt solutions and reported in Tables 4.1 and 4.2. The experimentally determined refractive index values of nitrate salt solution were correlated to the following equation,

$$nD = nD_w + am + bm^2 \tag{4.8}$$

where, nD is the predicted refractive index of solution and nD_w is the refractive index of water used for the preparation of solutions and its value is found to be 1.3325. *m* is molality and 'a' and 'b' are coefficients of Eq. (4.8). The regressed coefficients are reported in Table 4.6. The refractive indices at 298.15 K were observed to increase with increasing concentration.

Table 4.6: Regressed coefficients of refractive index for different electrolytes at 298.15 K

Electrolyte	a	b
$Ce(NO_3)_3$	0.0439	-0.0086
$La(NO_3)_3$	0.0441	-0.0088
$Pr(NO_3)_3$	0.0431	-0.0084
$Sm(NO_3)_3$	0.0434	-0.0081
$Eu(NO_3)_3$	0.0435	-0.0113
$RbNO_3$	0.0102	-0.0009
$CSNO_3$	0.0125	-0.0011
$Sr(NO_3)_2$	0.0263	-0.0028
$Y(NO_3)_3$	0.0421	-0.0076
$Ga(NO_3)_3$	0.0379	-0.0078

The cubic expansion coefficient (thermal isobaric expansibility) is given as

$$\alpha = \left(\frac{\partial \ln V}{\partial T}\right)_P = -\left(\frac{\partial \ln \rho}{\partial T}\right)_P \tag{4.9}$$

Applying Maxwell's relation to the differential of enthalpy,

$$dH = C_p dT + \left[V - T\left(\frac{\partial V}{\partial T}\right)_P\right] dP \tag{4.10}$$

Volumetric and thermal properties of a solution can be related as

$$\left(\frac{\partial C_p}{\partial P}\right)_T = -T\left(\frac{\partial^2 V}{\partial T^2}\right)_P \tag{4.11}$$

where, C_p is the isobaric heat capacity of the solutions.

In terms of cubic expansion coefficient, Eq. (4.11) can be written as

$$T\left(\frac{\partial^2 V}{\partial T^2}\right)_{P,m} = TV\left[\alpha^2 + \left(\frac{\partial \alpha}{\partial T}\right)_{P,m}\right] \tag{4.12}$$

The L.H.S of Eq. (4.12), i.e. $T\left(\frac{\partial^2 V}{\partial T^2}\right)$ can be directly expressed in terms of density as

$$T\left(\frac{\partial^2 V}{\partial T^2}\right)_{P,m} = T\left(\frac{1000 + mM_2}{\rho^2}\right) \times \left[\frac{2}{\rho}\left(\frac{\partial \rho}{\partial T}\right)^2_{P,m} - \left(\frac{\partial^2 \rho}{\partial T^2}\right)_{P,m}\right] \tag{4.13}$$

where, $\left(\frac{1000 + mM_2}{\rho^2(T,m)}\right)$ is the volume of the solution.

The cubic expansion coefficient can be used to interpret the ion-solvent interactions [33]. Variation of the cubic expansion coefficient with concentration at 298.15 K for different nitrate salt solutions is shown in Figs. 4.15 and 4.16.

It is evident from Figs. 4.15 and 4.16 that the nitrates of rubidium, cesium, strontium, yttrium and the lower lanthanides (La, Ce, Pr) follow the same trend while gallium, samarium and europium nitrates followed a different trend. The dissimilar behaviour shown by gallium, samarium and europium nitrates may be ascribed to the absence of ‘caging effect’ [34].

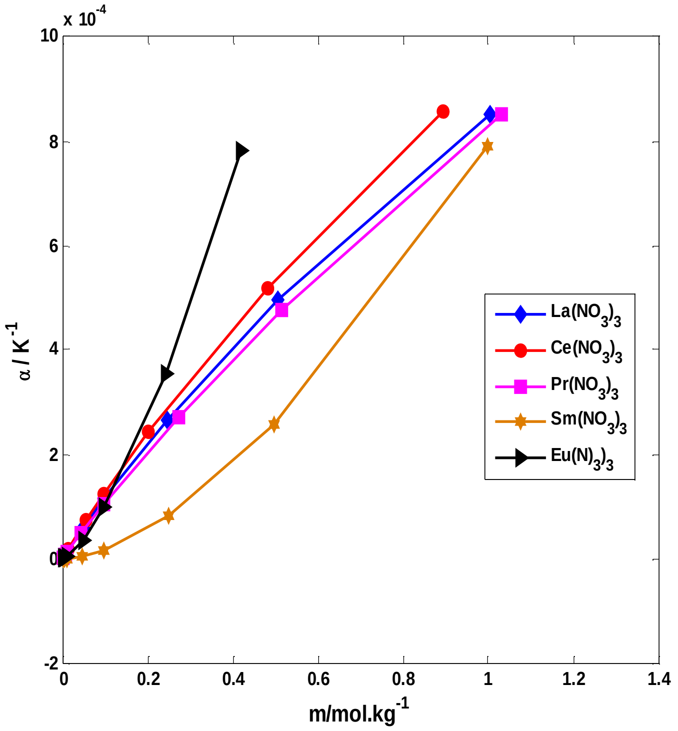

Fig. 4.15: Variation of cubic expansion coefficient of rare earth nitrates with concentration at 298.15K

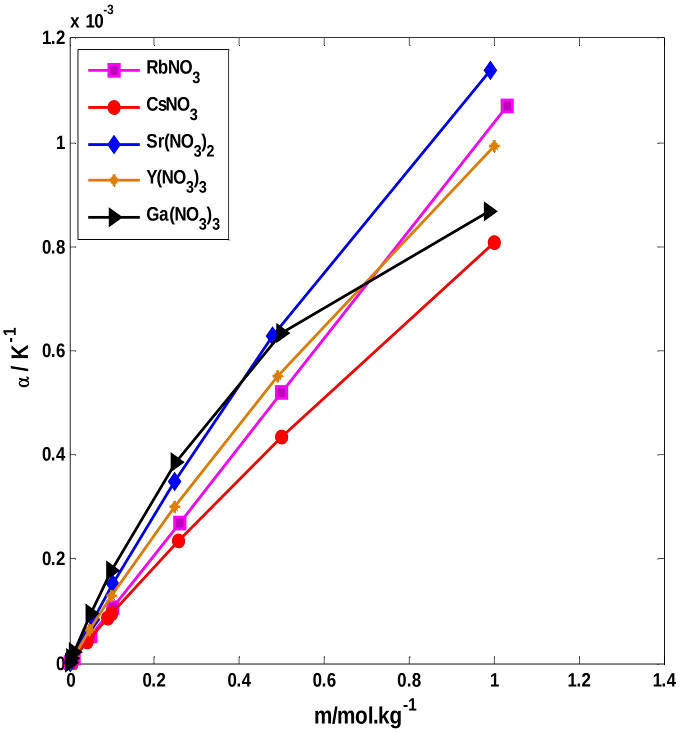

Fig. 4.16: Plot of cubic expansion coefficient of Rb, Cs, Sr, Y and Ga nitrates with concentration at 298.15 K

In the last decade, many researchers have emphasized that a_v is not the sole criterion for determining the structure making or breaking nature of any solute [35-38]. Hepler [38] has developed a technique for examining the sign of ($\partial^2V/\partial T^2$) for various solutes in terms of long range structure making or breaking capacity in aqueous solutions using the thermodynamic relation given in Eq. (4.13).

The variation of second derivative of volume at 298.15 K at different concentrations of aqueous nitrate salt solutions of lanthanides and Rb, Cs, Sr, Y and Ga are shown in Figs. 4.17 and 4.18 respectively.

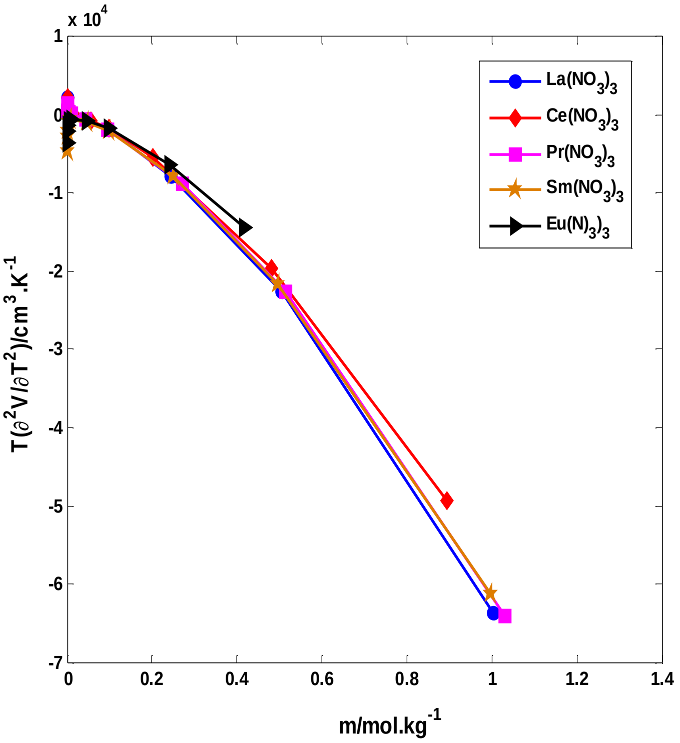

Fig. 4.17: Variation of $T(\partial^2V/\partial T^2)$ of rare earth nitrates with concentration at 298.15 K

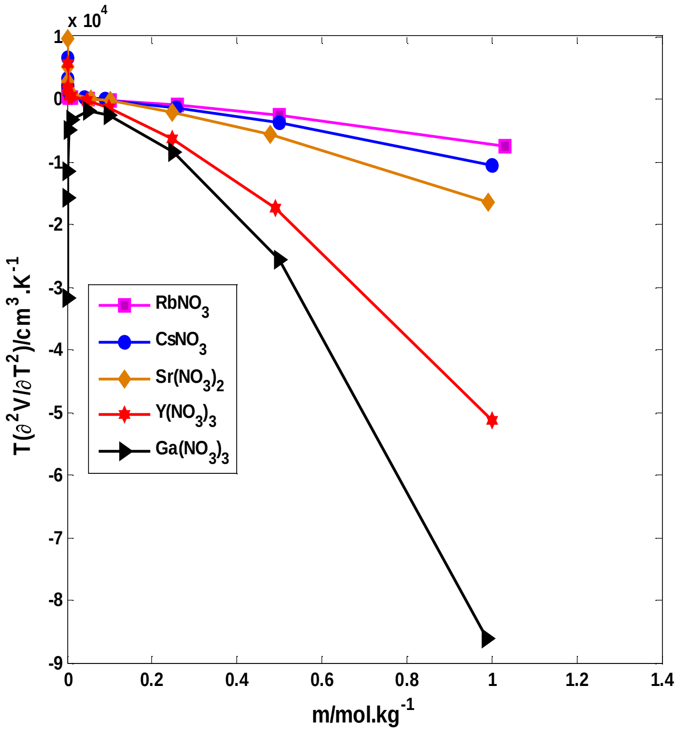

Fig. 4.18: Plot of $T(\partial^2V/\partial T^2)$ for Rb, Cs, Sr, Y and Ga nitrates with concentration at 298.15 K

On the basis of Hepler’s assumption, those solutes for which the second derivative of volume with temperature is negative or the first derivative of isobaric heat capacity with pressure is positive are expected to act as structure breakers and vice-versa.

The variation of second derivative of volume at 298.15 K and at different concentrations was found to be positive for Rb, Cs, Sr, Y, La, Ce and Pr nitrates at lower concentrations and negative for higher concentrations which implies that these nitrate salts act as structure makers at lower concentrations and as the concentration increases they act as structure breakers. As the variation is negative for all concentrations in the case of nitrates of gallium, samarium and europium, they act as structure breakers throughout the concentration range considered in the present study.

SUMMARY

In this Chapter, densities, refractive indices and volumetric properties of aqueous solutions of nitrates of rubidium, cesium, strontium, yttrium, gallium, cerium, lanthanum, praseodymium, europium, and samarium are reported at 298.15 K. Using the measured density values, apparent molal volume was calculated and correlated with Masson equation. The apparent molal volumes at infinite dilution and the experimental slope of Masson equation have been interpreted in terms of ion-solvent and ion-ion interactions, respectively. The apparent molal volume calculated at infinite dilution was also compared with the data reported in literature. Such a comparison facilitated the checking of the internal consistency of the measurements presented in this study.

The cubic expansion coefficient or the coefficient of thermal isobaric expansibility was calculated from the variation in density at 298.15 K. The variation of cubic expansion coefficient with concentration was also evaluated. It was observed that the cubic expansion coefficient increased with increasing concentration for all the aqueous nitrate solutions at 298.15 K. The variation in the second derivative of volume against concentration at 298.15 K and at constant pressure was calculated for predicting the structure maker and structure breaker behaviour of the electrolytes. Apparent molal volume, partial molal volume of the solvent, cubic expansion coefficient etc. of the aqueous solutions of nitrates have been discussed in terms of ionic contribution.

REFERENCES

1. C.W. Zhao, P.S. Ma, J.D. Li, J. Chem. Thermodyn., 37 (2005) 37
2. M.L. Parmer, D.S. Banyal, Indian J. Chem., 44A (2005) 1582
3. W.J. Crooks, J.D. Christian, Indian J. Chem., 43A (2004) 1872
4. E.G. Paneda, P. Guardado, A. Mastre, J. Soln. Chem., 33 (2004) 1277
5. Man Singh, J. Chem. Sci., 118 (2006) 269
6. M.L. Parmer, S.C. Attri, J. Mol. Liq., 136 (2007) 38
7. D.M. Swenson, E.M. Woolley, J. Chem. Thermodyn., 40 (2008) 54
8. R.E. Gibbson, O.H. Loeffler, J. Am. Chem. Soc., 70 (1948) 966
9. B.B. Owen, J.R. White, S. Smith, J. Am. Chem. Soc., 78 (1956) 3561
10. F. Steckel, S. Szapiro, Trans. Faraday Soc., 59 (1963) 331
11. W. Gildseth, A. Habenschuss, F.H. Spedding, J. Chem. Eng. Data, 17 (1972) 402
12. G.S. Kell, J. Chem. Eng. Data, 20 (1975) 97
13. G.S. Kell, J. Phys. Chem. Ref. Data, 6 (1977) 1109
14. C.T. Chen, R.A. Fine, F.J. Millero, J. Chem. Phys., 66 (1977) 2142
15. F.H. Spedding, M.J. Pikal, B.O. Ayers, J. Phys. Chem., 70 (1966) 2440
16. F.H. Spedding, P.F. Cullen, A. Habenschuss, J. Phys. Chem., 78 (1974) 1106

17. F.H. Spedding, L.E Shiers, M.A. Brown, J.L. Baker, L. Guitierrez, L.S. McDowell, A. Habenschuss, J. Phys. Chem., 79 (1975) 1087
18. F.H. Spedding, L.E. Shiers, M.A. Brown, J.L. Derer, D.L. Swanson, A. Habenschuss, J. Chem. Eng. Data, 20 (1975) 81
19. F.H. Spedding, V.W. Saeger, K.A. Gray, P.K. Boneau, M.A. Brown, C.W.D.J.L. Baker, L.E. Shiers, H.O. Weber, A. Habenschuss, J. Chem. Eng. Data, 20 (1975) 72
20. R. Marriott, Ph.D. Thesis, University of Lethbridge, Lethbridge, Alberta (1999)
21. J.A. Rard, J. Chem. Eng. Data, 32 (1987) 92
22. P. Atkins, G.T. Hefter, P. Singh, J. Soln. Chem., 20 (1991) 1059
23. T.M. Aminabhavi, S.S. Joshi, R.H. Balundgi, S.S. Shukla, Can. J. Chem., 69 (1991) 1028
24. Bijan Das, Can. J. Chem., 83 (2005) 2032
25. ASTM Standard D-1193, Specification for Reagent Water (2006)
26. ASTM Standard D-4052, Standard Test Method for Density and Relative Density of Liquids by Digital Density Meter (2002)
27. D.O. Masson, Phil. Mag., 79 (1929) 218
28. F.J. Millero, Chem. Rev., 71 (1971) 147
29. R.A. Marriot, A.W. Hakin, J.A. Rard, J. Chem. Thermodyn., 33 (2001) 643
30. A.W. Hakin, J.L. Liu, K. Erickson, J-V. Munoz, J.A. Rard, J. Chem. Thermodyn., 37 (2005) 153

31. S. Kumar, S.B. Koganti, J. Nucl. Sci. Technol., 34 (1997) 410

32. F.D. Leipziger, J.E. Roberts, J. Phys. Chem., 62 (1958) 1014

33. S. Cabani, G. Cont, E. Matteoli, J. Soln. Chem., 5 (1976) 751

34. F.J. Millero, “Structure and transport processes in water and aqueous solutions”, R.A. Horne, ed., Wiley Interscience, New York (1971) Chapter 15, pp. 622

35. M. Ben-Hamo, A. Apelblat and E. Manzurola, J. Chem. Thermodyn., 39 (2007) 1071

36. M.L. Parmer, D.S. Banyal, Indian J. Chem., 48A (2009) 1667

37. A. Apelblat, E. Manzurola, J. Chem. Thermodyn., 31 (1999) 869

38. L.G. Hepler, Can. J. Chem., 47 (1969) 4613

CHAPTER 5

TEMPERATURE DEPENDENCE OF VOLUMETRIC CHANGE AND STRUCTURAL INTERACTIONS IN AQUEOUS NITRATE SOLUTIONS

CHAPTER 5

TEMPERATURE DEPENDENCE OF VOLUMETRIC CHANGE AND STRUCTURAL INTERACTIONS IN AQUEOUS NITRATE SOLUTIONS

5.1 INTRODUCTION

The study of thermophysical properties of dilute aqueous electrolytes is of great importance in understanding the various interactions and the associated energies in aqueous solutions relevant to industrial, environmental and geochemical issues. Rare-earths that are produced in the fission of nuclear fuels such as U and Pu act as reactivity poisons [1]. In the aqueous route of reprocessing of nuclear spent fuels by the PUREX process to separate U and Pu from the fission products, the fuel along with its clad is chopped and dissolved in nitric acid, followed by solvent extraction with diluted Tri-butyl Phosphate (TBP). The aqueous phase resulting after the solvent extraction step contains the nitrates of all fission products and it is called as High Active Waste (HAW). The solvent TBP does not extract tri-valent actinides and lanthanides and hence, they follow the HAW path. Group partitioning methods are used to mutually separate these groups of elements. In the post-PUREX process, volumetric properties of solutes like density contributions of aqueous and organic species are exploited for precise modeling of solvent extraction.

When an electrolyte is added to water, it will dissociate into cations and anions, which will be surrounded by water molecules as well as the counter ions and the electrolyte solution will no longer behave as an ideal solution. The nonideality of the electrolyte solutions is attributed predominantly to the interactions of water–ion and ion–ion. For an understanding of the volumetric properties, detailed investigation of the structural interactions is required. The theory of molal volume has been discussed in the reviews by Redlich [2], Harned and Owen [3] and Redlich and Meyer [4]. Millero [5, 6] has discussed the partial molal volume at infinite dilution in detail and reported extensive data on partial molal volume [6].

The densities and apparent molal volumes of electrolytic solutions are widely used in the study of thermodynamic and transport properties. These properties include compressibility, expansibility, viscosity, conductivity and many more. The density data are required in mass balance and mass transfer calculations as well as in the designing of solvent extraction apparatus for the separation of organic and aqueous phases. The thermophysical properties of aqueous solutions provide information about molecular interactions present in the liquid state [7]. Experimental data on the physical properties such as density and refractive index are required for a complete understanding of the thermodynamic properties of aqueous solution as well as for practical chemical engineering work [8-12]. The influence of temperature on volumetric properties of aqueous solutions has been evaluated to obtain information about the structural effect of solute on the structure of water. The temperature dependence of partial molal volume at infinite dilution can be discussed in terms of solute hydration and a balance between different structural interactions between solute and water.

The thermodynamic [13-17], transport [18-20] and spectral [21-25] properties of the rare earth cations in aqueous solutions indicate that these properties are not smooth functions of ionic radii. The apparent molal volumes of dilute rare earth chlorides, perchlorates and nitrates at 298.15 K were reported by Spedding et al. [17, 26-29]. Chlorides and perchlorates are reported to form outer-sphere complexes with rare earth ions, while nitrate ion forms inner-sphere complex [30-45]. The volumetric effects due to different interactions occurring in the aqueous nitrate solutions have been investigated and discussed in this Chapter.

5.2 OVERVIEW OF EARLIER WORK

Extensive studies have been carried out on rare earth salt solutions at near ambient temperature and at ambient pressure [16, 17, 46-56]. In Chapter 4, the density, refractive index and volumetric properties of aqueous solutions of nitrates of rubidium, cesium, strontium, yttrium, gallium, cerium, lanthanum, praseodymium, europium, and samarium have been measured and reported at 298.15 K and 0.1 MPa. Studies have also been conducted at temperatures and pressures other than the ambient conditions [54, 57, 58].

Hakin et al. [46] measured the relative density and heat capacities of aqueous solutions of perchlorates of Y, Yb, Dy and Sm at the temperatures 288.15, 298.15, 313.15 and 328.15 K and at the pressure of 0.1 MPa using a Sodev 02D Vibrating Tube Densitometer. The measured properties were used to calculate apparent molar volume and apparent molar heat capacities of the perchlorate salt solution after incorporating a correction factor for the presence of acid. The calculated apparent molar properties were modeled at each temperature using Pitzer ion interaction equations to find out the apparent molar volume and apparent molar heat capacities at infinite dilution. Hakin et al. [47] also reported the experimental apparent molar volume and apparent molar heat capacities of the acidified aqueous solutions of chlorides of Y, Yb, Dy, Sm and Gd at T = 288.15, 298.15, 313.15 and 328.15 K and P = 0.1 MPa, which data were used in conjuction with Young's rule to calculate the apparent molar properties of the aqueous chloride salt solutions. The concentration dependence of apparent molar properties had been modeled using Pitzer ion interaction equation to find out apparent molar volumes and heat capacities at infinite dilution, which in turn were used to calculate single ion activity coefficients.

In a later work, Hakin et al. [48] measured the relative densities of the perchlorate solutions of Pr, Gd, Ho and Tm at the temperatures 288.15, 298.15, 313.15 and 328.15 K and at 0.1 MPa pressure using a Sodev O2D vibrating tube densitometer and relative massic heat capacities were measured at the same temperatures and pressure using a Picker flow microcalorimeter. Apparent molar volume and apparent molar heat capacities of the acidified salt solutions were calculated from the relative density and relative massic heat capacities from which the apparent molar properties of the salt solutions were derived by the application of Young's rule. The concentration dependence of the apparent molar properties was modeled using Pitzer ion-interaction equations to calculate the apparent molar properties at infinite dilution. The apparent molar volume and apparent molar heat capacities of the acidified solutions of nitrates of Pr, Gd, Ho and Y at T = 288.15, 298.15, 313.15 and 328.15 K and P = 0.1 MPa were calculated by Hakin et al. [49] and the concentration dependence of apparent molar properties of the aqueous nitrate solutions was studied by Pitzer ion-interaction equation The complex formation within the aqueous rare earth nitrate systems was discussed qualitatively from the concentration dependence of apparent molar volume and heat capacities.

Xiao et al. [54] measured the densities of aqueous solutions of $La(CF_3SO_3)_3$ and $Gd(CF_3SO_3)_3$ at the temperatures 278, 298 and 318 K and Pressures 1.0, 7.0, 30.0 MPa using vibrating tube densitometer. The apparent molar volumes obtained from density data were fitted into Pitzer equation. The standard partial molar volumes and the ion-interaction parameters had been determined by least square fitting of the experimental results. The standard partial molar volume of the anion was calculated at 298 K and 0.1 MPa from the partial molar volume of the cations.

Xiao et al. [55] estimated the apparent molar volume and apparent molar heat capacities of lanthanum chloride and perchlorates of lanthanum and gadolinium at T = 283, 298, 313, 328, 338 K from the results obtained by using a Picker flow microcalorimeter and a vibrating tube densitometer. The results were analysed by Pitzer equation to predict the standard partial molar volume and heat capacities and expression for excess properties. The temperature dependence of standard partial molar properties had been represented by a modified HKF model.

The apparent molar volumes and apparent molar heat capacities of perchlorates of Nd, Eu, Er and Yb had been measured by Xiao et al. [59] at the temperatures 283.2, 298.2, 313.2 and 328.2 K. The results were analysed by means of Pitzer equation to derive standard partial molar properties. Modified HKF model had been used to represent the temperature dependence of the standard molar properties within the experimental scatter.

The relative densities of the acidified aqueous solutions of ytterbium perchlorate were studied by Hakin et al. [57] at T = 348.15, 373.15, 398.15 and 423.15 K and P =10.0, 20.0 and 30.0 MPa using an optically coupled vibrating tube densitometer. The experimental apparent molar volume had been calculated from the density measurements and the apparent molar volume for aqueous perchlorate salts had been calculated using Young’s rule. The apparent molar volume at infinite dilution was calculated using Pitzer ion-interaction equations and the results had been compared with those values calculated using HKF equation of state.

The densities of aqueous solutions of $Gd(CF_3SO_3)_3$ at T = 373, 423 and 473 K and pressure 7.0 and 26.0 MPa were measured and reported by Xiao et al. [58] using a vibrating tube densitometer. The temperature and pressure dependence of the standard partial molar volume and the virial coefficients in the Pitzer equation were expressed by empirical functions using compressibility of water as an independent variable.

5.3 EXPERIMENTAL

Analytical Reagent grade chemicals and reagents were used in this study. They were dried in a vacuum desiccator for several days and used directly. ASTM Grade-1 water as per ASTM D-1193 [60] was used in the experiments for reagent/solution preparation and as water standard. All other experimental details are described in Section 2.2 of Chapter 2.

For density measurement a precise vibrating-tube densitometer (Anton Paar DMA-5000) coupled with a 30-station autosampler SP-3m was used. Densitometer was provided with Peltier thermostats for maintaining the desired sample temperature with an accuracy of ± 0.001 K. The precision in the density measurements was found to be ± 1×10^{-6} $g.cm^{-3}$. Density measurements were made in complete conformation to ASTM-D4052 [61].

5.4 RESULTS AND DISCUSSION

The apparent molal volume of solutes (designated as 2) in the solutions at the temperature 298.15 K was calculated using the following equation:

$$\mathrm{V}_{2,\phi} = \frac{1000}{m\rho\rho^{0}}(\rho^{0} - \rho) + \frac{M_2}{\rho} \tag{5.1}$$

where $V_{2,\phi}$ is the apparent molal volume, m is the molality, M_2 is the molecular weight of the solute and ρ^0 and ρ are the densities of water and of the solution, respectively. The calculated apparent molal volume was correlated with Masson's equation [62] as follows:

$$V_{2,\phi} = V_{2,\phi}{}^{0} + a_v\sqrt{m} \tag{5.2}$$

where, $V_{2,\phi}{}^{0}$ is the limiting apparent molal volume, also known as partial molal volume, m is the molality and a_v is an empirical constant determined from experimental results. The slope of the plot between $V_{2,\phi}$ and $\sqrt{m}$ gives the value of a_v, which represents the solute-solute interaction and the intercept gives the value of $V_{2,\phi}{}^{0}$, which represents solute-solvent interaction.

Equating Eqs. (5.1) and (5.2) and rearranging, the following equation is obtained for density of the solution [63]:

$$\frac{\rho}{\rho^{0}} = 1.00 + a_0 m + b_0 m^{1.5} \tag{5.3}$$

$$\text{where } a_0 = \frac{M_2 - \rho^{0} \times V_{2,\phi}{}^{0}}{10^3} \tag{5.4}$$

$$\text{and } b_0 = -\frac{a_0}{10^3} \tag{5.5}$$

Thermodynamically, the variation in volume with temperature is given by

$$\alpha = \left(\frac{\partial \ln V}{\partial T}\right)_P = -\left(\frac{\partial \ln \rho}{\partial T}\right) \tag{5.6}$$

Upon integration, Eq. (5.6) gives

$$\frac{V_T}{V_0} = \exp\{\alpha(T - T_0)\} \tag{5.7}$$

Since $\frac{V_T}{V_0} = \frac{\rho_0}{\rho_T}$

$$\frac{\rho_0}{\rho_T} = \exp\{\alpha(T - T_0)\} \tag{5.8}$$

Here α is the cubic expansion coefficient (thermal isobaric expansibility) and it is a function of temperature. Thus, it is assumed that the coefficients of Eq. (5.3) will have the temperature dependence in the form

$$\frac{\rho_{T(K)}}{\rho^0_{T(K)}} = 1 + \overline{a_0}m + \overline{b_0}m^{1.5} \tag{5.9}$$

where, $\overline{a_0} = a_0[1 + a_1(T - 298.15K) + a_2(T - 298.15K)^2]$ (5.10)

and $\overline{b_0} = b_0[1 + b_1(T - 298.15K) + b_2(T - 298.15K)^2]$ (5.11)

$\rho^0_{T(K)}$ is the density of water at the experimental temperature, T. The density of ASTM Grade-I water at 298.15 K was taken as 0.997043 g/cm^3. The densities of aqueous nitrate salt solutions at different temperatures are given in Tables 5.1 to 5.10 respectively. From the variation in density with temperature, it is observed that at lower concentrations, the change in density with temperature is not significant; however, as the concentration increased the density was found to increase. With increase in temperature the density decreased.

Table 5.1: Densities of $La(NO_3)_3$ at different temperatures

	Molality of $La(NO_3)_3$ (mol.kg^{-1})									
T (K)	0.0002	0.0007	0.0013	0.0043	0.0093	0.0497	0.0979	0.2450	0.5045	1.0045
293.15	0.998274	0.998449	0.998574	0.999426	1.000777	1.011655	1.024332	1.061323	1.122021	1.221215
298.15	0.997119	0.997293	0.997418	0.998265	0.999608	1.010413	1.023011	1.059761	1.120089	1.218730
303.15	0.995722	0.995894	0.996019	0.996862	0.998195	1.008938	1.021461	1.057999	1.117988	1.216115
308.15	0.994107	0.994278	0.994404	0.995240	0.996569	1.007255	1.019713	1.056057	1.115734	1.213382
313.15	0.992290	0.992458	0.992586	0.993417	0.994741	1.005376	1.017774	1.053948	1.113337	1.210538
318.15	0.990287	0.990455	0.990581	0.991409	0.992730	1.003320	1.015663	1.051679	1.110803	1.207584
323.15	0.988108	0.988275	0.988401	0.989227	0.990544	1.001092	1.013388	1.049259	1.108139	1.204529
328.15	0.985767	0.985931	0.986060	0.986881	0.988195	0.998706	1.010959	1.046699	1.105353	1.201373
333.15	0.983271	0.983434	0.983560	0.984380	0.985691	0.996173	1.008386	1.043996	1.102446	1.198122
338.15	0.980624	0.980788	0.980913	0.981731	0.983038	0.993493	1.005668	1.041169	1.099426	1.194773
343.15	0.977839	0.978000	0.978128	0.978941	0.980249	0.990677	1.002807	1.038221	1.096290	1.191334

Table 5.2: Temperature dependence of densities of $Ce(NO_3)_3$

	Molality of $Ce(NO_3)_3$ ($mol.kg^{-1}$)									
T (K)	0.0002	0.0009	0.0025	0.0063	0.0138	0.0562	0.0984	0.2024	0.4811	0.8941
293.15	0.998294	0.998471	0.998928	0.999984	1.002025	1.013419	1.024544	1.050956	1.116177	1.201338
298.15	0.997135	0.997312	0.997766	0.998814	1.000844	1.012159	1.023213	1.049458	1.114278	1.198953
303.15	0.995739	0.995915	0.996366	0.997408	0.999426	1.010677	1.021663	1.047758	1.112212	1.196438
308.15	0.994123	0.994297	0.994746	0.995784	0.997794	1.008984	1.019913	1.045870	1.109990	1.193800
313.15	0.992307	0.992478	0.992928	0.993959	0.995961	1.007097	1.017975	1.043806	1.107620	1.191039
318.15	0.990304	0.990475	0.990922	0.991949	0.993944	1.005030	1.015861	1.041580	1.105113	1.188171
323.15	0.988125	0.988296	0.988744	0.989764	0.991752	1.002797	1.013584	1.039201	1.102471	1.185188
328.15	0.985784	0.985952	0.986400	0.987417	0.989401	1.000404	1.011154	1.036676	1.099704	1.182100
333.15	0.983290	0.983454	0.983902	0.984916	0.986893	0.997866	1.008576	1.034012	1.096811	1.178911
338.15	0.980636	0.980807	0.981196	0.982268	0.984235	0.995174	1.005861	1.031210	1.093799	1.175619
343.15	0.977853	0.978024	0.978173	0.979472	0.981441	0.992353	1.003003	1.028284	1.090679	1.172230

Table 5.3: Densities of $Pr(NO_3)_3$ at different temperatures

	Molality of $Pr(NO_3)_3$ (mol.kg^{-1})									
T (K)	0.0003	0.0064	0.0018	0.0052	0.0111	0.0441	0.0965	0.2724	0.5142	1.0311
293.15	0.998303	0.998423	0.998730	0.985624	1.001281	1.010147	1.024097	1.067113	1.122224	1.223502
298.15	0.997147	0.997265	0.997573	0.989121	1.000106	1.008915	1.022774	1.065519	1.120299	1.221009
303.15	0.995750	0.995868	0.996171	0.987408	0.998691	1.007449	1.021229	1.063728	1.118203	1.218384
308.15	0.994135	0.994251	0.994555	0.985408	0.997058	1.005772	1.019480	1.061755	1.115952	1.215641
313.15	0.992317	0.992433	0.992734	0.983123	0.995229	1.003900	1.017545	1.059617	1.113555	1.212782
318.15	0.990314	0.990430	0.990731	0.980607	0.993213	1.001849	1.015434	1.057318	1.111019	1.209819
323.15	0.988138	0.988250	0.988550	0.977806	0.991025	0.999628	1.013159	1.054874	1.108351	1.206749
328.15	0.985795	0.985905	0.986205	0.974757	0.988672	0.997245	1.010728	1.052284	1.105560	1.203579
333.15	0.983296	0.983407	0.983706	0.971336	0.986166	0.994713	1.008153	1.049564	1.102648	1.200309
338.15	0.980652	0.980759	0.981056	0.966574	0.983514	0.992036	1.005435	1.046711	1.099616	1.196943
343.15	0.977865	0.977973	0.978272	0.961864	0.980722	0.989223	1.002584	1.043737	1.096472	1.193482

Table 5.4: Densities of $Sm(NO_3)_3$ in the temperature range 293.15-343.15 K

	Molality of $Sm(NO_3)_3$ (mol.kg^{-1})									
T (K)	0.0002	0.0005	0.0009	0.0044	0.0091	0.0470	0.0980	0.2497	0.4972	0.9989
293.15	0.998260	0.998363	0.998454	0.999477	1.000825	1.011501	1.025797	1.066062	1.127542	1.235255
298.15	0.997102	0.997207	0.997293	0.998313	0.999653	1.010263	1.024475	1.064504	1.125630	1.232759
303.15	0.995706	0.995806	0.995895	0.996909	0.998240	1.008795	1.022928	1.062745	1.123548	1.230129
308.15	0.994088	0.994189	0.994278	0.995288	0.996613	1.007116	1.021182	1.060805	1.121311	1.227383
313.15	0.992272	0.992372	0.992461	0.993466	0.994784	1.005243	1.019246	1.058692	1.118924	1.224524
318.15	0.990266	0.990366	0.990457	0.991460	0.992772	1.003189	1.017134	1.056419	1.116396	1.221554
323.15	0.988087	0.988186	0.988279	0.989275	0.990584	1.000963	1.014857	1.053996	1.113739	1.218479
328.15	0.985745	0.985844	0.985936	0.986933	0.988228	0.998580	1.012428	1.051429	1.110955	1.215300
333.15	0.983247	0.983346	0.983439	0.984429	0.985661	0.996045	1.009829	1.048721	1.108018	1.212023
338.15	0.980601	0.980699	0.980723	0.981775	0.982652	0.993271	1.006840	1.045794	1.104705	1.208646
343.15	0.977811	0.977914	0.977001	0.978748	0.978538	0.989675	1.001951	1.042161	1.099500	1.205099

Table 5.5: Densities of $Eu(NO_3)_3$ at different temperatures

	Molality of $Eu(NO_3)_3$ ($mol.kg^{-1}$)								
T (K)	0.0002	0.0007	0.0014	0.0046	0.0099	0.0478	0.0981	0.2421	0.4187
293.15	0.998271	0.998405	0.998610	0.999531	1.000932	1.011594	1.025405	1.063685	1.106601
298.15	0.997113	0.997248	0.997451	0.998367	0.999799	1.010358	1.024092	1.062149	1.104823
303.15	0.995717	0.995849	0.996055	0.996962	0.998401	1.008892	1.022552	1.060410	1.102860
308.15	0.994100	0.994231	0.994436	0.995341	0.996775	1.007215	1.020811	1.058488	1.100733
313.15	0.992283	0.992413	0.992620	0.993517	0.994941	1.005345	1.018881	1.056394	1.098449
318.15	0.990279	0.990408	0.990616	0.991509	0.992909	1.003291	1.016775	1.054137	1.096021
323.15	0.988102	0.988230	0.988436	0.989327	0.990658	1.001070	1.014504	1.051729	1.093452
328.15	0.985762	0.985886	0.986091	0.986978	0.988217	0.998690	1.012078	1.049177	1.090751
333.15	0.983252	0.983364	0.983593	0.984482	0.985333	0.996153	1.009502	1.046488	1.087923
338.15	0.980500	0.980509	0.980822	0.981835	0.982250	0.993476	1.006788	1.043611	1.084972
343.15	0.977453	0.977325	0.975830	0.978955	0.978888	0.990631	1.003769	1.039629	1.081881

Table 5.6: Densities of $RbNO_3$ from 293.15 to 343.15 K

	Molality of $RbNO_3$ ($mol.kg^{-1}$)									
T (K)	0.0002	0.0007	0.0014	0.0050	0.0104	0.0495	0.1019	0.2582	0.4991	1.0324
293.15	0.998239	0.998281	0.998369	0.998709	0.999305	1.003381	1.008791	1.024710	1.048741	1.099737
298.15	0.997082	0.997123	0.997213	0.997548	0.998139	1.002183	1.007555	1.023347	1.047206	1.097863
303.15	0.995686	0.995726	0.995814	0.996147	0.996735	1.000749	1.006082	1.021768	1.045465	1.095809
308.15	0.994069	0.994108	0.994197	0.994527	0.995114	0.999101	1.004399	1.019985	1.043534	1.093593
313.15	0.992253	0.992290	0.992378	0.992708	0.993290	0.997253	1.002521	1.018016	1.041434	1.091222
318.15	0.990250	0.990287	0.990373	0.990700	0.991282	0.995221	1.000463	1.015876	1.039171	1.088708
323.15	0.988070	0.988107	0.988194	0.988519	0.989096	0.993019	0.998232	1.013572	1.036754	1.086058
328.15	0.985729	0.985769	0.985852	0.986174	0.986753	0.990654	0.995844	1.011116	1.034192	1.083280
333.15	0.983234	0.983259	0.983352	0.983674	0.984246	0.988136	0.993305	1.008512	1.031491	1.080378
338.15	0.980586	0.980465	0.980707	0.981029	0.981597	0.985473	0.990613	1.005716	1.028653	1.077358
343.15	0.977807	0.976887	0.977906	0.978241	0.978808	0.982669	0.987766	1.002466	1.025555	1.074219

Table 5.7: Variation of densities of $CsNO_3$ at different temperatures

	Molality of $CsNO_3$ (mol.kg^{-1})									
T (K)	0.0001	0.0005	0.0010	0.0055	0.0425	0.0890	0.0983	0.2552	0.4987	1.0012
293.15	0.998253	0.998315	0.998395	0.999045	1.004624	1.011010	1.012281	1.034389	1.067859	1.133907
298.15	0.997096	0.997155	0.997236	0.997883	1.003424	1.009773	1.011037	1.033013	1.066292	1.131977
303.15	0.995700	0.995758	0.995839	0.996483	1.001991	1.008306	1.009561	1.031422	1.064519	1.129868
308.15	0.994084	0.994143	0.994223	0.994863	1.000344	1.006626	1.007873	1.029624	1.062559	1.127589
313.15	0.992268	0.992325	0.992406	0.993046	0.998496	1.004750	1.005992	1.027640	1.060420	1.125154
318.15	0.990265	0.990321	0.990401	0.991038	0.996464	1.002692	1.003925	1.025482	1.058116	1.122569
323.15	0.988086	0.988144	0.988221	0.988857	0.994260	1.000461	1.001690	1.023158	1.055657	1.119844
328.15	0.985746	0.985800	0.985879	0.986512	0.991893	0.998073	0.999296	1.020681	1.053051	1.116987
333.15	0.983250	0.983302	0.983379	0.984016	0.989372	0.995531	0.996748	1.018054	1.050305	1.113999
338.15	0.980598	0.980660	0.980735	0.981360	0.986707	0.992835	0.994054	1.015291	1.047423	1.110891
343.15	0.977813	0.977863	0.977942	0.978577	0.983894	0.990012	0.991223	1.012391	1.044413	1.107667

Table 5.8: Densities of $Sr(NO_3)_2$ at different temperatures

	Molality of $Sr(NO_3)_2$ (mol.kg^{-1})									
T (K)	0.0001	0.0003	0.0009	0.0035	0.0091	0.0547	0.1008	0.2471	0.4793	0.9921
293.15	0.998452	0.998499	0.998598	0.999033	0.999994	1.007521	1.015233	1.039141	1.075902	1.152507
298.15	0.997296	0.997345	0.997441	0.997875	0.998825	1.006284	1.013930	1.037638	1.074114	1.150199
303.15	0.995899	0.995947	0.996042	0.996473	0.997416	1.004814	1.012400	1.035930	1.072148	1.147746
308.15	0.994283	0.994331	0.994428	0.994854	0.995790	1.003138	1.010666	1.034036	1.070018	1.145169
313.15	0.992467	0.992514	0.992611	0.993032	0.993964	1.001264	1.008745	1.031971	1.067737	1.142474
318.15	0.990463	0.990511	0.990606	0.991028	0.991952	0.999210	1.006647	1.029740	1.065309	1.139664
323.15	0.988285	0.988333	0.988429	0.988846	0.989768	0.996986	1.004386	1.027358	1.062750	1.136746
328.15	0.985943	0.985989	0.986085	0.986500	0.987418	0.994606	1.001968	1.024835	1.060058	1.133726
333.15	0.983445	0.983490	0.983590	0.984000	0.984915	0.992071	0.999403	1.022172	1.057246	1.130610
338.15	0.980800	0.980841	0.980942	0.981352	0.982261	0.989395	0.996699	1.019378	1.054314	1.127395
343.15	0.978013	0.978056	0.978155	0.978565	0.979472	0.986582	0.993862	1.016460	1.051268	1.124088

Table 5.9: Densities of $Y(NO_3)_3$ from 293.15 to 343.15 K

	Molality of $Y(NO_3)_3$ ($mol.kg^{-1}$)									
T (K)	0.0001	0.0005	0.0009	0.0047	0.0098	0.0467	0.0997	0.2472	0.4901	1.0013
293.15	0.998444	0.998550	0.998635	0.999512	1.000748	1.009157	1.020914	1.052484	1.099702	1.188021
298.15	0.997290	0.997396	0.997478	0.998349	0.999576	1.007924	1.019595	1.050939	1.097823	1.185576
303.15	0.995894	0.995998	0.996079	0.996945	0.998166	1.006457	1.018055	1.049200	1.095786	1.183014
308.15	0.994278	0.994382	0.994464	0.995327	0.996538	1.004787	1.016319	1.047283	1.093601	1.180348
313.15	0.992461	0.992564	0.992647	0.993505	0.994710	1.002921	1.014393	1.045199	1.091278	1.177582
318.15	0.990458	0.990560	0.990644	0.991497	0.992698	1.000875	1.012296	1.042965	1.088825	1.174716
323.15	0.988279	0.988382	0.988464	0.989316	0.990513	0.998660	1.010035	1.040583	1.086246	1.171757
328.15	0.985936	0.986037	0.986121	0.986971	0.988164	0.996287	1.007623	1.038060	1.083547	1.168708
333.15	0.983440	0.983539	0.983624	0.984470	0.985661	0.993764	1.005069	1.035409	1.080735	1.165567
338.15	0.980792	0.980895	0.980981	0.981822	0.983012	0.991097	1.002372	1.032629	1.077810	1.162335
343.15	0.978003	0.978104	0.978189	0.979032	0.980222	0.988294	0.999541	1.029726	1.074771	1.159013

Table 5.10: Variation in the densities of $Ga(NO_3)_3$ with temperature

	Molality of $Ga(NO_3)_3$ ($mol.kg^{-1}$)									
T (K)	0.0001	0.0005	0.0009	0.0046	0.0099	0.0492	0.0990	0.2493	0.4995	0.9899
293.15	0.998233	0.998333	0.998259	0.999185	1.000293	1.008132	1.017844	1.046649	1.089892	1.160442
298.15	0.997075	0.997176	0.997099	0.998023	0.999123	1.006913	1.016663	1.045167	1.088122	1.158242
303.15	0.995677	0.995777	0.995694	0.996620	0.997715	1.005458	1.015188	1.043480	1.086187	1.155925
308.15	0.994062	0.994161	0.994074	0.995001	0.996088	1.003794	1.013409	1.041620	1.084105	1.153500
313.15	0.992244	0.992341	0.992253	0.993179	0.994263	1.001933	1.011237	1.039585	1.081881	1.150968
318.15	0.990241	0.990336	0.990242	0.991168	0.992249	0.999889	1.008621	1.037394	1.079520	1.148337
323.15	0.988063	0.988155	0.988058	0.988983	0.990059	0.997673	0.985265	1.035053	1.077031	1.145612
328.15	0.985721	0.985811	0.985710	0.986634	0.987705	0.995296	0.973510	1.032571	1.074425	1.142789
333.15	0.983223	0.983311	0.983206	0.984130	0.985193	0.992768	0.968369	1.029951	1.071696	1.139880
338.15	0.980575	0.980668	0.980554	0.981477	0.982537	0.990095	0.962359	1.027202	1.068858	1.136878
343.15	0.977780	0.977880	0.977763	0.978675	0.979728	0.987281	0.949098	1.024328	1.065907	1.133790

The coefficients of Eqs. (5.10) and (5.11) and the standard deviation for the aqueous solutions of nitrates have been listed in Table 5.11.

Table 5.11: Regressed coefficients of density for different electrolytes

Solute	a_0	a_1	a_2	b_0	b_1	b_2	Std.dev.
$Ce(NO_3)_3$	2.96E-01	-2.00E-04	4.77E-06	-6.55E-02	9.08E-05	-2.15E-06	4.14E-02
$Eu(NO_3)_3$	2.94E-01	7.90E-05	-4.65E-06	-4.29E-02	-3.10E-04	1.25E-05	3.26E-02
$Sm(NO_3)_3$	2.98E-01	1.20E-04	-6.81E-06	-4.33E-02	-2.30E-04	1.02E-05	3.11E-02
$La(NO_3)_3$	2.85E-01	-2.03E-04	4.80E-06	-4.62E-02	9.56E-05	-2.04E-06	1.74E-02
$Pr(NO_3)_3$	2.80E-01	-1.73E-04	3.63E-06	-4.22E-02	6.28E-05	-8.14E-07	3.69E-01
$RbNO_3$	1.04E-01	-7.00E-05	5.00E-07	-1.40E-03	-1.20E-06	9.00E-07	9.80E-03
$CSNO_3$	1.45E-01	-9.00E-05	2.00E-06	-2.40E-03	3.00E-05	-4.00E-07	8.80E-03
$Sr(NO_3)_2$	1.72E-01	-2.00E-04	3.00E-06	-9.00E-03	9.00E-05	-1.30E-06	1.24E-02
$Y(NO_3)_3$	2.40E-01	-2.00E-04	4.90E-06	-3.87E-02	8.00E-05	-2.00E-06	1.45E-02
$Ga(NO_3)_3$	5.00E-04	-3.00E-04	-4.00E-05	-4.78E-02	2.00E-04	5.00E-05	6.94E-01

Equation (5.2) is valid for a fixed temperature. For studying the dependence of temperature on apparent molal volume, a quadratic equation was assumed for the variation of apparent molal volume against temperature. This equation could be written as

$$V_{2,\phi} = V_{2,\phi}^{298.15K}[1 + A(T - 298.15K) + B(T - 298.15K)^2] \tag{5.12}$$

where, A and B are the coefficients of Eq. (5.12). The variation of apparent molal volume of the nitrate salt solutions with temperature and concentration are plotted in Figs. 5.1 to 5.10.

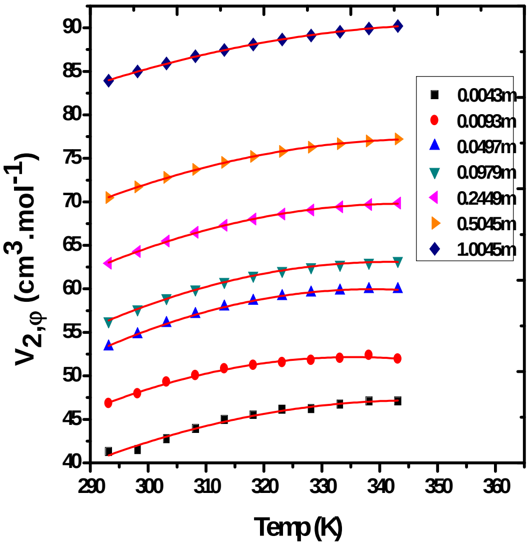

Fig. 5.1: Variation of apparent molal volume of $La(NO_3)_3$ with temperature

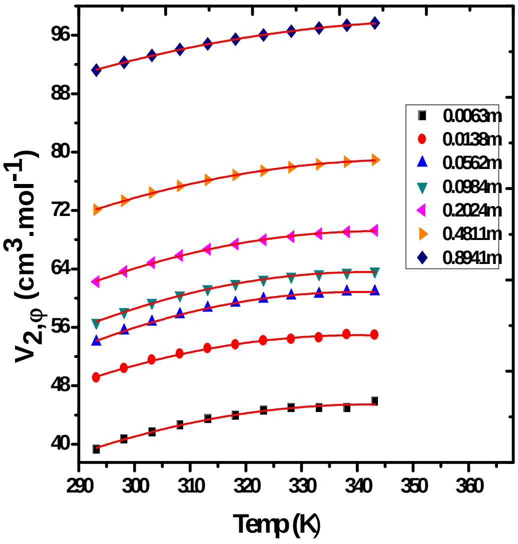

Fig. 5.2: Temperature dependence of apparent molal volume of $Ce(NO_3)_3$

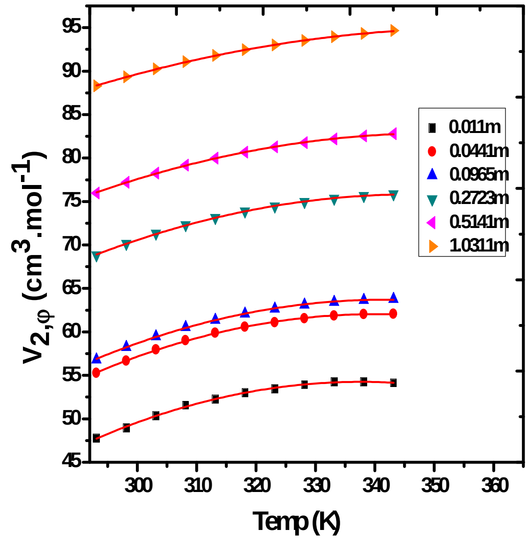

Fig. 5.3: Plot of variation of apparent molal volume of $Pr(NO_3)_3$ with temperature

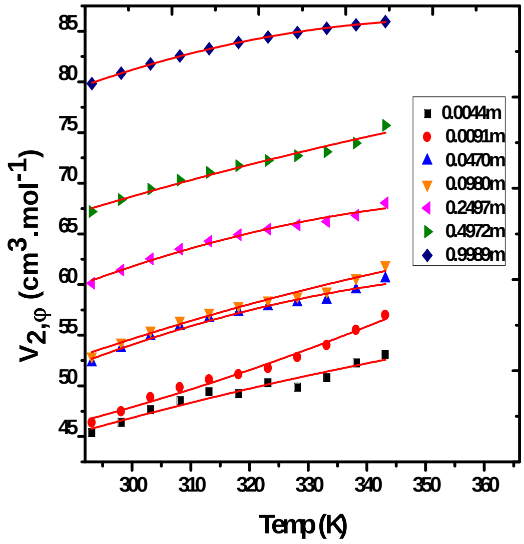

Fig. 5.4: Apparent molal volume of $Sm(NO_3)_3$ vs. temperature

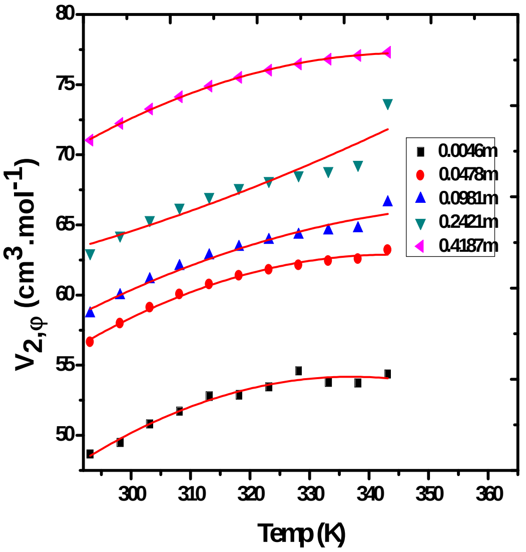

Fig. 5.5: Effect of temperature on apparent molal volume of $Eu(NO_3)_3$

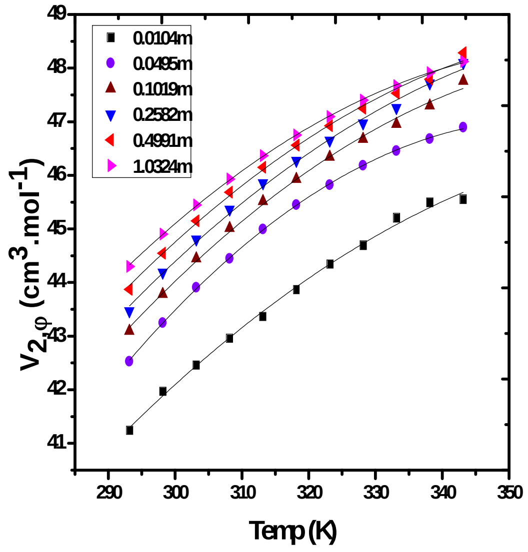

Fig. 5.6: Variation of apparent molal volume of $RbNO_3$ with temperature

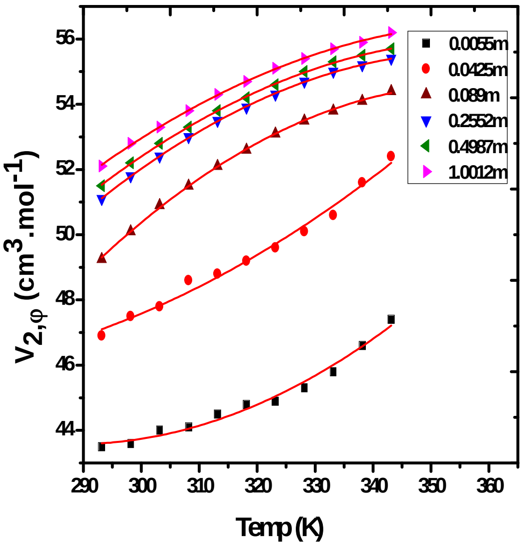

Fig. 5.7: Plot of variation of apparent molal volume of $CsNO_3$ with temperature

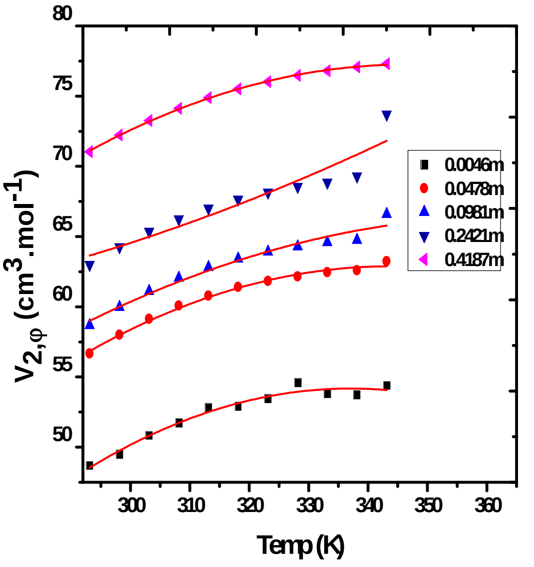

Fig. 5.8: Temperature dependence of apparent molal volume of $Sr(NO_3)_2$

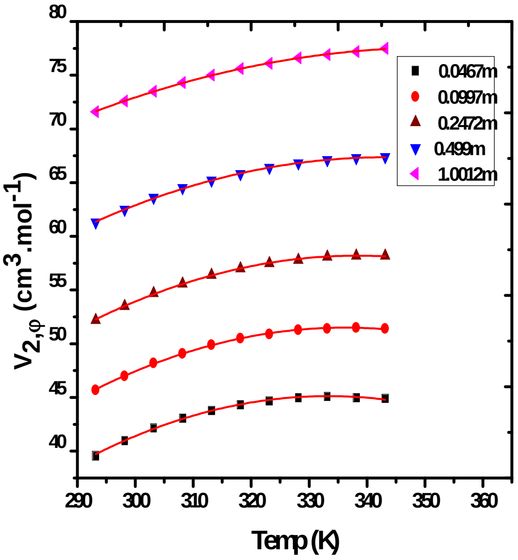

Fig. 5.9: Change in apparent molal volume of $Y(NO_3)_3$ with temperature

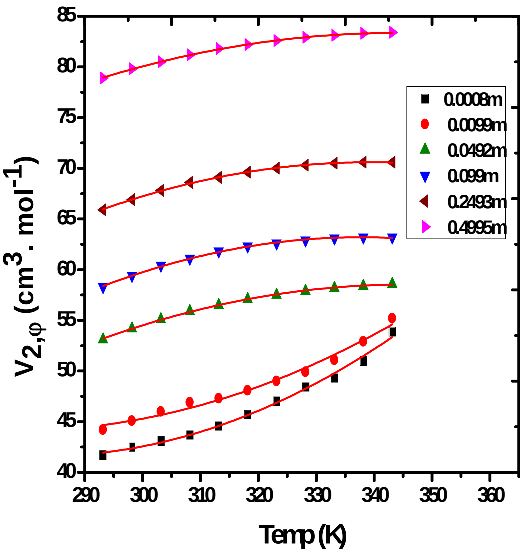

Fig. 5.10: Apparent molal volume of $Ga(NO_3)_3$ vs. temperature

For different temperatures and concentration, the cubic expansion coefficient given as Eq. (5.6) can be written as

$$\alpha(T,m) = \left(\frac{\partial \ln V(T,m)}{\partial T}\right)_P \tag{5.13}$$

Applying Maxwell's relation for differential of enthalpy we get,

$$dH = C_p dT + \left[V - T\left(\frac{\partial V}{\partial T}\right)_P\right] dP \tag{5.14}$$

The relation between volumetric and thermal properties of a solution can be written as

$$\left(\frac{\partial C_p}{\partial P}\right)_T = -T\left(\frac{\partial^2 V}{\partial T^2}\right)_P \tag{5.15}$$

where, C_p is the isobaric heat capacity of the solutions.

In terms of cubic expansion coefficient, Eq. (15) takes the form

$$T\left(\frac{\partial^2 V}{\partial T^2}\right)_{P,m} = TV\left[\alpha^2(T,m) + \left(\frac{\partial \alpha(T,m)}{\partial T}\right)_{P,m}\right] \tag{5.16}$$

The left hand side of Eq. (16) can be directly expressed in terms of derivative of density as

$$T\left(\frac{\partial^2 V}{\partial T^2}\right)_{P,m} = T\left(\frac{1000+mM_2}{\rho^2(T,m)}\right)\times\left[\frac{2}{\rho(T,m)}\left(\frac{\partial \rho(T,m)}{\partial T}\right)^2_{P,m} - \left(\frac{\partial^2 \rho(T,m)}{\partial T^2}\right)_{P,m}\right] \tag{5.17}$$

where, $\left(\frac{1000+mM_2}{\rho^2(T,m)}\right)$ is the volume of solution.

The cubic expansion coefficient can be used to interpret the ion-solvent interactions [64]. Variation in the cubic expansion coefficient of the aqueous nitrate salt solutions with temperature is shown in Figs. 5.11 to 5.20 respectively.

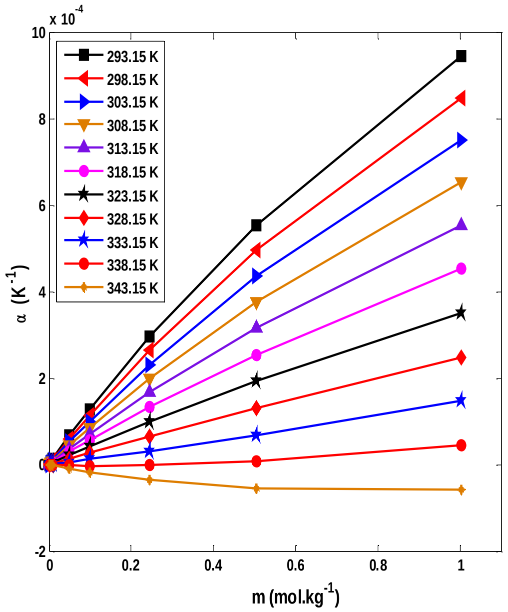

Fig. 5.11: Temperature and concentration effect on cubic expansion coefficient of La(NO$_3$)$_3$

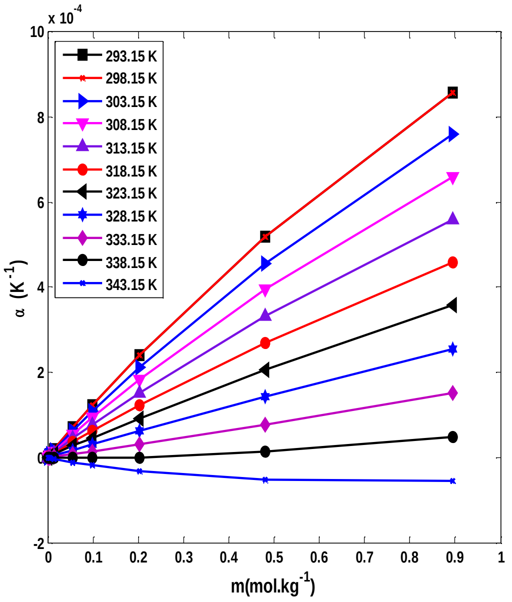

Fig. 5.12: Plot of temperature and concentration dependence of cubic expansion coefficient for Ce(NO$_3$)$_3$

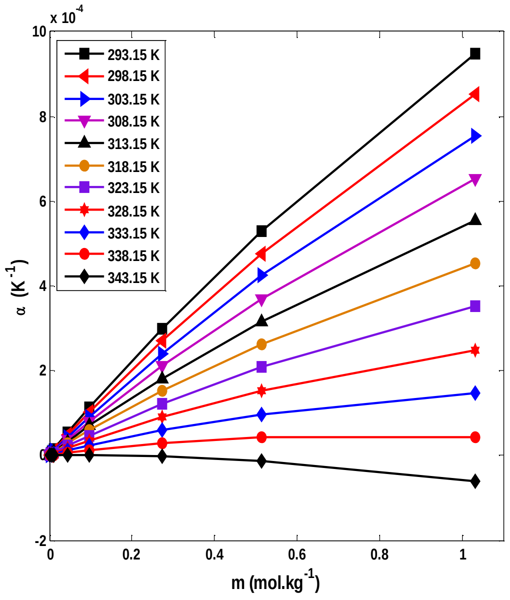

Fig. 5.13: Variation of cubic expansion coefficient of $Pr(NO_3)_3$ with temperature and concentration

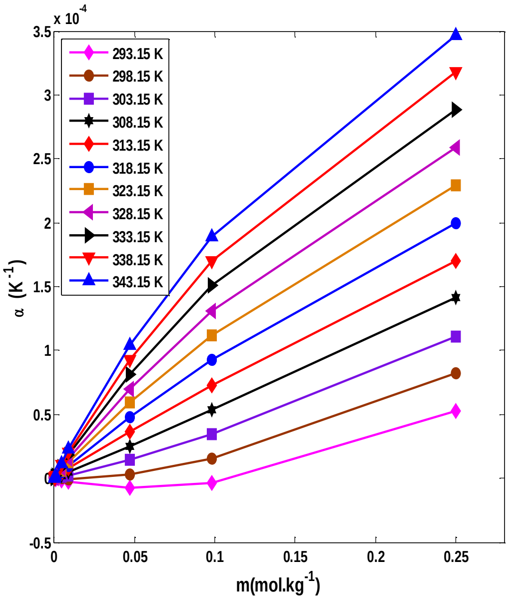

Fig. 5.14: Cubic expansion coefficient of $Sm(NO_3)_3$ vs. temperature at different concentrations

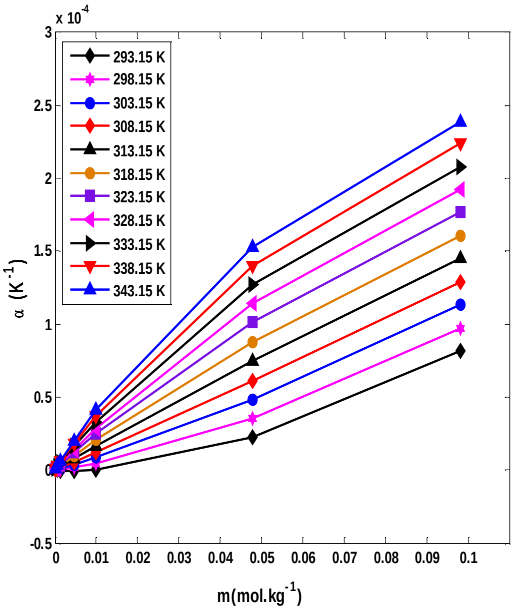

Fig. 5.15: Effect of temperature and concentration on cubic expansion coefficient of $Eu(NO_3)_3$

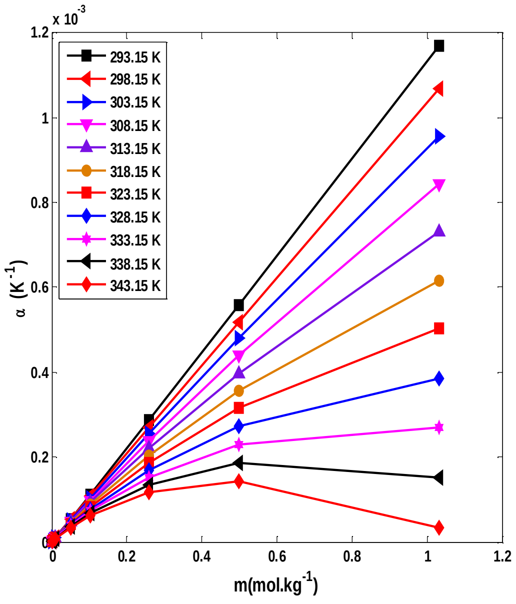

Fig. 5.16: Plot of temperature and concentration dependence of cubic expansion coefficient for $RbNO_3$

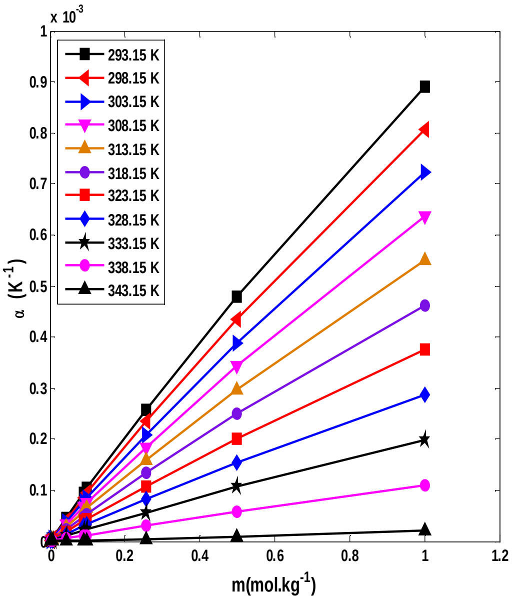

Fig. 5.17: Temperature and concentration effect on cubic expansion coefficient of $CsNO_3$

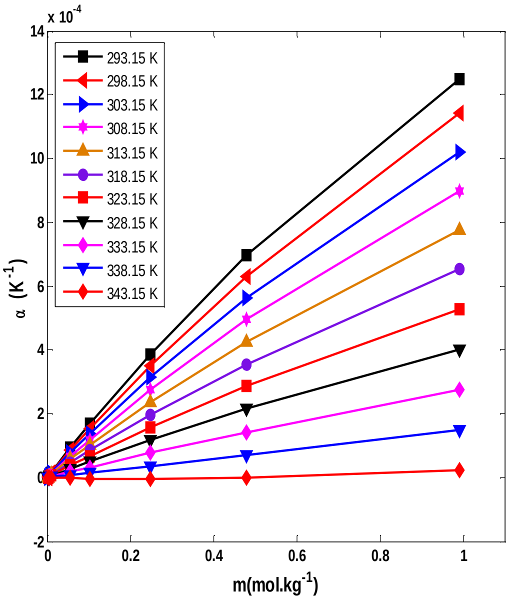

Fig. 5.18: Variation of cubic expansion coefficient of $Sr(NO_3)_2$ with temperature and concentration

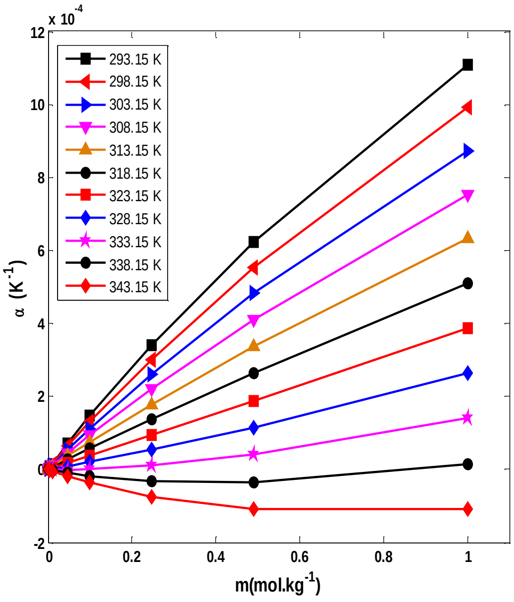

Fig. 5.19: Effect of temperature and concentration on cubic expansion coefficient of $Y(NO_3)_3$

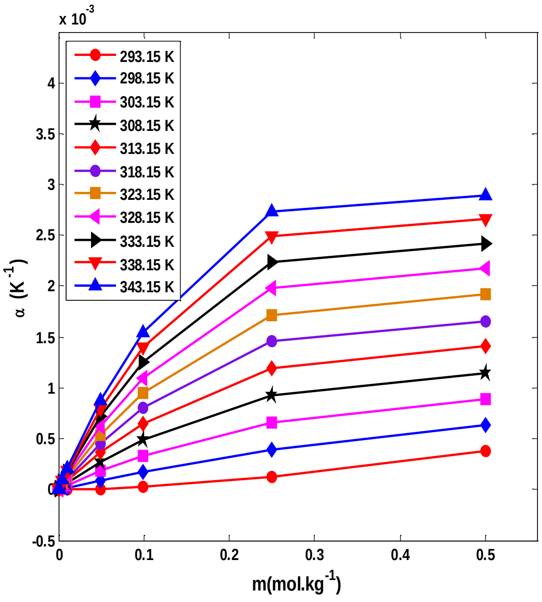

Fig. 5.20: Cubic expansion coefficient of $Ga(NO_3)_3$ vs. temperature at different concentrations

It is evident from these figures that the value of α decreases with increase in temperature for the nitrates of rubidium, cesium, strontium, yttrium and the lower lanthanides (La, Ce and Pr) which implies that they behave like common electrolytes [5, 6], because in common electrolytes the cubic expansion coefficient should decrease with the rise in temperature. At low temperatures, the water around the ions will be loosely bound, giving rise to higher value of expansivity. The behaviour exhibited by the nitrates of gallium, samarium and europium may be ascribed to the absence of 'caging effect' [5].

In the last decade, many researchers have emphasized that a_v is not the sole criterion for determining the structure making or breaking nature of any solute [65-68]. Hepler [68] has developed a technique for examining the sign of $\left(\frac{\partial^2 V}{\partial T^2}\right)$ for various solutes in terms of long range structure making or breaking capacity in aqueous solutions using the thermodynamic relation given in Eq. (5.15). The variation of second derivative of volume with temperature for the aqueous solutions of nitrates at different concentrations is shown in the Figs. 5.21 – 5.30 respectively.

Based on Hepler's assumption, those solutes for which the second derivative of volume with temperature is negative or the first derivative of isobaric heat capacity with pressure is positive are considered to act as structure breakers and vice-versa.

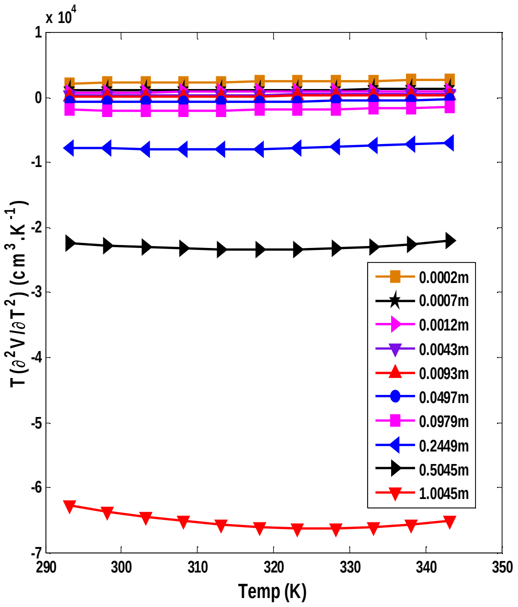

Fig. 5.21: Plot of T($\partial^2V/\partial T^2$) vs. temperature for La(NO_3)$_3$

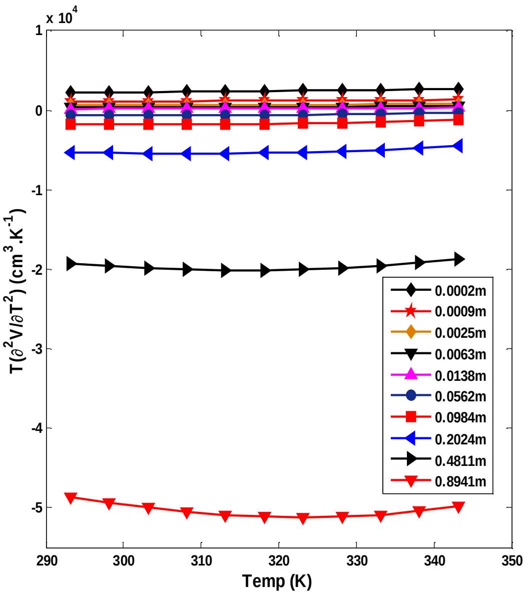

Fig. 5.22: Graph of T($\partial^2V/\partial T^2$) with temperature for Ce(NO_3)$_3$

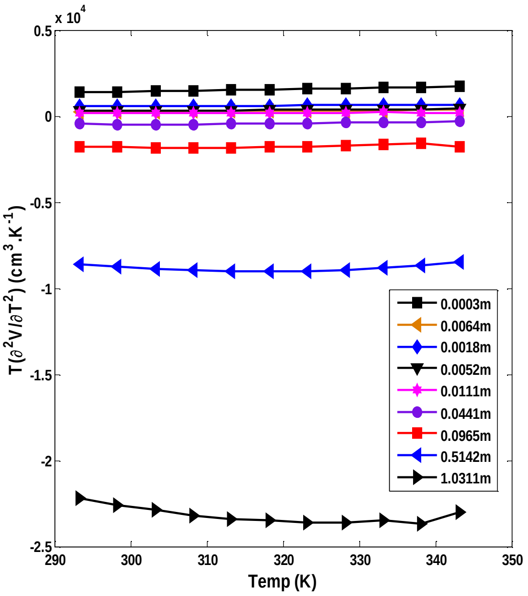

Fig. 5.23: Effect of temperature on T($\partial^2V/\partial T^2$) for Pr(NO_3)$_3$

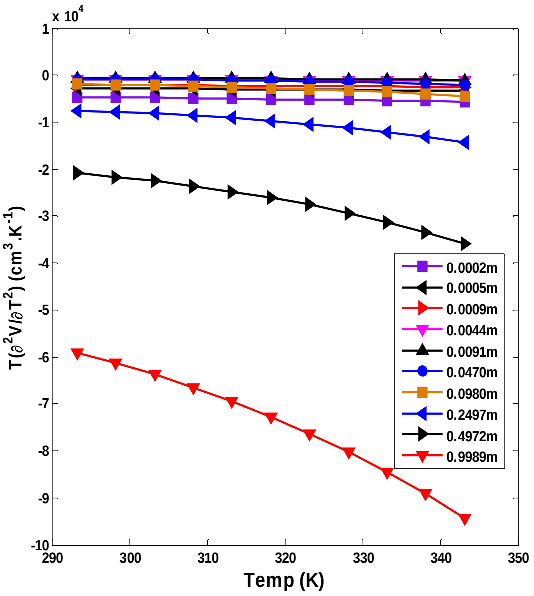

Fig. 5.24: Temperature dependence of T($\partial^2V/\partial T^2$) for Sm(NO_3)$_3$

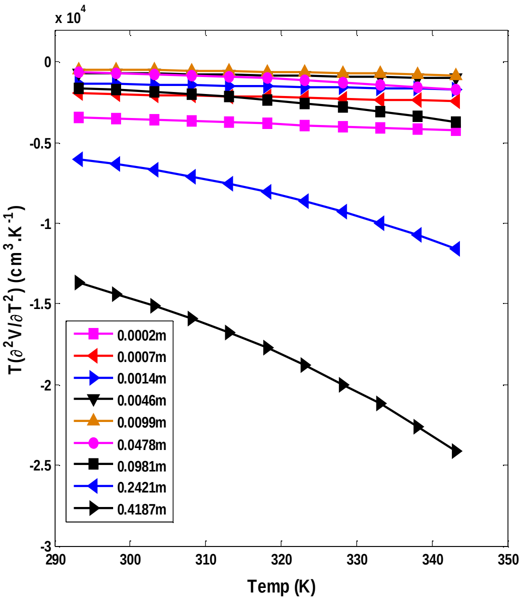

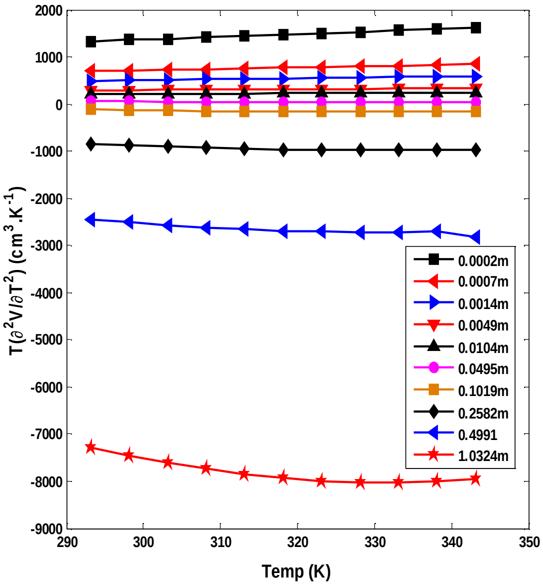

Fig. 5.25: $T(\partial^2V/\partial T^2)$ vs. temperature plot for $Eu(NO_3)_3$

Fig. 5.26: Effect of temperature on $T(\partial^2V/\partial T^2)$ for $RbNO_3$

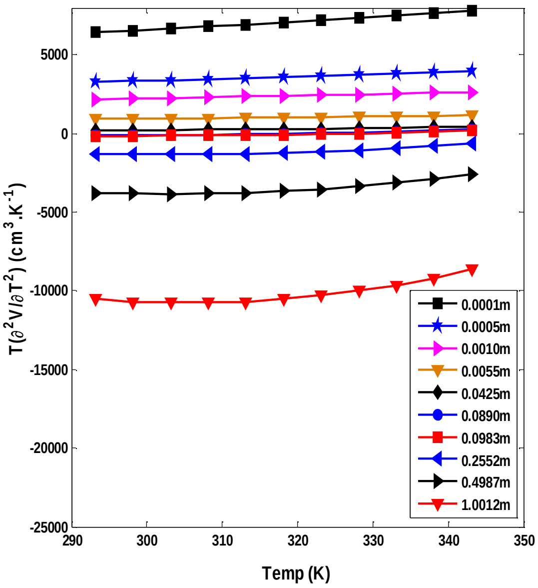

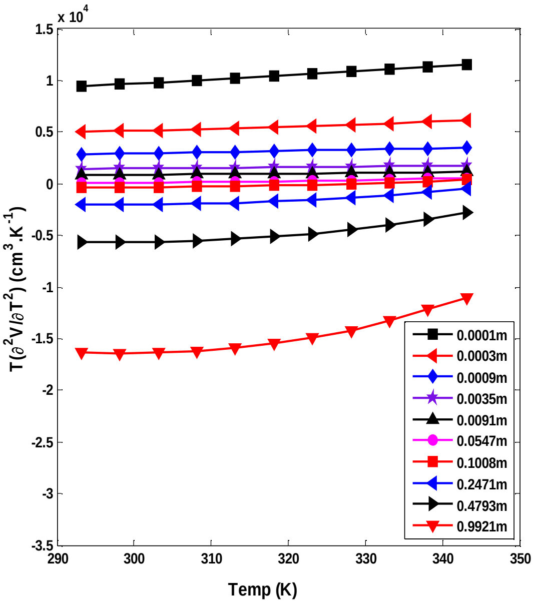

Fig. 5.27: $T(\partial^2V/\partial T^2)$ vs. temperature plot for $CsNO_3$

Fig. 5.28: Temperature dependence of $T(\partial^2V/\partial T^2)$ for $Sr(NO_3)_2$

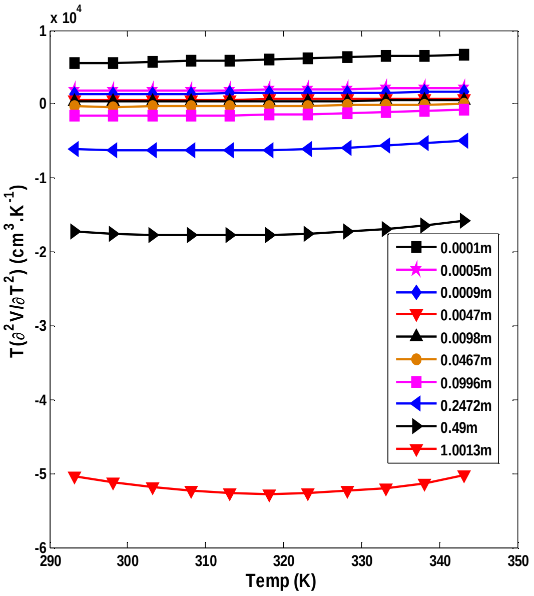

Fig. 5.29: Variation of T($\partial^2V/\partial T^2$) with temperature for $Y(NO_3)_3$

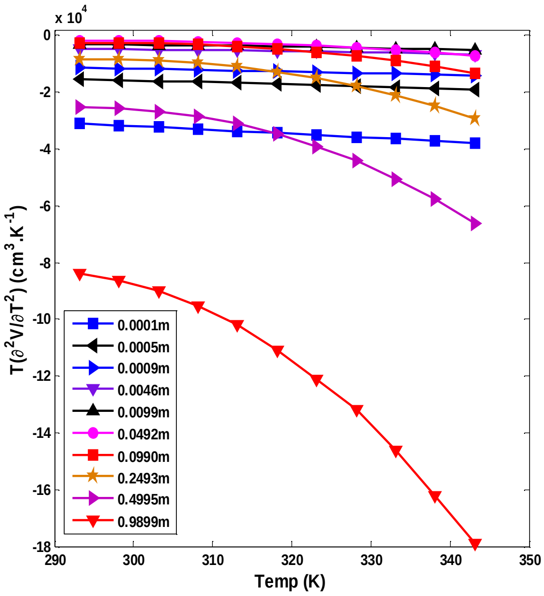

Fig. 5.30: Graph of T($\partial^2V/\partial T^2$) with temperature for $Ga(NO_3)_3$

The variation in the second derivative of volume with temperature was found to be positive for the nitrates of Rb, Cs, Sr, Y, La, Ce and Pr at lower concentrations and negative for higher concentrations which implies that those nitrate salts acting as structure makers at lower concentrations act as structure breakers as the concentration increases. However, the nitrates of gallium, samarium and europium exhibited negative variation in the second derivative of volume with temperature for all concentrations indicating that they act as structure breakers at all concentrations.

SUMMARY

Chapter 5 is an extension of Chapter 4, in which a detailed and systematic study of the density, structural behaviour and volumetric properties of aqueous solutions of nitrates of rubidium, cesium, strontium, yttrium, gallium, cerium, lanthanum, praseodymium, europium and samarium has been discussed in the temperature range 293.15 - 343.15 K with 5 K interval. The temperature dependence of density and apparent molal volume was correlated by a second order polynomial. The studies revealed that the density decreased with increase in temperature and apparent molal volume increased with increase in the concentration as well as with temperature, indicating an increase in solute-solvent interaction.

The cubic expansion coefficient or the coefficient of thermal isobaric expansibility was calculated from the variation of density with temperature. The variation of cubic expansion coefficient with concentration was also evaluated. The variation of second derivative of volume with temperature at constant pressure and concentration predicts the structure maker and structure breaker behaviour of the electrolytes. The cubic expansion coefficient values estimated based on Hepler’s assumption, revealed that the values decreased with increase in temperature for the nitrates of rubidium, cesium, strontium, yttrium, lanthanum, cerium and praseodymium and the opposite behaviour shown by the nitrates of gallium, samarium and europium may be due to the absence of caging effect. From the variation observed in the second derivative of volume with temperature at constant pressure and concentration, it is predicted that rubidium, cesium, strontium, yttrium, lanthanum, cerium and praseodymium nitrates act as structure makers at lower concentrations and structure breakers at higher concentrations. The nitrates of gallium, samarium and europium exhibited structure breaker behaviour at all concentrations and temperatures.

REFERENCES

1. Proc. 6th OECD/NEA Information Exchange Meeting on Actinide and Fission Products Partitioning and Transmutation, EUR 19783 EN, Madrid, Spain, 2000
2. O. Redlich, J. Phys. Chem., 44 (1940) 619
3. H.S. Harned, B.B. Owen, “The physical chemistry of electrolytic solutions”, 3rd ed., Reinhold, New York, N. Y. (1958)
4. F.H. Spedding, J.A. Rard, V.W. Saeger, J. Chem. Eng. Data, 19 (1974) 373
5. F. J. Millero, Chem. Rev.71 (1971) 147
6. F.J. Millero, “Water and aqueous solutions”, R.A. Horne, ed., Wiley-Interscience, New York, N. Y. (1972) Chap. 13, 14
7. A. Ali, S. Hyder, A.K. Nain, J. Mol. Liq., 79 (1999) 89
8. R. Francesconi, F. Comelli, C. Castellari, J. Chem. Eng. Data, 45 (2000) 544
9. U.S. Vural, H. Yuruk, V. Muradoglu, Russ. J. Phys. Chem., 77 (2003) 1091
10. U.S. Vural, V. Muradoglu, H. Yuruk, Russ. J. Phys. Chem., 78 (2004) 33
11. U.S. Vural, Russ. J. Phys. Chem., 79 (2005) 1096
12. A.H. Hind, E. McLaughlin, A.R. Ubbelohde, J. Chem. Soc. Faraday Trans., 56 (1960) 331
13. F.H. Spedding, G. Atkinson, “The structure of electrolytic solutions”, W. J. Hamer ed., Willey, New York, N. Y. (1959) Chap. 22
14. F.H. Spedding, D.A. Csejka, C.W. DeKock, J. Phys. Chem., 70 (1966) 2423

15. F.H. Spedding, P.F. Cullen, A. Habenschuss, J. Phys. Chem., 78 (1974) 1106

16. F.H. Spedding, K.C. Jones, J. Phys. Chem., 70 (1966) 2450

17. F.H. Spedding, M.J. Pikal, B.O. Ayers, J. Phys. Chem., 70 (1966) 2440

18. F.H. Spedding, M.J. Pikal, J. Phys. Chem., 70 (1966) 2430

19. F.H. Spedding, J.A. Rard, J. Phys. Chem., 78 (1974) 1435

20. F.H. Spedding, J.A. Rard, V.W. Saeger, J. Chem. Eng. Data, 19 (1974) 373

21. D.G. Karraker, Inorg. Chem., 7 (1968) 437

22. W.B. Lewis, J.A. Jackson, J.E. Lemons, H. Taube, J. Chem. Phys., 36 (1962) 694

23. L.O. Morgan, J. Chem. Phys., 38 (1963) 2788

24. W.C. Mundy, F.H. Spedding, J. Chem. Phys., 59 (1973) 2183

25. K. Nakamura, K. Kawamura, Bull. Chem. Soc. Japan, 44 (1971) 330

26. F.H. Spedding, L.E. Shiers, M.A. Brown, J.L. Baker, L. Guitierrez, L.S. McDowell, A. Habenschuss, J. Phys. Chem., 79 (1975) 1087

27. F.H. Spedding, V.W. Saeger, K.A. Gray, P.K. Boneau, M.A. Brown, C.W. DeKock, J.L. Baker, L.E. Shiers, H.O. Weber, A. Habenschuss, J. Chem. Eng. Data, 20 (1975) 72

28. F.H. Spedding, L.E. Shiers, M.A. Brown, J.L. Derer, D.L. Swanson, A. Habenschuss, J. Chem. Eng. Data, 20 (1975) 81

29. F.H. Spedding, P.F. Cullen, A. Habenschuss, J. Phys. Chem., 78 (1974) 1106

30. A. Angnostopoulos, P.O. Sakellaridis, J. Inorg. Nucl. Chem., 32 (1970) 1740

31. N.A. Coward, R.W. Kiser, J. Phys. Chem., 70 (1966) 213

32. D.F. Peppard, G.W. Mason, I. Hucher, J. Inorg. Nucl. Chem., 24 (1962) 881

33. D.L. Nelson, D.E. Irish, J. Chem. Phys., 54 (1971) 4479

34. J. Knoeck, J. Anal. Chem., 41 (1969) 2069

35. K. Nakamura, K. Kawamura, Bull. Chem. Soc. Japan, 44 (1971) 330

36. J. Reuben, D. Fiat, J. Chem. Phys., 51 (1969) 4909

37. H.E. Silber, N. Scheinin, G. Atkinson, J. Grecsek, J. Chem. Soc., Faraday Trans. 2,68 (1972) 1200

38. R. Garnsey, D.W. Ebdon, J. Am. Chem. Soc., 91 (1969) 50

39. G.R. Choppin, W.F. Strazik, J. Inorg. Chem., 4 (1965) 1250

40. K. Bukietynska, G.R. Choppin, J. Chem. Phys., 52 (1970) 2875

41. G.R. Choppin, D.E. Henrie, K. Buijs, Inorg. Chem., 5 (1966) 1743

42. B.M.L. Bansal, S.K. Patil, H.D. Sharma, J. Inorg. Nucl. Chem., 26 (1964) 993

43. I. Abrahamer, Y. Marcus, J. Inorg. Nucl. Chem., 30 (1968) 1563

44. F.H. Spedding, S. Jaffe, J. Am. Chem. Soc., 76 (1954) 884

45. R.E. Hester, R.A. Plane, Inorg. Chem., 3 (1964) 769

46. A.W. Hakin, M.J. Lucas, J.L. Liu, K. Erickson, A. Madhavji, J. Chem. Thermodyn., 35 (2003) 775

47. A.W. Hakin, M.J. Lucas, J.L. Liu, K. Erickson, J. Chem. Thermodyn., 35 (2003) 1861
48. A.W. Hakin, J.L. Liu, K. Erickson, J-V. Munoz, J. Chem. Thermodyn., 36 (2004) 773
49. A.W. Hakin, J.L. Liu, K. Erickson, J-V. Munoz, J.A. Rard, J. Chem. Thermodyn., 37 (2005) 153
50. R.A. Marriot, A.W. Hakin, J.A. Rard, J. Chem. Thermodyn., 33 (2001) 643
51. F.H. Spedding, J.L. Baker, J.P. Walters, J. Chem. Eng. Data, 20 (1975) 189
52. F.H. Spedding, J.P. Walters, J.L. Baker, J. Chem. Eng. Data, 20 (1975) 438
53. F.H. Spedding, J.L. Baker, J.P. Walters, J. Am. Chem. Soc., 24 (1979) 298
54. C. Xiao, P.R. Tremaine, J. Chem. Eng. Data, 41 (1996) 1075
55. C. Xiao, P.R. Tremaine, J. Chem. Thermodyn., 28 (1996) 43
56. C. Xiao, P.R. Tremaine, J. Soln. Chem., 26 (1997) 277
57. A.W. Hakin, M.J. Lucas, J.L. Liu, J. Chem. Thermodyn., 36 (2004) 759
58. C. Xiao, J.M. Simonson, P.R. Tremaine, J. Chem. Thermodyn., 31 (1999) 1055
59. C. Xiao, P.R. Tremaine, J. Chem. Thermodyn., 29 (1997) 827
60. ASTM Standard D-1193, Specification for Reagent Water (2006)
61. ASTM Standard D-4052, Standard Test Method for Density and Relative Density of Liquids by Digital Density Meter (2002)

62. D.O. Masson, Phil. Mag., 79 (1929) 218

63. S. Kumar, S.B. Koganti, J. Nucl. Sci. Technol., 34 (1997) 410

64. S. Cabani, G. Cont and E. Matteoli, J. Soln. Chem., 5 (1976) 751

65. M. Ben-Hamo, A. Apelblat and E. Manzurola, J. Chem. Thermodyn., 39 (2007) 1071

66. M.L. Parmer and D.S. Banyal, Indian J. Chem., 48A (2009) 1667

67. A. Apelblat and E. Manzurola, J. Chem. Thermodyn., 31 (1999) 869

68. L.G. Hepler, Can. J. Chem., 47 (1969) 4613

CHAPTER 6

VOLUMETRIC AND VISCOMETRIC STUDY OF AQUEOUS SOLUTIONS OF PEG-200, PEG-400 AND [HMIm]Br SYSTEM

CHAPTER 6

VOLUMETRIC AND VISCOMETRIC STUDY OF AQUEOUS SOLUTIONS OF PEG-200, PEG-400 AND [HMIm]Br SYSTEM

6.1 INTRODUCTION

Solvents are necessary to dissolve solids, to lower the viscosity, to regulate temperatures, to recover compounds by means of extraction and crystallisation, as reaction medium and for cleaning purposes. Along with water, several organic compounds (especially volatile organic compounds) are used as solvent in chemical processes. Nevertheless, on the list of damaging chemicals, solvents rank highly, because most of the solvents are volatile liquids that are difficult to contain. The volatile organic compounds (VOCs) have a negative impact on the environment with regard to human health and safety, combined with their volatility and flammability. Therefore, efforts are being taken worldwide to develop solvent-free processes as well as to develop environmentally benign ‘green’ solvents such as ionic liquids, polyethylene glycol (PEG) and supercritical fluids. There are several advantages in replacing volatile organic compounds with water and other green solvents. The most obvious are their low cost, reduced flammability and toxicity and reduced environmental risk caused by the discharge of effluents. The ‘green’ solvents also lead to improved performance in the separation processes, resulting in the development of economical and ecological viable processes over the use of conventional solvents.

6.1.1 IONIC LIQUID

Ionic liquids (ILs) are considered as ‘young chemicals’ having a variety of applications in different areas of chemical industry such as a viable media for potentially green synthesis and separation media, as well as for novel applications, where the unique properties of the IL materials provide new options based on their different physical and chemical properties [1]. Ionic liquids are defined as salts with the melting temperatures below the boiling temperature of water [2]. Most of the salts identified in the literature as ILs are liquids at room temperature, and often at substantially lower temperatures [3-6]. ILs are composed of organic cations and different anions. They are referred to as ‘designer solvents’ as one can design them for different functions by changing the cation and anion and their physical properties can be optimised for a specific application [7-10]. ILs are also being explored as possible environmentally benign solvents [11-14]. Researchers have identified the ILs to be more than a solvent and have several applications in electrochemistry, biological media, catalysis, organic synthesis, and so on [15-20]. Thermal stability, high thermal conductivity, large electrochemical window, non-flammability and negligible vapour pressure [21-25] are some of their unique properties which make them an innovative solvent for the replacement of volatile organic compounds [26-28] currently used in industries [29, 30] and making them environmentally compatible [31]. Employing ionic liquids in industries could lead to a reduction in VOC emission and to a more cost effective use of starting material as ionic liquids are recyclable [3-5, 32, 33]. In order to utilise such valuable ionic liquids for different commercial applications, information about their thermophysical properties like density, refractive index, activity, vapour pressure, conductivity, viscosity, etc. are essential [34, 35]. Numerical values of these properties have significance in design and control of the chemical processes involving ILs [36-

39]. ILs are extensively used for the extraction of metal ions in solvent extraction [40-42]. Ionic liquid is being used as a green solvent in various R&D activities in nuclear fuel cycle such as recovery and purification of nuclides of interest from spent nuclear fuel matrices [43-45]. The ionic liquids, 1,3-dialkyl imidazolium salts have became popular as solvents, reagents, catalysts and as materials in large-scale chemical applications.

6.1.2 POLY (ETHYLENE) GLYCOL

Polyethylene glycol, PEG with the structural formula as $HO–(CH_2CH_2O)_n–H$, is a linear polyether compound, soluble in water and most of the organic solvents [46]. Materials with molecular weight less than 100,000 are usually called PEGs while higher molecular weight polymers are classified as PEOs [47]. PEG is loaded with variety of properties with various applications from industrial manufacturing to medicine. Its interesting properties include non- toxicity, easy recyclability, formation of aqueous two phase system with aqueous solutions of other polymers and salts [48, 49], formation of complexes with metal cations and so forth. PEG is used in areas like catalysis [50], biotechnology and medicine [51, 52], in pharmaceutical preparation and cosmetics [53], aqueous biphasic system as alternative separation media [54, 55], in bioconversion as aqueous two phase system (ATPS) [56-58], as solvent and phase transfer catalyst in organic synthesis [59, 60]. However, the use of aqueous PEG solutions and related materials in chemical reactions is not focused much in review articles. Unlike VOCs, low molecular weight liquid PEGs are non-volatile. The vapour density for low molecular weight PEG is greater than 1 relative to air as per the available MSDS data, and this is consistent with the industry standard for the selection of alternative solvents to VOCs [49]. PEG also has low flammability and is biodegradable.

The study of the physicochemical properties of PEG + water system is gaining importance due to its wide spread application. Knowledge of thermodynamic and thermophysical properties of polymer solutions is important for practical purposes. Properties of PEG have been partly studied by various research groups [61-70]. Among the different thermophysical properties, density has enormous importance as far as various industrial applications are concerned. The volumetric properties of these macromolecules are important in understanding solute-solute and solute-solvent interactions, since they may give an indirect insight into the conformational features of the polymer solute in the solution. Furthermore, the dependence of these properties on composition and temperature is of considerable interest from a theoretical point of view, because it may lead to a better understanding of the fundamental behaviour of polymer solutions [66-70].

The present study is aimed at measuring the various thermophysical properties of the ionic liquid 1-hexyl-3-methyl imidazolium bromide at 298.15 K and 0.1 MPa. The study also covers the measurement of the thermophysical properties of PEG-200 and PEG-400 in the temperature range 293.15-343.15 K and pressure 0.1 MPa.

6.2 OVERVIEW OF EARLIER WORK

The thermophysical properties of PEGs and ionic liquids have been studied extensively to extract important information about them [61-86]. Tawfik and Teja [61] measured experimentally the densities of five polyethylene glycols (ethylene glycol, diethylene glycol, triethylene glycol, tetraethylene glycol and pentaethylene glycol) in the temperature range 398 - 423 K using a vibrating tube densitometer. They had correlated the densities with a modified Rackett equation and formulated a generalized relation for the homologues of polyethylene glycols.

Muller and Rasmussen [62] measured the densities of aqueous solutions of mono-, di-, tri- and tetraethylene glycols along with poly(ethylene glycol) of average molecular weight 400 at the temperatures 298.15, 308.15, 318.15 and 328.15 K using an oscillating tube densitometer. They had calculated the excess volume from the measured data. Densities of aqueous solutions of PEG of average molecular weight 2000 and 10000 were also reported for a limited concentration range at 328.15 K.

Gonzalez-Tello et al. [63] obtained a linear relationship between density and PEG concentration in the temperature range 277 to 298 K, from the densities and viscosities measured for concentrated aqueous solutions of PEGs (10-50 mass %) with average molecular masses of 8000, 3350 and 1000. Han et al. [64] measured the density and viscosity of binary mixtures of PEG and water over the whole concentration range at six temperatures in the range 298.15 - 323.15 K, and had estimated the deviation in excess molar volume and viscosity. The excess properties were correlated with Redlich-Kister equation.

Zhang et al. [65] determined the density and viscosity of PEG 300 + water over the whole concentration range at five temperatures (298.15 K to 318.15 K). The measured data were fitted into an equation for calculating excess molar volume and viscosity deviation. The computed results were fitted into Redlich-Kister equation to obtain the coefficients and to estimate the percentage deviation between the experimental and calculated quantities.

Eliassi et al. [69] used PEGs with molecular weights 400 (385-415), 4000 (3500-4500), 6000 (5000-7000) and double distilled water for their studies. Density measurements were carried out at the temperatures 300.15, 310.15, 313.15, 318.15, 323.15 and 328.15 K. A constant temperature water bath was used to control the temperature. The measured densities were expressed in terms of mass fraction and by using fitted polynomial expressions and Gibbs-Duhem equation, partial molar volume of PEG and H_2O of various mixtures were computed. Kirincic and Cvetoklofutar [70] measured the density of PEGs of molecular weight ranging from 300 to 3500 using digital densitometer and thermal stability was controlled by digital thermometer. From the measured data, the apparent specific volume of the solute and solvent were calculated. The specific excess volume of the solutions and the coefficient of the virial expansion of the excess property were evaluated and interpreted in terms of solute-solute and solute-solvent interactions.

Gardas et al. [71] calculated the apparent molar properties and the isoentropic compressibility of aqueous solutions of imidazolium chloride, 1-methyl imidazolium chloride and 1-butyl-3-methyl imidazolium chloride from the measured speed of sound and density at 298.15 K. The results had been correlated with hydrophobic hydration, hydrophobic interactions and water structural changes in aqueous media.

Lal et al. [72] measured the density and speed of sound for aqueous solutions of ionic liquids with 1-butyl-3-methylimidazolium as cation and with different anions at different concentration and temperatures. Apparent molar properties and infinite dilution properties were calculated from the measured values and the results were interpreted in terms of ionic liquid-water interaction.

The density, refractive index and dynamic viscosity of two ionic liquids containing 1-benzyl-3-methyl-imidazolium cation with two different anions was reported by Deive et al. [73] as a function of temperature. They had calculated the volumetric properties and correlated the relation between density and refractive index with different equations. Liu et al. [74] measured the density, refractive index, viscosity, specific conductance and surface tension of systems involving imidazolium based ionic liquids and water.

Gardas et al. [75] reported the experimental density values at different temperatures ranging from 293.15 to 313.15 K, speed of sound and osmotic coefficients at 298.15 K for aqueous solutions of 1-ethyl-3-methyl imidazolium bromide and osmotic coefficients at 298.15 K for aqueous solutions of 1-butyl-3-methyl imidazolium chloride. The experimental data were used to calculate molar properties, compressibility, expansivity, internal pressure, activity and activity coefficients. Widegren and Magee [76] measured the physical properties of binary mixture of 1-hexyl-3-methylimidazolium bis (trifluoromethylsulfonyl)imide with water. The densities and dynamic viscosity were measured in the temperature range 258.15 to 373.15 K, kinetic viscosity at 293.15 to 298.15 K and speed of sound through the mixture at 283.15 to 343.15 K.

Esperanca et al. [77, 78] determined the speed of sound in the pure ionic liquids (1-propyl-3-methylimidazolium bis(trifluoromethylsulfonyl)amide $[C_3mim]^+[Tf_2N]^-$ and (1-pentyl-3-methylimidazolium bis(trifluoromethylsulfonyl)amide $[C_5mim]^+[Tf_2N]^-$ and their densities. The temperature and pressure range of measurement for the speed of sound were $298 < T / K < 338$ and $0.1 < p / MPa < 200$ respectively. Density measurements had been performed over a broad range of temperature (298 < T / K > 333) and pressure (0.1 < p / MPa < 60).

6.3 EXPERIMENTAL

6.3.1 CHEMICALS

Analytical grade PEG-200 (approximate molecular weight range: 190-210) and PEG-400 (molecular weight range: 380-420) were purchased from BDH (Mumbai) and Aldrich (Germany) respectively and were used without further purification. The IR spectra of 1-hexyl-3-methyl imidazolium bromide [HMIm]Br obtained from io-li-tec, GmbH was examined and it was used without further purification.

6.3.2 GENARAL PROCEDURE

ASTM Grade-1 water as per ASTM D-1193 [87] with a resistivity of 18.2 MΩ·cm at 298.15 K and TOC < 15 ppb from a MILLIPORE Simplicity system was used in the experiments for reagent/solution preparation and as water standard. Water for density standard was drawn from the water-purifier immediately before the experiments and it was degassed in an ultrasonic bath (TEC-110H) at 35 kHz for 60 s. The other experimental details have been discussed in Chapter 2 of this thesis.

6.3.3 MEASUREMENT OF DENSITY AND REFRACTIVE INDEX

Density and refractive index measurements were carried out using a precise vibrating-tube densitometer coupled with Anton Paar ABBEMAT RXA-156 refractometer and a 30-station auto sampler SP-3m. Densitometer and refractometer had Peltier thermostats for maintaining the desired sample temperature. Density measurements were made in complete conformation to ASTM-D4052 [88].

6.3.4 MEASUREMENT OF WATER ACTIVITY

Water activity was measured by a thermodynamic water activity meter [89] with a built-in thermoelectric Peltier element module for maintaining the temperature of sample. Samples were loaded in polystyrene cups and placed into the activity meter. The activity meter was standardized using a two-step procedure. In the first step, purified and degassed Millipore water was used as a standard ($a_w = 1.000$). In the second step, five immobilized electrolyte solutions, in sealed tablets supplied by M/s. Novasina were used as standards. These solutions were ~25 % LiCl ($a_W = 0.113$), ~25 % $MgCl_2.6H_2O$ ($a_W = 0.328$), ~25 % NaCl ($a_W = 0.753$), 25 % $BaCl_2.2H_2O$ ($a_W = 0.901$) and ~20 % K_2SO_4 ($a_W = 0.973$). The uncertainty estimated was ± 0.1 K for temperature and ± 0.003 for a_w values.

6.3.5 MEASUREMENT OF VISCOSITY

The viscosity of the pure components and their mixture with water were measured with a Canon-Fenske viscometer [90] with an accuracy of ± 0.2 %. The flow time was determined using a digital timer with the least-count of 0.01 s.

6.4 RESULT AND DISCUSSION

6.4.1 IONIC LIQUID

The ionic liquid investigated was 1-hexyl-3-methyl imidazolium bromide ([HMIm]Br), the structure of which is shown in Fig. 6.1. The IR spectra obtained for ascertaining its purity is shown in Fig.6.2 (3079.8cm^{-1}, 2931.5 cm^{-1}, 2860.2 cm^{-1}, 1642.9 cm^{-1}, 1465.7 cm^{-1}, 1166.8 cm^{-1} and 1627.8 cm^{-1}).

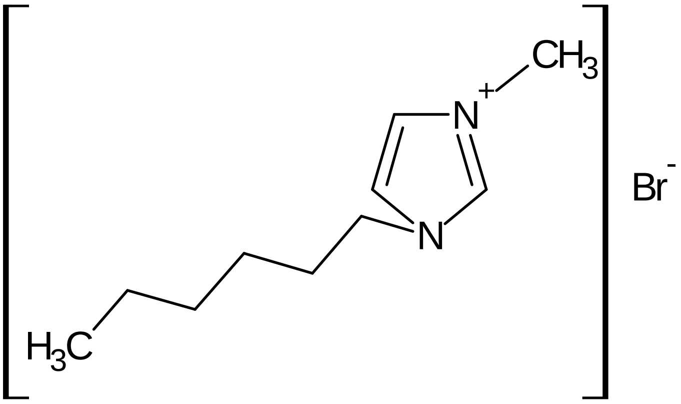

Fig.6.1: Structure of [HMIm]Br

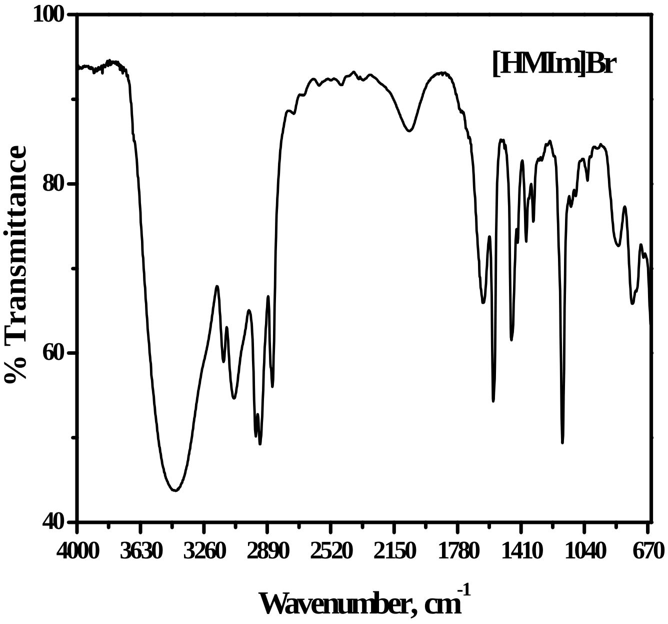

Fig.6.2: IR data of aqueous solutions of pure [HMIm]Br

The theory behind the correlation of density, apparent molal volume and refractive index at 298.15 K has been discussed in Chapter 4.

6.4.1.1 CORRELATION OF DENSITY

The experimental density data (shown in Table 6.1) could be correlated by the following equation:

$$\frac{\rho}{\rho^{0}} = 1.00 + 0.049\frac{m}{m_0} - 0.009(\frac{m}{m_0})^{1.5} \tag{6.1}$$

The density of ASTM Grade-I water at 298.15 K was taken as 0.997043 g/cm^3 [87]. The mean deviation and standard deviation were 0.9063 x 10^{-3} % and -0.3958 x 10^{-3} % respectively.

Table 6.1: Experimental density data for [HMIm] Br at 298.15 K

Conc (mol. Kg^{-1})	Expt. Density (g/cm^3)	Pred. Density (g/cm^3)	Residuals* (g/cm^3)	Deviations** %
0.0000	0.9970	0.9970	0.0000	0.0000
0.0016	0.9971	0.9971	0.0000	-0.0023
0.0028	0.9971	0.9971	0.0000	-0.0009
0.0034	0.9971	0.9971	0.0000	-0.0009
0.0043	0.9973	0.9973	0.0000	-0.0014
0.0054	0.9973	0.9973	0.0000	-0.0008
0.0079	0.9974	0.9974	0.0000	-0.0001
0.0082	0.9974	0.9974	0.0000	0.0006
0.0101	0.9975	0.9975	0.0000	0.0003
0.0155	0.9978	0.9978	0.0000	0.0008
0.0231	0.9987	0.9987	0.0000	0.0004
0.0351	0.9991	0.9991	0.0000	-0.0004

*Calculated as ρ_{pred}-ρ_{expt}.

**Calculated as 100*(ρ_{pred}-ρ_{expt})/ ρ_{expt}

A good match between experimental and predicted values was observed (shown in Fig. 6.3). The variation of density with concentration is shown in Fig. 6.4.

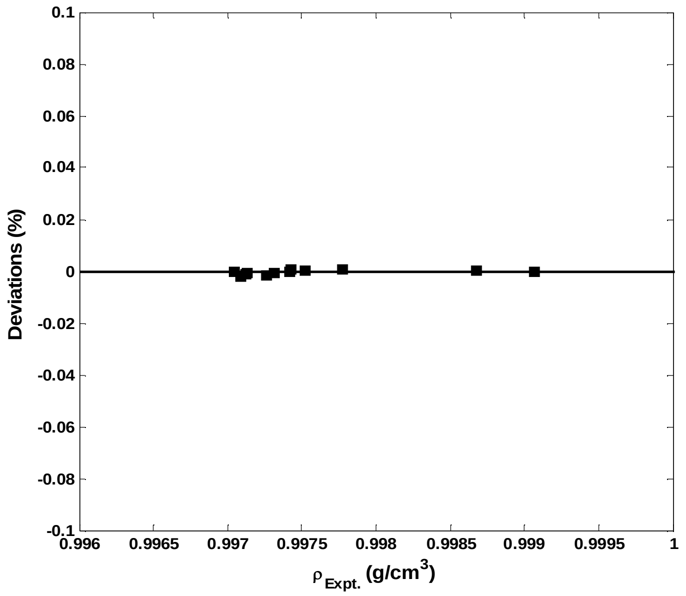

Fig.6.3: Plot of deviations for density of aqueous solutions of [HMIm] Br at 298.15 K

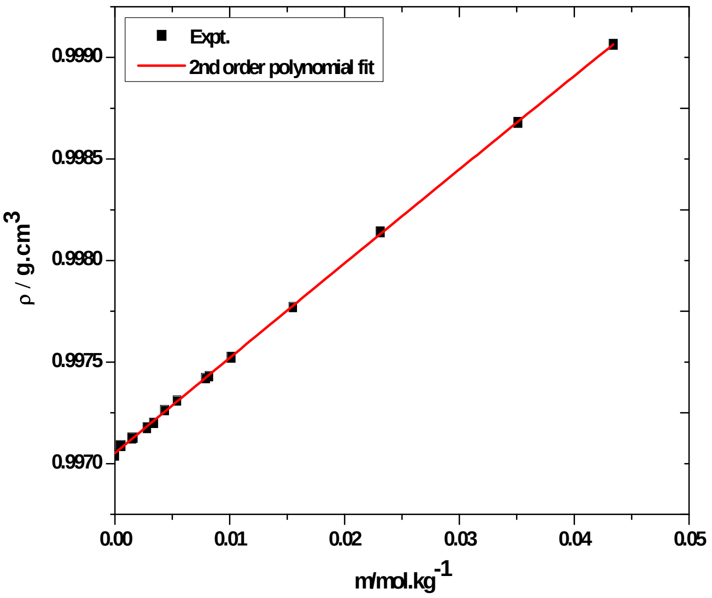

Fig.6.4: Variation of density of aqueous solutions of [HMIm] Br with concentration at 298.15K

6.4.1.2 CORRELATION OF APPARENT MOLAL VOLUME

The apparent molal volumes for aqueous solutions of [HMIm] Br at 298.15 K were calculated and correlated with the equations described in Chapter 4. The calculated apparent molal volume values are given in Table 6.2. The first few values were omitted in the regression analysis. The following equation is obtained after correlation:

$$V_{2,\phi}^{298.15K} = 195.39 + 31.74\sqrt{m} \tag{6.2}$$

Equation (6.2) gives the value of $V_{2,\phi}^{0}$ as 195.39 $cm^3.mol^{-1}$ and a_v as 31.74 $cm^3.dm^{3/2}.mol^{-3/2}$. $V_{2,\phi}^{0}$ is a large positive value for all concentrations indicating the presence of strong solute-solvent interaction. The positive values of $V_{2,\phi}^{0}$ and a_v imply that there is no cation-anion penetration.

Table 6.2: Apparent molal volume values of [HMIm] Br as a function of concentration

molality ($mol.kg^{-1}$)	$V_{2,\varphi}$ ($cm^3.mol^{-1}$)
0.0016	193.78
0.0043	196.17
0.0054	197.93
0.0079	199.57
0.0082	200.36
0.0101	200.01
0.0155	200.52
0.0351	200.67
0.0434	200.64

The variation of apparent molal volume with concentration is shown in Fig.6.5.

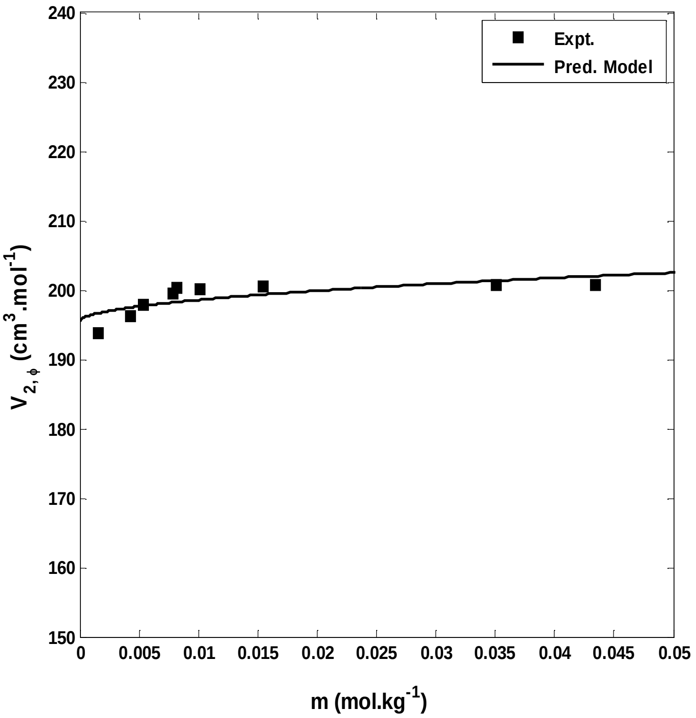

Fig. 6.5: Apparent molal volume of aqueous solution of [HMIm]Br at 298.15 K

6.4.1.3 CORRELATION OF REFRACTIVE INDEX

Experimental refractive index values are listed in Table 6.3. The correlated equation is given as

$$nD = 1.3324 + 0.0386m - 0.0021m^2 \tag{6.3}$$

From the correlation, $^{n}D_{w}$ is calculated to be 1.3324 and the coefficients are 0.0386 and -0.0021 respectively. The variation of refractive index for aqueous solutions of [HMIm]Br with concentration at 298.15 K and 0.1 MPa is given in Fig. 6.6.

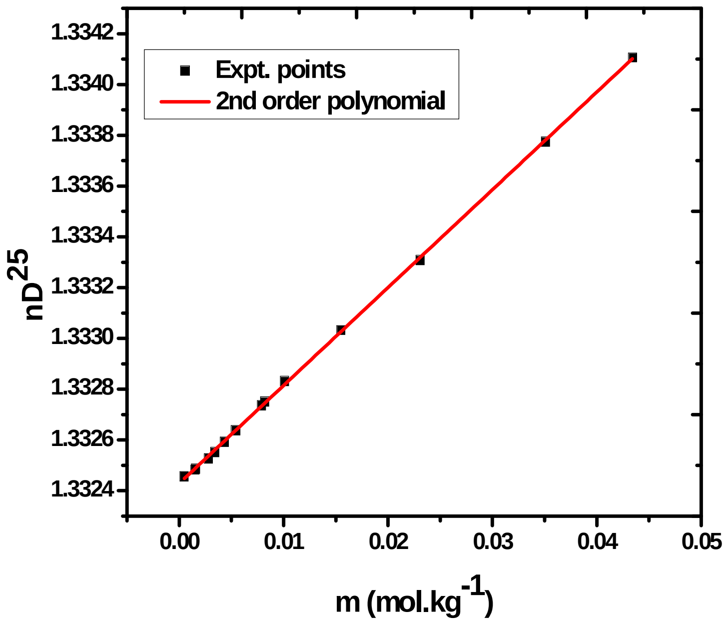

Fig.6.6. Refractive index of aqueous solutions of [HMIm] Br vs.concentration at 298.15 K

6.4.1.4 WATER ACTIVITY AND VAPOUR PRESSURE MEASUREMENT

Water activity (a_w) describes the equilibrium amount of water available for hydration of materials. Water activity is defined as the equilibrium relative humidity expressed as a fraction. Vapour pressures were estimated from the experimentally determined water activity values using the equation

$$P = a_w \times P^0 \tag{6.4}$$

where p = 3.1686 kPa at 298.15 K. Experimental water activity and calculated vapour pressure values are also shown in Table 6.3.

Table 6.3: Refractive index, water activity, and vapour pressure of aqueous solution of [HMIm] Br at 298.15 K and 0.1 MPa

Conc. $mol.kg^{-1}$	Refractive index nD^{25}	water activity a_w	Vapour pressure kPa
0	1.332428	1.000	3.1686
0.0005	1.332456	0.999	3.1654
0.0015	1.332483	0.998	3.1623
0.0016	1.332487	0.998	3.1623
0.0028	1.332528	0.997	3.1591
0.0034	1.332553	0.996	3.1559
0.0043	1.332593	0.996	3.1559
0.0054	1.332638	0.995	3.1528
0.0079	1.332737	0.994	3.1496
0.0082	1.332752	0.994	3.1496
0.0101	1.332832	0.993	3.1464
0.0155	1.333033	0.991	3.1401
0.0231	1.333308	0.990	3.1369
0.0351	1.333775	0.987	3.1274
0.0434	1.334107	0.986	3.1242

The variation of water activity and vapour pressure for aqueous solutions of [HMIm]Br with concentration at 298.15 K and 0.1 MPa are shown in Figs. 6.7 and 6.8 respectively.

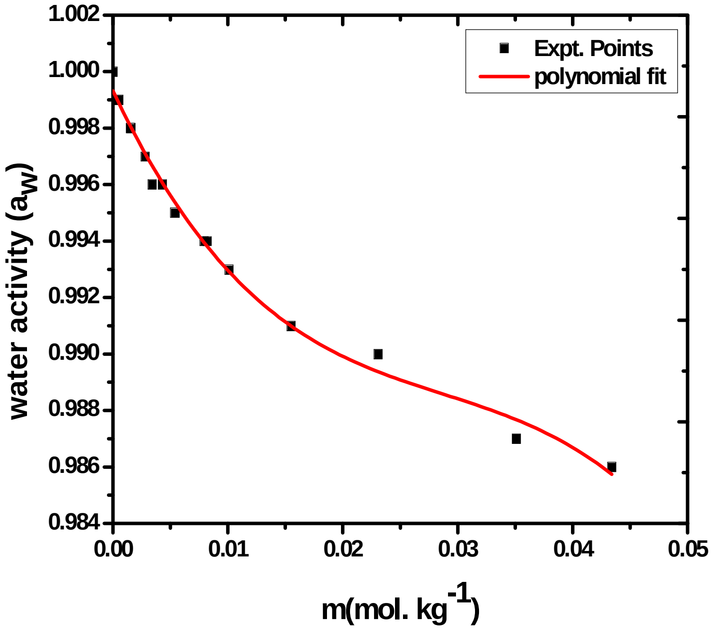

Fig. 6.7: Plot of the variation of water activity of aqueous solution of [HMIm] Br with concentration at 298.15 K

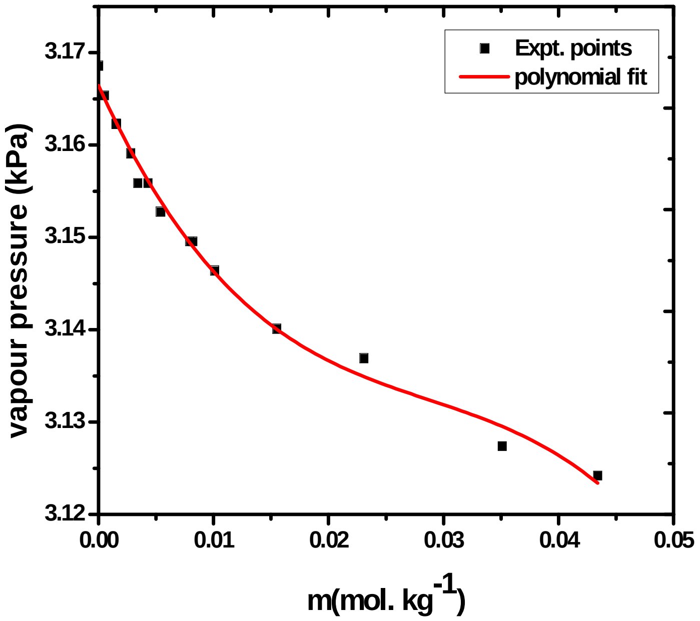

Fig. 6.8: Vapour pressure variation with concentration for aqueous solution of [HMIm] Br at 298.15K

6.4.1.5 EXCESS PROPERTIES

Excess molar volume of a solution is a thermodynamic property and is defined as the amount of volume which is in excess to that of an ideal solution at the same conditions of composition, temperature, and pressure and is given as

$$V_m^E = V_m - V_m^{ideal} \qquad (6.5)$$

where, V_m and V_m^{ideal} are the molar volumes of the solution and and that of pure components, respectively. Excess molar volumes of aqueous [HMIm]Br solution were calculated using Eq. (6.6), which was obtained after rearranging Eq. (6.5), using mole fractions, molar masses and densities to represent the volumes of solution and pure components.

$$V_m^E / cm^3.mol^{-1} = X_1 M_1 \left(\frac{1}{\rho} - \frac{1}{\rho_0} \right) + X_2 M_2 \left(\frac{1}{\rho} - \frac{1}{\rho_1} \right) \qquad (6.6)$$

where $V_m{}^E$ is the excess molar volume; M_1 and M_2 are the molar masses of water and [HMIm]Br respectively; X_2 is the mole fraction of [HMIm]Br; ρ is the density of aqueous [HMIm]Br solutions; and ρ_0 and ρ_1 are the densities solvent and pure solute respectively.

The excess molar volume was correlated with a Redlich-Kister-type equation by least-squares fitting given by Eq. (6.7).

$$V_m^E / cm^3.mol^{-1} = X_1 X_2 \sum_{i=0}^{n} A_i (2X_i - 1)^i \qquad (6.7)$$

where, A_i are the adjusted coefficients.

Excess refractive index was also calculated in the same manner using Redlich-Kister polynomial. The values of excess volume and excess refractive index calculated are reported in Table 6.4.

Table 6.4: Excess volume and excess refractive index values of aqueous solution of [HMIm]Br

X_2	V^E ($cm^3. mol^{-1}$)	nD^E
9.87E-06	-2.16E-05	2.49E-05
2.71E-05	-5.88E-05	6.83E-05
2.85E-05	-6.16E-05	7.18E-05
5.12E-05	-1.09E-04	1.29E-04
6.08E-05	-1.29E-04	1.53E-04
7.76E-05	-1.62E-04	1.95E-04
9.83E-05	-2.03E-04	2.46E-04
1.42E-04	-2.83E-04	3.53E-04
1.47E-04	-2.92E-04	3.66E-04
1.83E-04	-3.54E-04	4.55E-04
2.80E-04	-5.01E-04	6.90E-04
4.16E-04	-6.62E-04	1.01E-03
6.33E-04	-8.03E-04	1.51E-03
7.81E-04	-8.21E-04	1.84E-03

The variations of excess volume and excess refractive index with mole fraction of solute are shown in Figs. 6.9 and 6.10 respectively.

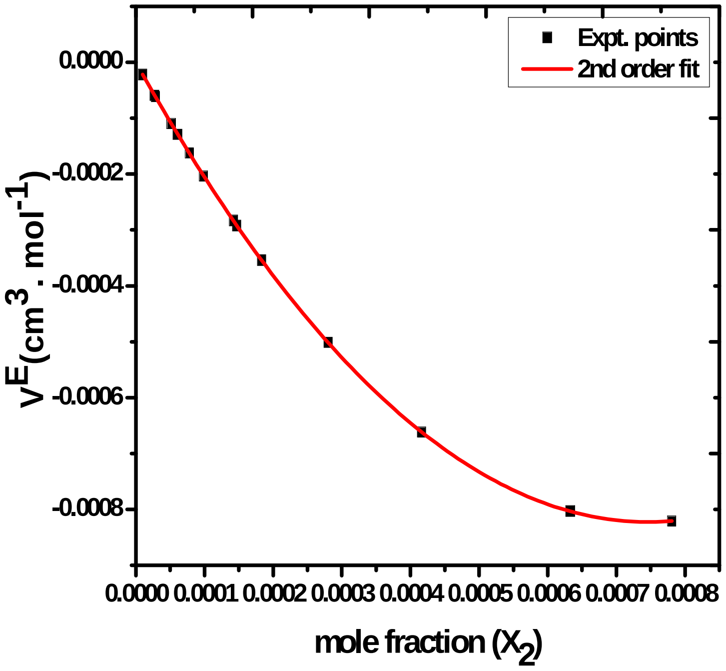

Fig.6.9. Plot of excess volume of aqueous solution of [HMIm]Br at 298.15K

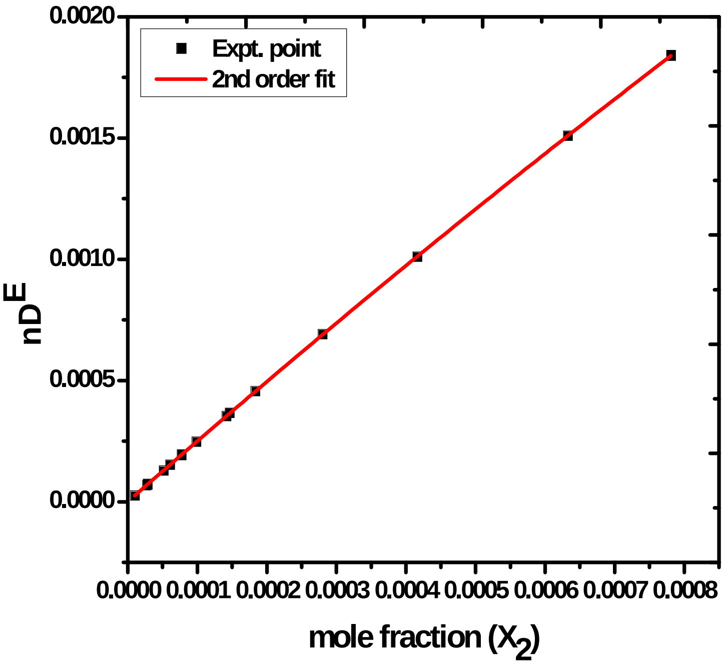

Fig.6.10. Excess refractive index vs. mole fraction for aqueous solution of [HMIm]Br at 298.15 K

Excess volume is the resultant contribution of physical, chemical and structural effects. The physical contribution involving non-specific interactions between the real species of a mixture contribute positive value to V^E. The chemical interactions involving charge transfer type forces result in a decrease in volume and contribute negative value to V^E. The structural contributions are mostly negative which arise from changes of free volume and various other effects. In the present study, excess volume is found to be negative as is common in completely miscible solvents. The negative excess volume generally indicates contraction in volume upon mixing. It reflects the compactness of the solution i.e. existence of net attractive interaction between dissimilar molecules which could be contributed by hydrogen bonding interactions.

6.4.2 POLY (ETHYLENE) GLYCOL

5.4.2.1 DENSITY

The variation in the experimental densities with temperature for aqueous solutions of PEG-200, PEG-400 and pure PEGs are shown in Figs. 6.11 to 6.13 respectively. The densities decreased with increase in temperature in a regular pattern. The variation of density with temperature followed the same theory as explained in Chapter 5.

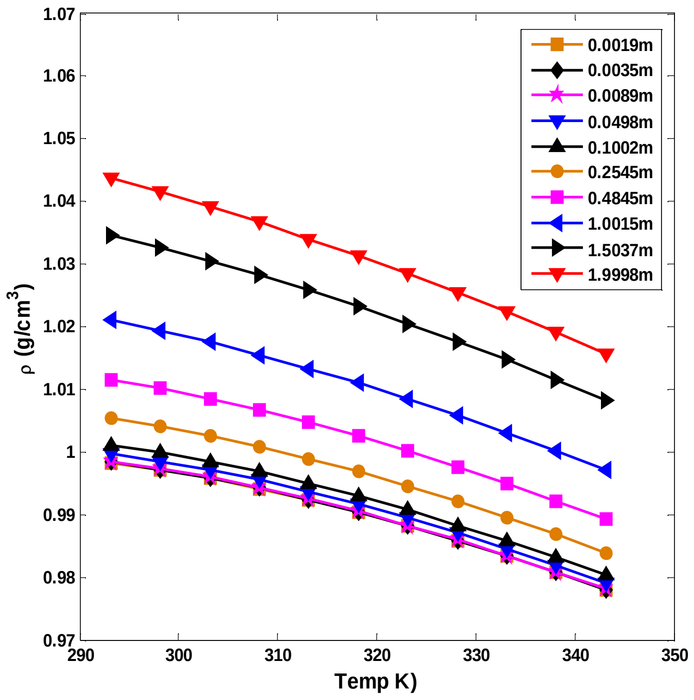

Fig. 6.11: Variation of density of aqueous solutions of PEG 200 with temperature

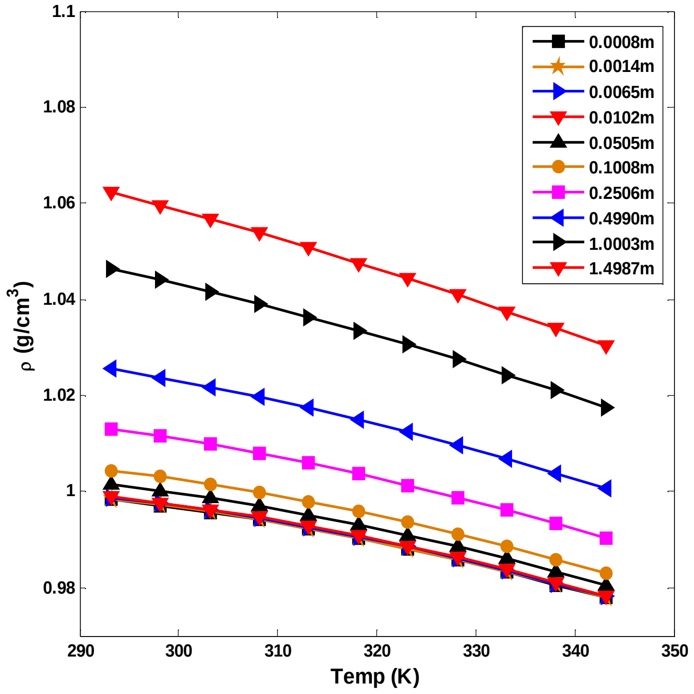

Fig. 6.12: Temperature dependence of density for aqueous solutions of PEG 400

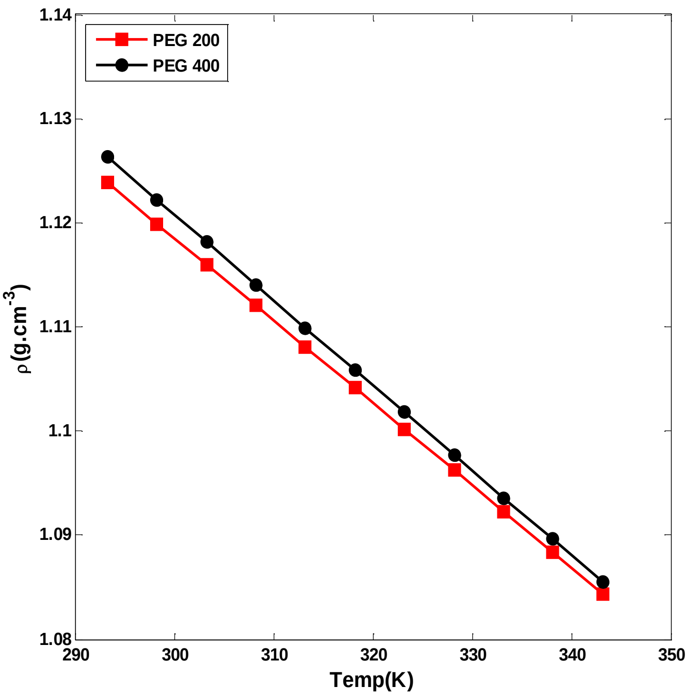

Fig. 6.13: Plot of density vs. temperature
for pure PEG-200 and PEG 400

Regressed coefficients and standard deviation for the variation of density with temperature have been listed in Table 6.5.

Table 6.5: Regressed coefficients of density for aqueous solutions of different PEGs at different temperature

Solute	a_0	a_1	a_2	b_0	b_1	b_2	Std.dev.
PEG-200	2.49E-02	-5.10E-05	4.30E-07	3.99E-03	-4.60E-05	3.20E-07	0.0627
PEG-400	6.28E-02	-1.60E-04	1.30E-06	3.70E-04	-8.50E-05	4.20E-07	0.0049

6.4.2.2 APPARENT MOLAL VOLUME

The apparent molal volume for aqueous solutions of PEG-200 and PEG-400 at different temperatures and concentration were calculated as per the equations discussed in

Chapter 5. The apparent molal volumes thus obtained were correlated with Masson equation to get $V_{2,\phi}^{0}$. The values of $V_{2,\phi}^{0}$ at different temperatures for aqueous solutions of PEG-200 and PEG-400 are given in Table 6.6.

Table 6.6: $V_{2,\phi}^{0}$ values for aqueous solutions of PEG-200 and PEG-400 for different temperature

Temp(K)	PEG-200	PEG-400
	$V_{2,\phi}^{0}$ ($cm^3.mol^{-1}$)	$V_{2,\phi}^{0}$ ($cm^3.mol^{-1}$)
293.15	170.61	336.84
298.15	171.29	338.37
303.15	171.94	339.84
308.15	172.60	341.29
313.15	173.26	342.72
318.15	173.92	344.17
323.15	174.61	345.62
328.15	175.31	347.09
333.15	176.00	348.57
338.15	176.72	350.08
343.15	177.44	351.60

From the table, it is observed that $V_{2,\varphi}^{0}$ has a large positive which indicates strong solute-solvent interaction.

The different apparent molal volume values are given in Tables 6.7 and 6.8 respectively.

Table 6.7: Apparent molal volume of aqueous solutions of PEG-200 at different temperatures and molalities (m)[a]

T (K)	0.0035	0.0089	0.0498	0.1002	0.2545	0.4845	1.0015	1.5037	1.9998	2.5003
293.15	138.90	152.97	163.40	169.90	170.49	170.98	170.33	173.57	169.84	169.76
298.15	137.90	152.88	163.90	170.55	171.18	171.68	171.07	174.29	170.67	170.60
303.15	138.65	154.10	164.50	171.25	171.85	172.38	171.79	174.99	171.47	171.43
308.15	138.16	154.33	165.30	171.87	172.53	173.07	172.52	175.69	172.26	172.24
313.15	138.75	154.68	165.87	172.50	173.21	173.77	173.23	176.4	173.04	173.03
318.15	138.78	154.83	166.45	173.18	173.87	174.45	173.94	177.1	173.81	173.83
323.15	139.32	155.70	167.4	173.86	174.58	175.16	174.66	177.81	174.59	174.61
328.15	138.99	156.73	167.85	174.57	175.29	175.87	175.39	178.53	175.36	175.40
333.15	139.81	157.20	168.66	175.25	176.00	176.58	176.13	179.26	176.14	176.19
338.15	140.55	157.94	169.55	175.93	176.72	177.31	176.87	180.00	176.93	176.99
343.15	140.39	158.66	169.97	176.63	177.45	178.05	177.63	180.74	177.72	177.79

[a] ‘*m*’ is in mol/kg

Table 6.8: Apparent molal volume of aqueous solutions of PEG-200 at different temperatures and molalities (m)

T (K)	0.0014	0.0065	0.0102	0.0505	0.1008	0.2506	0.499	1.0003	1.4987	1.7694
293.15	272.03	300.97	330.33	332.77	336.73	336.97	336.64	336.62	336.19	336.14
298.15	272.25	302.85	331.58	334.07	338.24	338.50	338.26	338.30	337.98	337.97
303.15	270.63	303.12	332.87	335.33	339.74	339.99	339.81	339.94	339.71	339.75
308.15	270.61	302.65	334.11	336.62	341.17	341.48	341.35	341.53	341.40	341.50
313.15	269.79	304.82	335.68	337.99	342.67	342.94	342.86	343.11	343.07	343.22
318.15	270.31	305.07	336.85	339.36	344.11	344.45	344.38	344.69	344.73	344.92
323.15	272.18	307.78	338.33	340.89	345.55	345.93	345.90	346.27	346.38	346.62
328.15	274.73	309.79	339.94	342.21	347.07	347.44	347.43	347.84	348.03	348.31
333.15	271.92	310.09	341.39	343.65	348.55	348.96	348.98	349.43	349.68	350.00
338.15	272.25	312.50	343.25	345.02	350.11	350.46	350.53	351.03	351.35	351.70
343.15	271.70	311.48	344.51	346.38	351.6	352.01	352.11	352.64	353.02	353.40

molality ‘*m*’ is in mol/kg

6.4.2.3 REFRACTIVE INDEX

Refractive indices for aqueous solutions of PEGs and pure PEGs were measured at 298.15 K and 0.1 MPa. The measured values for the aqueous solutions of PEGs are listed in Table 6.9.

Table 6.9: Values of refractive index for the aqueous solutions of PEG-200 and PEG-400 at 298.15 K

PEG-200		PEG-400	
Concentration (mol.kg^{-1})	Refractive index (nD)	Concentration (mol.kg^{-1})	Refractive index (nD)
0.0019	1.332595	0.0008	1.332556
0.0035	1.332598	0.0014	1.332587
0.0089	1.332717	0.0065	1.332849
0.0498	1.333701	0.0102	1.333037
0.1002	1.334830	0.0505	1.335019
0.2545	1.338139	0.1008	1.337430
0.4845	1.343115	0.2506	1.344214
1.0015	1.350435	0.4990	1.354118
1.5037	1.361094	1.0003	1.370541
1.9998	1.368228	1.4987	1.383264
2.5003	1.374712	1.7694	1.389109

The experimentally determined refractive index values of PEG solutions (reported in Table 6.9) were correlated by the following equation:

$$nD = nD_w + am + bm^2 \tag{6.8}$$

where nD is the predicted refractive index of the solution and nD_w is the refractive index of water used for the preparation of solution, *m* is molality of PEG in water and a and b are coefficients. The plot for the variation of refractive index with concentration for PEG-200 and PEG-400 solutions at 298.15 K and 0.1 MPa is shown in Fig. 6.14.

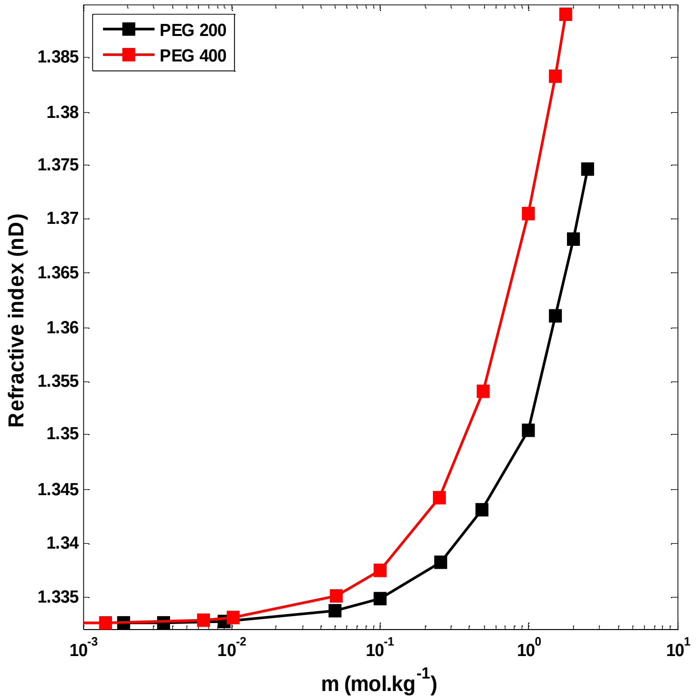

Fig. 6.14: Refractive index of aqueous solutions of PEG-200 and PEG-400 vs. concentration

6.4.2.4 VISCOSITY

Viscosity can be calculated from the density data using Eq. (6.9).

$$\frac{\eta_s}{\rho_s t_s} = \frac{\eta_1}{\rho_1 t_1} \tag{6.9}$$

where, η_s is the viscosity of the standard, ρ_s is the density of standard, t_s is the flow time of standard, η_1 is the viscosity of the sample, ρ_1 is the density of the sample and t_1 is the flow time of the sample. The viscosity values calculated for PEG solutions (given in Table 6.10) were correlated to the following equation:

$$\eta = a_1 + b_1 m + c_1 m^2 \tag{6.10}$$

where, η is the predicted viscosity of solution, m is molality of PEG in water, a_1 is a constant, b_1 and c_1 are coefficients for the above equation. The refractive index and viscosities of pure PEGs are listed in Table 6.11.

Table 6.10: Viscosities of aqueous solutions of PEG-200 and PEG-400 at 298.15 K

PEG-200		PEG-400	
Conc. (mol/kg)	Viscosity (cP)	Conc. (mol/kg)	Viscosity (cP)
0.0019	0.892	0.0008	0.941
0.0035	0.900	0.0014	0.943
0.0089	0.933	0.0065	0.955
0.0498	0.963	0.0102	0.969
0.1002	0.979	0.0505	1.020
0.2545	1.059	0.1008	1.141
0.4845	1.235	0.2506	1.375
1.0015	1.489	0.4990	1.888
1.5037	2.027	1.0003	3.322
1.9998	2.433	1.4987	5.145
2.5003	2.977	1.7694	6.898

Table 6.11: Refractive index and viscosity of pure PEGs at 298.15 K

Solute	Refractive index	Viscosity (cP)
PEG-200	1.456413	47.481
PEG-400	1.464575	87.914

The regressed coefficient values for refractive index and viscosity of aqueous solutions of PEG-200 and PEG-400 are given in Table 6.12.

Table 6.12: Regressed coefficients for refractive index and viscosities of aqueous solutions of PEGs at 298.15 K

Property	Coefficients	PEG-200	PEG-400
Refractive index	a	0.0208	0.0466
	b	-0.0016	-0.0084
Viscosity	a_1	0.9171	0.9728
	b_1	0.5217	1.0861
	c_1	0.121	1.2325

6.4.2.5 EXCESS PROPERTIES

Excess refractive index for aqueous solutions of PEGs was calculated from the individual values at 298.15 K as per the equation:

$$nD^{E} = nD^{mix} - \left(X_1 nD^1 + X_2 nD^2\right) \tag{6.11}$$

where, nD^{mix} is the refractive index of the mixture, nD^1 and nD^2 are the refractive indices of pure water and pure PEGs respectively; X_1 and X_2 are the mole fractions of the pure components. The excess refractive indices are also represented by a Redlich-Kister type equation, which is given below:

$$nD^{E} = X_1 X_2 \sum_{i=0}^{n} B_i (2X_1 - 1)^i \tag{6.12}$$

where, B_i are the adjusted coefficients.

Similarly, excess viscosity for aqueous solutions of PEGs was calculated from the individual values at 298.15 K as per the equation:

$$\eta^E = \eta^{mix} - \left(X_1\eta^1 + X_2\eta^2\right) \tag{6.13}$$

where, η^{mix} is the viscosity of the mixture, η^1 and η^2 are the viscosities of pure water and pure PEGs respectively; X_1 and X_2 are the mole fractions of the pure components.

Redlich-Kister equation for viscosity can be written as

$$\eta^E / cP = X_1 X_2 \sum_{i=0}^{n} C_i (2X_1 - 1)^i \tag{6.14}$$

where, C_i are the adjusted coefficients. The variation of excess refractive index and excess viscosity with mole fraction for PEG-200 and PEG-400 are shown in Figs. 6.15 and 6.16 respectively.

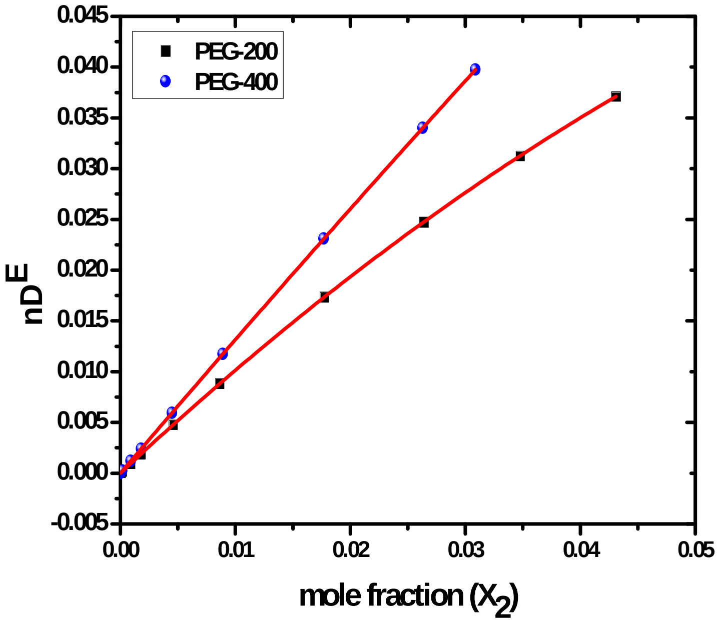

Fig. 6.15: Plot of excess refractive index for aqueous solutions of PEG-200 and PEG-400

The excess refractive indices of both the PEG-water mixtures are positive throughout the composition range, which could be due to weak structural interactions.

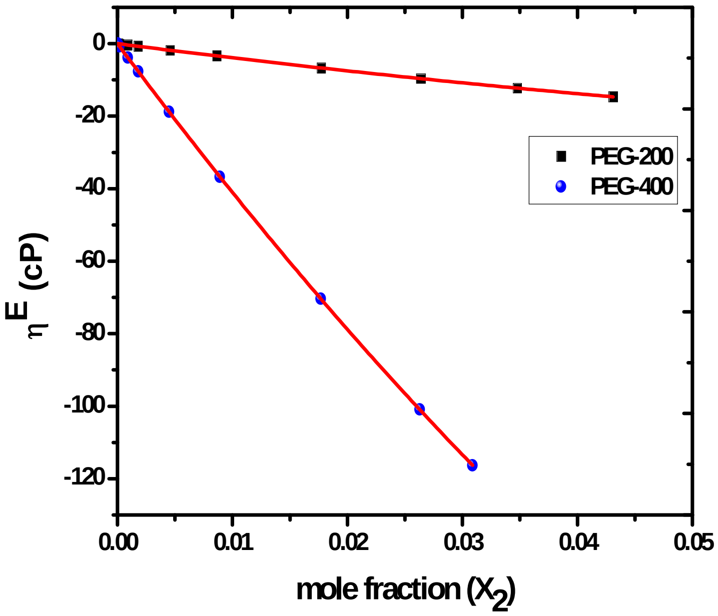

Fig. 6.16: Variation of excess viscosity with mole fraction for aqueous solutions of PEG-200 and PEG-400

The values of excess viscosity are negative over the whole composition range which indicates that dispersion forces are dominant in these systems, as it has been reported that dispersion forces are dominant in the systems where the component molecules have different molecular sizes.

Excess volume was calculated as per Eq. (6.6) described earlier. Excess volume for different temperatures was calculated using the densities at different temperatures, for aqueous PEG solutions. The excess volumes were correlated with Redlich-Kister polynomial as given in Eq. (6.7). The variation of excess volume with mole fraction for aqueous solutions of PEG-200 and PEG-400 are shown in Figs. 6.17 and 6.18 respectively.

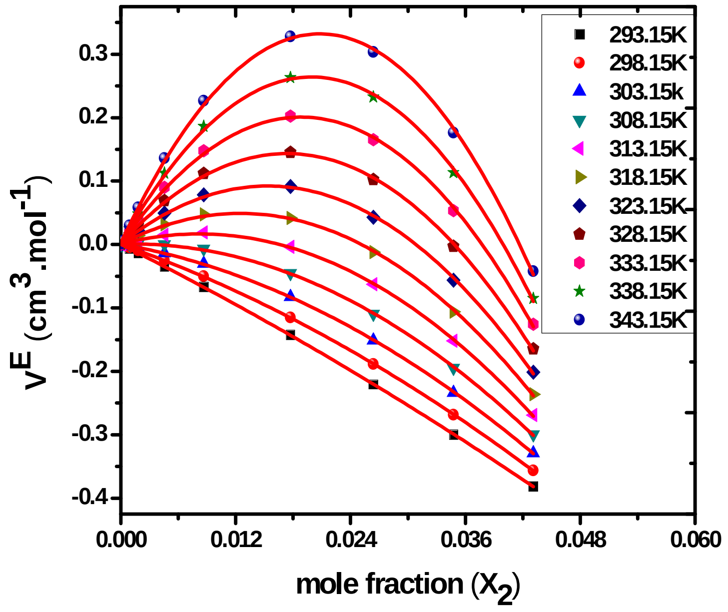

Fig. 6.17: Excess volume of aqueous solutions of PEG-200 vs. mole fraction

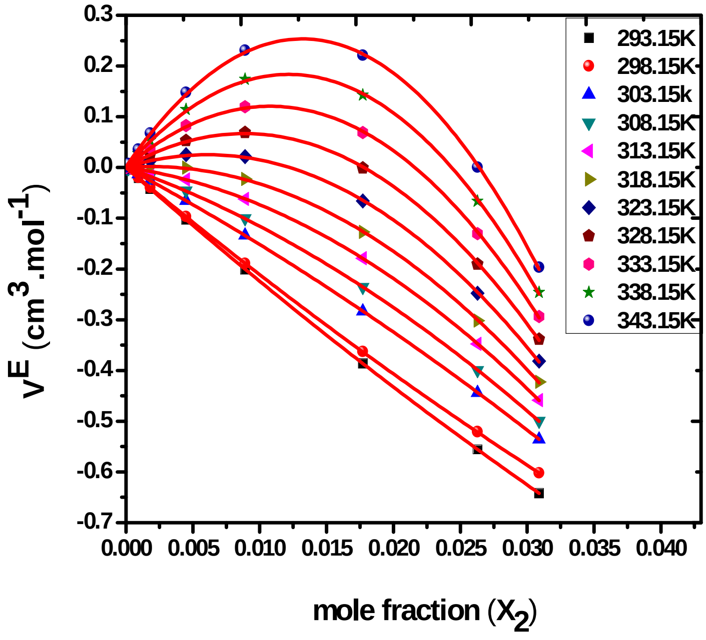

Fig. 6.18: Variation of excess volume of aqueous solutions of PEG-400 with mole fraction

It could be seen from Figs. 6.17 and 6.18 that the excess volume is negative for lower temperatures; however, as the temperature increases, it moves towards positive side, which might be due to the weakening of the hydrogen bonds and structures in the liquid. The resulting tendency as observed could thus, be explained as a balance between these contributions. Negative excess volumes usually indicate contraction in volumes upon mixing. Probably, the presence of extensive intermolecular H-bonding between water and PEG (within PEG + water) is responsible for the negative values of excess volumes. Specifically, the H-bonding between the –O– of water and the terminal –H of PEGs and that between the –H of water and the –O– of the terminal –OH of PEGs could be the major contributor here. Relatively weaker H-bonding between the –H of water and the –O– of the $–H_2C–O–CH_2–$ of PEGs may also contribute to the large negative excess volumes within (PEG + water).

The interactions within the mixture were affected by the temperature and composition of the mixture. The interactions become weaker as the temperature of the mixture is increased. This result could be due to weakening of hydrogen-bonding as the temperature increases which results in the solvent structure loosing, and thus, leading to more ideal mixing behaviour. Positive sign is also attributed to dispersion forces (London interactions) which are likely to be operative in all cases.

6.4.2.6 CUBIC EXPANSION COEFFICIENT AND STRUCTURAL BEHAVIOUR

Calculation of cubic expansion coefficients from densities and prediction of the structure maker and structure breaker behaviour from the variation in the second derivative of volume with temperature for different temperatures have been explained in Chapter 5. The variation in cubic expansion coefficient with concentration for different PEGs are shown in Figs. 6.19 and 6.20.

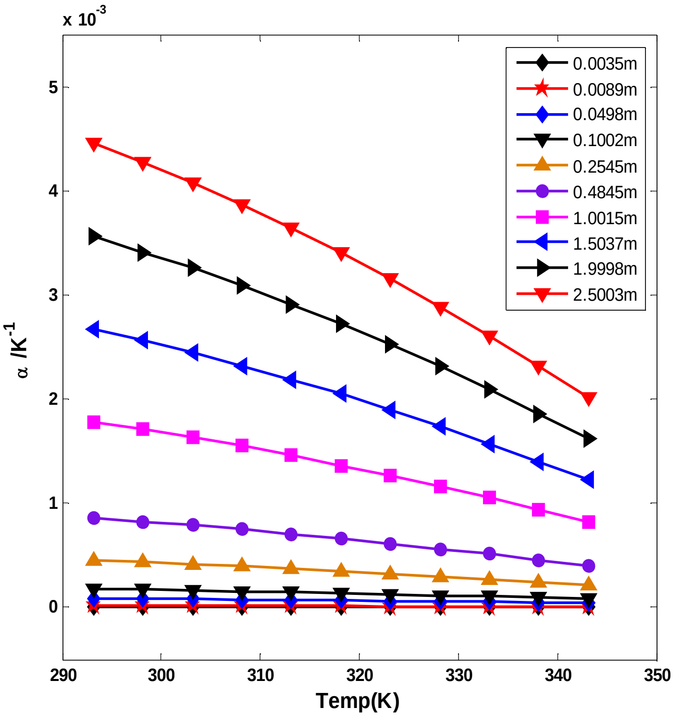

Fig. 6.19: Plot of cubic expansion coefficient of aqueous solutions of PEG 200 vs. temperature

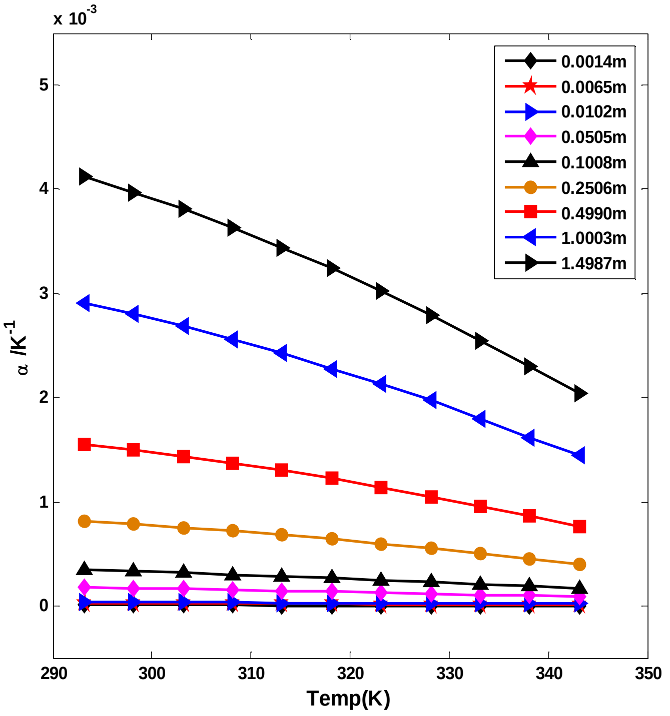

Fig. 6.20: Cubic expansion coefficient vs. temperature plot for aqueous solutions of PEG 400

The cubic expansion coefficient decreases with increasing temperature for both the PEGs which imply that they behave like common electrolytes. At lower concentrations, the change was not significant, but as the concentration increases a predominant change was observed which could be due to the change in volume. The variation of the second derivative of volume with temperature at constant pressure and composition for the aqueous solutions of PEG-200 and PEG-400 is plotted in Figs. 6.21 and 6.22 respectively.

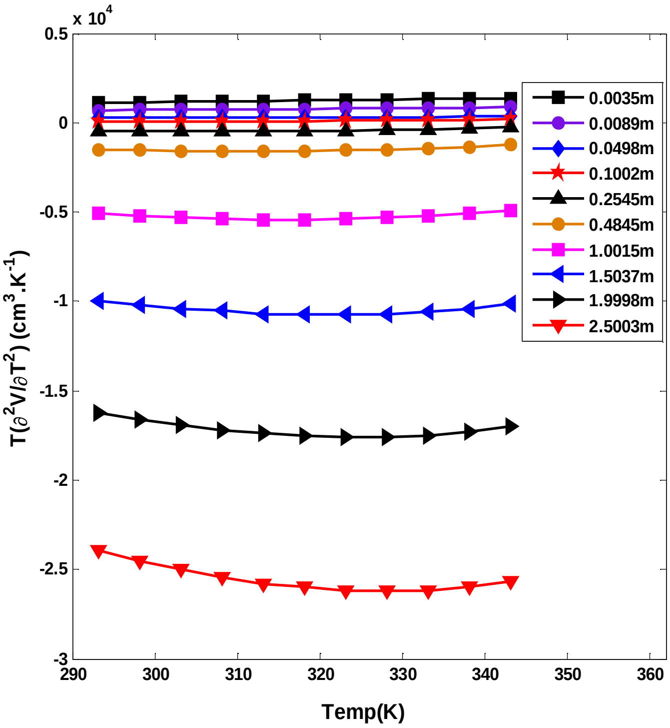

Fig. 6.21: Variation of second derivative of volume with temperature for aqueous solution of PEG-200

According to Hepler [91], the change in heat capacity with pressure or the change in the second derivative of volume with temperature is related to the changes in the structure of water. He proposed that the solutes for which the second derivative of volume with temperature is negative (i.e. derivative of *Cp* with pressure is positive) will act as structure breakers and vice-versa.

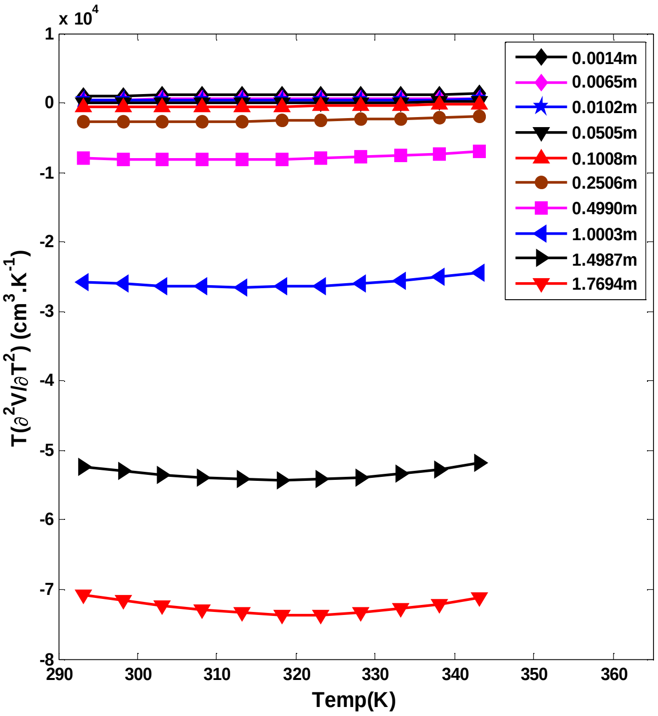

Fig. 6.22: Effect of temperature on second derivative of volume for aqueous solution of PEG-400

Figures 6.21 and 6.22 reveal that the value of the second derivative of volume with temperature is positive up to ~0.1 m for PEG-200 and up to ~0.05 m for PEG-400 at all temperatures and for all other concentrations it becomes negative i.e. both the PEGs behave as structure makers at all temperatures for lower concentrations and as structure breakers at higher concentrations.

SUMMARY

In this Chapter a detailed study on the thermophysical properties of aqueous solutions of 1-hexyl-3-methyl imidazolium bromide ([HMIm]Br) at 298.15 K is presented. Density (ρ), refractive index (nD^{25}) and water activity (a_w) of pure and aqueous dilute solutions of [HMIm]Br were experimentally measured at 298.15 K and at atmospheric pressure. The measured values were used to estimate apparent molal volume ($V_{2,\varphi}$), excess volume (V^E) and excess refractive index (nD^E). The apparent molal volumes estimated were correlated with Masson equation for extracting information about structural interactions. The excess quantities were correlated to Redlich-Kister equation. Vapour pressure of the solutions were calculated from the measured values of water activity.

The density (ρ), refractive index (nD) and viscosity (η) of binary aqueous solutions of PEG-200 and PEG-400 including those of pure liquids were measured over the entire composition range at 298.15 K and the effect of temperature on these properties was also investigated. The experimental data were used to calculate apparent molal volume ($V_{2,\varphi}$), excess volume (V^E), excess refractive index (nD^E) and excess viscosity (η^E). The calculated apparent molal volume was fitted into Masson equation for obtaining information about ion-ion and ion-solvent interactions and the excess quantities were correlated to Redlich-Kister equation to obtain the coefficients. Cubic expansion coefficient was calculated and structure maker and structure breaker behaviour of these solutes has been evaluated. The variation of these parameters with composition has been discussed with regard to structural interaction. The dependence of volume on concentration threw light on the long range electrostriction of water by the solute ions.

REFERENCES

1. R.D. Rogers, K.R. Seddon, "Ionic liquids as green solvents- progress and prospects", ACS Symposium Series 856, American Chemical Society, Washington, DC (2003)
2. J.S. wilkes, Green Chem., 4 (2002) 73
3. A.B. Pereiro, A. Rodriguez, J. Chem. Thermodyn., 38 (2006) 651
4. A.B. Pereiro, A. Rodriguez, J. Chem. Thermodyn., 39 (2006) 978
5. M.T. Zafarani-mottar, H. Shekaari, J. Chem. Thermodyn., 37 (2005) 1029
6. N.V. Plechkova, K.R. Seddon, Chem. Soc. Rev., (2008) 1
7. N.V. Plechkova, K.R. Seddon, Chem. Soc. Rev., (2008) 123
8. R.D. Rogers, R.P. Swatloski, S.K. Spear, J. Am. Chem. Soc., (2002) 4974
9. C.T. Wu, K.N. Marsh. J. Chem. Eng. Data, 48 (2003) 486
10. A.J. Carmichael, K.R. Seddon, J. Phys. Org. Chem., 13 (2000) 591
11. J.F. Brennecke, E.J. Maginn, AIChE J., 47 (2001) 2384
12. J.D. Holbrey, K.R. Seddon, Clean Products Processes, 1 (1999) 223
13. K.R. Seddon, A. Stark, M. Torres, Pure Appl. Chem., 72 (2000) 1391
14. K.R. Seddon, A. Stark, M. Torres, Pure. Appl. Chem., 72 (2000) 2275
15. T. Welton, Chem. Rev., 99 (1999) 2071

16. K.A. Venkatesan, T.G. Srinivasan, P.R.V. Rao, J. Radiochem. Nucl. Sci., 10 (2009) R1-R6
17. N.V. Plechkova, K.R. Seddon, Chem. Soc. Rev., 37 (2008) 123
18. T. Tseuda, C.L. Hussey, “Electrochemical application of room-temperature ionic liquids”. The Electrochemical Society interface, In Tech, sanghai, china (2007)
19. P.R.V. Rao, K.A. Venkatesan, T.G. Srinivasan, Progress in Nucl. Energy, 50 (2008) 449
20. J.A. Whitehead, J. Zhang, N. Pereira, A. McCluskey, G.A. Lawrence, Hydrometall., 88 (2007) 109
21. M.J. Earle, J.M.S.S. Esperanca, M.A. Gilea, J.N. Canongia lopes, L.P.N. Rebelo, J.W. Magee, K.R. Seddon, J.A. Widegren, “The distillation and volatility of ionic liquids”, Nature, 439 (2006) 831
22. Dz. H. Zaitsau, G.J. Kabo, A.A. Strechan, J. Phys. Chem. A, 110 (2006) 7303
23. J.L. Anthony, E.J. Maggin, J.F. Brennecke, J. Phys. Chem. B, 105 (2001) 10942
24. J. Dupont, R.F. de Souza, P.A.Z. Suarez, Chem. Rev., 102 (2002) 3667
25. M.T. Zafarani-mottar, H. Shekaari, J. Chem. Thermodyn., 38 (2006) 1377
26. J.L. Karr, A.M. Jesinowski, J.A. berberich, R. Moulton, J. Am. Soc., 125 (2003) 4125
27. C.F. Poole, J. Chromatogr A, 1037 (2004) 49

28. M. Freemantle, Chem. Eng. News, 76 (1998) 32

29. A. Heintz, J.K. Lehman, J. Chem. Eng. Data, 48 (2003) 472

30. P. Bhujrajh, N. Deenadayalu, J. Chem. Thermodyn., 38 (2006) 278

31. M.J. Earle, K.R. Seddon, Pure Appl. Chem.,72 (2000) 1391

32. U. Domanska, A. Pobudkowska, J. Soln. Chem., 35 (2006) 311

33. K.R. Seddon, J. Chem. Tech. Biotechnol., 68 (1997) 351

34. T.M. Letcher, U. Domanska, A. Marciniak, M. Marcianiak, J. Chem. Eng. Data, 50 (2005) 1294

35. J. Ranke, A. Othman, P. Fan, A. Muller, Int. J. Mol. Sci., 10 (2009) 1271

36. N.V. Plechkova, K.R. Seddon, Chem. Soc. Rev., (2008) 1

37. N.V. Plechkova, K.R. Seddon, Chem. Soc. Rev., (2008) 123

38. E. Gomez, B. Gonzalez, J. Chem. Eng. Data, 51 (2006) 2096

39. G.P. Smith, A.S. Dworkin, R.M. Pagni, S.P. Zingg, J. Am. Chem. Soc., 111 (1989) 525

40. S. Dai, Y.H. Ju, C.E. Barnes, J. Chem. Soc. Dalton Trans., 8 (1999) 1201

41. J. Luczak, M. Joskowska, J. Hupka, Physicochemical Problems of Mineral Processing, 42 (2008) 223

42. A.E. Visser, R.P. Swatloski, W.M. Reichert, S.T. Griffin, R.D. Rogers, Ind. Eng. Chem. Res., 39 (2000) 3596

43. A. Rout, K.A. Venkatesan, T.G. Srinivasan, P.R.V. Rao, Radiochim. Acta, 97 (2009) 719

44. A. Rout, K.A. Venkatesan, T.G. Srinivasan, P.R.V. Rao, Sep. Purif. Technol., 76 (2011) 238

45. K. Binnemans, Chem. Rev.,107 (2007) 2592

46. G.M. Powell, Handbook of Water Soluble Gums and Resins, McGraw Hill, New York, (1980)

47. J. Kahovec, R.B. Fox, K. Hatada, Pure Appl. Chem., 74 (2002) 1921

48. L.R. Pratt Chem. Rev., 102 (2002) 2625

49. M.A. Abraham, L. Moens, “Clean Solvents, Alternative Media for Chemical Reactions and Processing”, ACS Symposium Series 819, American Chemical Society, Washington, DC. (2002)

50. C.M. Starks, C.L. Liotta, M. Halpern, “Phase-Transfer Catalysis: Fundamentals, Applications and Industrial Perspectives”, Chapman & Hall, New York, 158 (1994)

51. J.M. Harris, “Poly(ethylene glycol) Chemistry: Biotechnical and Biomedical Applications”, ed., Plenum Press, New York, 1992.

52. J.M. Harris, S. Zalipsky, “Poly(ethylene glycol) Chemistry and Biological Applications”, ACS Symposium Series 680, American Chemical Society, Washington, DC (1997)

53. Encyclopedia of Polymer Science and Technology, John Willey and Sons, Inc. (1996)

54. J.G. Huddleston, H.D. Willauer, S.T. Griffin, R.D. Rogers, Ind. Eng. Chem. Res. 38 (1999) 2523

55. L. Mei,, D. Lin, Z. Zhu, Z. Han, J. Chem. Eng. Data 40 (1995) 1168

56. F. Tjerneld , H.O Johansson, Int. Rev. Cytol., 192 (2000) 137

57. R. Hatti-Kaul, Mol. Biotechnol., 19 (2001) 269

58. R. Hatti-Kaul, Methods in Biotechnology, Vol. 11, Aqueous Two-Phase Systems, Methods and Protocols, ed., Human Press, NJ, (2000) p. 411.

59. G.E. Totten, N.A. Clinton, J. Macromol. Sci. Rev. Macromol. Chem. Phys., C28, 293. (1988)

60. G.E. Totten, N.A. Clinton, and P.L. Matlock J. Macromol. Sci. Rev. Macromol. Chem. Phys., C38 (1998) 77

61. W.Y. Tawfik, A.S. Teja, Chem. Eng. Sci., 44 (1989) 921

62. E.A. Muller, P. Rasmussen J. Chem. Eng. Data, 36 (1991) 214

63. P. Gonzalez-Tello, F. Camacho, G. Blazquez, J. Chem. Eng. Data, 39 (1994) 611

64. F. Han, J. Zhang, G. Chen, X. Wei, J. Chem. Eng. Data, 53 (2008) 2598

65. N. Zhang, J. Zhang, Y.Zhang, J. Bai, T. Huo, X. Wei, Fluid Phase Equil., 313 (2012) 7

66. Y. Song, P.M. Mathias, D. Tremblay, C.C. Chen, Ind. Eng. Chem. Res., 42 (2003) 2415
67. I. Inamura, Y. Jinbo, Y. Akiyama, Y. Kubo, Bull. Chem. Soc. Jpn., 68 (1995) 2021
68. I. Inamura, Polym. J., 18 (1986) 269
69. A. Eliassi, H. Modarress, G.A. Mansoori, J. Chem. Eng. Data, 43 (1998) 719
70. S. Kirincic, A. Cvetoklofutar, Fluid phase Equil., 149 (1998) 233
71. R.L. Gardas, D.L. Dagade, S.S. Terdale, J.A.P. Coutinho, K.J. Patil, J. Chem. Thermodyn., 40 (2008) 695
72. B. Lal, M. Sahin, E. Ayranci, J. Chem Thermodyn., 54 (2012) 142
73. F.J. Deive, M.A. Rivas, A. Rodriguez, J. Chem. Thermodyn., 43 (2011) 487
74. W. Liu, L. Cheng, Y. Zhang, H. Wang, M. Yu, J. Mol. Liq., 140 (2008) 68
75. R.L. Gardas, D.L. Dagade, J.A.P. Coutinho, K.J. Patil, J. Phys. Chem. B, 112 (2008) 3380
76. J.A. Widegren, E.J.W. Magee, J. Chem. Eng. Data, 52 (2007) 2331
77. J.M.S.S. Esperanca, H.J.R. Guedes, M. Blesic, L.P.N. Rebelo, J. Chem. Eng. Data, 51 (2006) 237
78. J.M.S.S. Esperanca, Z.P. Visak, H.J.R. Guedes, K.R. Seddon, L.P.N. Rebelo, J. Chem. Eng. Data, 51 (2006) 2009
79. A. Heintz, J. Chem. Thermodyn., 37 (2005) 525

80. S.P. Verevkin, J. Safarov, E. Bich, E. Hassel, A. Heintz, Fluid Phase Equil., 236 (2005) 222
81. T.V. Vasiltsova, S.P. Verevkin, E. Bich, A. Heintz, R. Bogel-Lukasik, U. Domanska, J. Chem. Eng. Data, 51 (2006) 213
82. I.A. Sumartschenkowa, S.P. Verevkin, T.V. Vasiltsova, E. Bich, A. Heintz, M.P. Shevelyova, G.J. Kabo, J. Chem. Eng. Data, 51 (2006) 2138
83. K. Kim, S. Park, S. Choi, H. Lee, J. Chem. Eng. Data, 49 (2004) 1550
84. X. Jiang, J. Wang, C. Li, L. Wang, Z. Wang, J. Chem. Thermodyn., 39 (2007) 841
85. A.B. Pereiro, J.L. Legido, A. Rodríguez, J. Chem. Thermodyn., 39 (2007) 1168
86. L.E. Ficke, R.R. Novak, J.F. Brennecke, J. Chem. Eng. Data,55 (2010) 4946
87. ASTM Standard D1193, Standard Specification for Reagent Water (2011)
88. ASTM Standard D4052, Standard test method for density and relative density of liquids by digital density meter (2002)
89. Lab-Master Operation Manual, M/s. NOVASINA, Switzerland (2009)
90. ASTM D445-11a, Standard Test Method for Kinematic Viscosity of Transparent and Opaque Liquids (and Calculation of Dynamic Viscosity) (2006)
91. L.G. Hepler, Can. J. Chem., 47 (1969) 4613

CHAPTER 7

BRIEF SUMMARY OF THE THESIS WORK AND FUTURE PROSPECTIVE

CHAPTER 7

BRIEF SUMMARY OF THE THESIS WORK AND FUTURE PROSPECTIVE

7.1 SUMMARY

When an electrolyte is dissolved in water, it dissociates into cations and anions, which will be surrounded by water molecules as well as the counter ions and the electrolyte solution ceases to behave as an ideal solution. The nonideality in the electrolyte solutions is attributed mainly to the interactions of water–ion and ion–ion. Thermodynamic properties including activity coefficients at infinite dilution and other thermophysical and volumetric properties find applications in the development of reliable predictive models for systems containing aqueous solutions.

The knowledge of individual ionic activity coefficients is important for the study of equilibrium processes involving electrolyte solutions as well as for processes involving ion-exchange and pollution control. Activity coefficients can also be used in the prediction of rate constant, equilibrium constant, chemical potentials, solubility product and for the separation of a species from a mixture of substances. In this work, the single ion activity coefficients of chloride, nitrate, potassium and sodium ions had been measured. The emf values measured for aqueous solutions of nitrates and chlorides of sodium and potassium by pH/ISE meter were substituted in Nernst equation to calculate the single ion activity coefficient. Mean ionic activity coefficient determined by taking the geometric mean of the calculated values was compared with the literature data.

Excess molal volumes and partial molal volumes can be considered as a basis for understanding some of the molecular interactions (such as dispersion forces and hydrogen-bonding interactions) in binary mixtures. Excess molal volume is one of the useful parameters in the development of technological processes of a reactive system, and to predict vapour-liquid equilibria by incorporating into appropriate equation of state (EoS) models.

Partial molal volume of a substance at infinite dilution in a mixture is the change in volume per mole of added substance to a large volume of the added component. Data on the partial molal volume at infinite dilution provide useful information about the interactions and are of great importance in characterizing the structure and properties of solutions.

The aqueous nitrate salts of fission products such as rare earth, alkali and alkaline earths, obtained from nuclear fission are very important from a socio-economic perspective. A complete thermodynamic investigation of the rare earths in aqueous solution is essential to understand how these ions behave in solvents such as water. Similarly, PEG solutions and ionic liquids which serve as new solvents are also assuming importance from the extraction point of view. Hence, thermophysical and partial molal properties of the aqueous solutions of PEG-200, PEG-400, [HMIm] Br, rare earth and some other nitrate salts have been determined over an extended temperature range. Nitrate anion was used because the fission products exist as nitrate salts in aqueous phase in the solvent extraction step of PUREX process. The thermophysical property measurements reported in this thesis have provided precise volumetric, viscometric and structural behaviour data for aqueous solutions of $RbNO_3$, $CsNO_3$, $Sr(NO_3)_2$, $Y(NO_3)_3$, $Ga(NO_3)_3$, $La(NO_3)_3$, $Ce(NO_3)_3$, $Pr(NO_3)_3$, $Sm(NO_3)_3$, $Eu(NO_3)_3$, PEG-200, PEG-400 and [HMIm]Br in the temperature range 293.15 –

343.15 K in 5 K interval and at the ambient pressure of 0.1 MPa. The data on apparent molal volume at infinite dilution reported in the literature upheld the internal consistency of the calculated values in this thesis work.

The thermophysical and volumetric property measurements carried out at 298.15 K and 0.1 MPa, and reported in Chapter 4 have been performed at higher temperatures up to 343.15 K and reported in Chapter 5. Chapter 5 presents the density data for aqueous solutions of $RbNO_3$, $CsNO_3$, $Sr(NO_3)_2$, $Y(NO_3)_3$, $Ga(NO_3)_3$, $La(NO_3)_3$, $Ce(NO_3)_3$, $Pr(NO_3)_3$, $Sm(NO_3)_3$ and $Eu(NO_3)_3$ over the temperature range 293.15-343.15 K in 5 K interval. These measurements facilitated the determination of apparent molal volume at infinite dilution, cubic expansion coefficient and prediction of structural behaviour of the aqueous nitrate solutions at different temperatures.

The study of volumetric properties of aqueous nitrate solutions had been extended to Poly ethylene glycol-200 and Poly ethylene glycol-400 in the temperature range 293.15 - 343.15 K in 5 K interval and 1-hexyl-3-methyl imidazolium bromide ([HMIm]Br) at 298.15 K. The densities, refractive indices and viscosities were measured for PEG-200 and PEG-400. Apparent molal volume, partial molal volume, cubic expansion coefficient, structural behaviour and excess properties were derived as a function of temperature. From the measured data for density, refractive index and water activity of [HMIm]Br, volumetric and excess properties and vapour pressure had been calculated. The excess properties were correlated to Redlich-Kister equation and the following important conclusions have been derived from this study:

- The values of partial molal volume of the solvent (i.e. apparent molal volume at infinite dilution) were positive and large for all concentrations showing strong solute-solvent interaction, which increase gradually with increasing temperature and concentration. The increase in the magnitude of interaction might be attributed to the increase in solvation. In the case of ionic solutes there were no cation-anion penetrations.

- The cubic expansion coefficient (α) decreased with increasing temperature for the nitrates of rubidium, cesium, strontium, yttrium and lower lanthanides like lanthanum, cerium and praseodymium which implies that they behave like common electrolytes. Gallium, samarium and europium nitrates showed the opposite behaviour. The largest value of α at the lowest temperature indicated that water around the solute was loosely bound, giving rise to higher value of expansivity.
- With the aid of Hepler’s assumption, it is concluded that aqueous nitrates of cesium, rubidium, strontium, yttrium, lanthanum, cerium and praseodymium act as structure makers at lower concentrations and structure breakers at higher concentrations. However, gallium, samarium and europium nitrates exhibited structure breaking behaviour at all concentrations and temperatures.
- The ion-solvent interaction was predominating in [HMIm]Br over the entire concentration range investigated. The excess molal volume was found to be negative as is common in completely miscible solvents. The negative excess molal volume indicated contraction in volume upon mixing. The positive excess refractive index could be due to weak structural interactions.
- In PEG + water system, strong solute-solvent and negligible solute-solute interactions have been predicted, which increased with increasing temperature. The negative excess volume at lower temperatures moved towards positive side as the temperature increased. The negative excess volumes could be attributed to the increase in the ordering of the systems, partially due to the formation of

either hydrogen bonds or structured liquids. Intermolecular hydrogen bonding may occur between the –O- of water and the terminal –H of PEGs and the –H of water and the –O- of the terminal –OH of PEG. With increase in temperature, weakening of the hydrogen bonds and structures in the liquid were predicted, due to which excess volume became positive. Weak structural interactions resulted in the positive excess refractive index also. The negative excess viscosity over the whole composition range indicated that the dispersion forces were dominant in these systems. The decrease in the cubic expansion coefficient with increase in temperature for both the PEGs implied that they were behaving like common electrolytes. At lower concentration, the change was not significant, but as the concentration increased a drastic change was observed which could be due to the change in volume. According to Hepler's concept, PEG behaves as a structure maker at all temperatures for lower concentrations and structure breaker at higher concentrations.

An attempt has been made to model the dependence of temperature and concentration on the apparent molal properties of each system investigated for the thesis, using an equation of state commonly referred to as the density model. Wherever possible, the results of this model were compared with those results from models previously reported in the literature.

The studies presented in this thesis have indicated that more detailed and precise thermodynamic data are essential in understanding the equilibrium properties of solutions beyond 298.15 K and 0.1 MPa. Although an attempt has been made for a thorough investigation on the thermodynamic properties of aqueous electrolyte systems, they are not extensive enough to fully explain the properties related to structural interactions.

7.2 FUTURE EXPERIMENTAL WORK

Experimental work should be focused towards evaluating the partial molal properties of electrolytes and non-electrolyte solutions of not only binary but also multi-component solutions. The data available in literature for multi-component electrolyte solutions, particularly for non-aqueous electrolyte solutions, are inadequate. Further, measurement of thermodynamic properties of aqueous systems require to be extended up to at least 350 K for predicting suitable model equations to extrapolate the information acquired from experiments.

7.2.1 AQUEOUS ELECTROLYTE SYSTEM

Although single ion activity coefficient data are available for single component system, multicomponent aqueous systems require further investigation. Data need to be generated to evaluate the contribution due to the presence of interfering ions while measuring the single ion activity coefficient of a particular species. The same study could be extended to multi-solvent systems.

Thermodynamic data have been generated for the nitrates of some rare earth and fission products. A systematic study to investigate the partial molal properties of aqueous nitrates of all alkali, alkaline-earth and rare earths over extended temperatures and pressures is desirable to have the data base and to provide a deep insight into solute-solvent and solute-solute interactions. Theoretical models should be developed to predict solute-solvent and solute-solute interactions within aqueous solutions and the experimentally measured properties should be validated by model predicted values. The studies envisaged can be extended to solvents other than water.

7.2.2 AQUEOUS NON-ELECTROLYTE SYSTEMS

The analysis presented in Chapter 6 involves measurement of properties over a narrow range of temperature and ambient pressure. Future direction in this area could be to include input data set at high temperatures and pressures. Binary solutions of PEG with salts, other polymer solutions or different ionic liquids can be investigated to obtain valuable thermophysical properties.

7.2.3 NON-AQUEOUS SYSTEM

Single ion activity coefficient measured can be extended to non-aqueous electrolyte systems like electrolyte-alcohol or electrolyte-water-alcohol with different ISEs. Data on these systems will be useful particularly, for understanding the behaviour of liquid-liquid systems.

PUBLICATIONS

JOURNALS

1. **Debasmita Dash**, S. Kumar, C. Mallika, U. K. Mudali, "New data on activity coefficients of potassium, nitrate and chloride ions in aqueous solutions of KNO_3 and KCl by Ion Selective Electrodes", *ISRN Chemical Engineering*, published online, vol. 2012 (2012) doi:10.5402/2012/730154
2. **Debasmita Dash**, S. Kumar, C. Mallika, U. K. Mudali, "Thermophysical, volumetric and excess properties of aqueous solutions of 1-hexyl-3-methyl imidazolium bromide at 298.15 K and 0.1 Mpa", *ISRN Physical Chemistry*, published online, vol. 2013 (2013) http://dx.doi.org/10.1155/2013/475296
3. **Debasmita Dash**, S. Kumar, C. Mallika, U. K. Mudali, "Density, viscosity, refractive index, volumetric and excess properties of binary mixtures of poly (ethylene glycol) and water at 298.15 K and 0.1 MPa", *Internatl. J. Thermophys.* (Under review)
4. **Debasmita Dash**, S. Kumar, C. Mallika, U. K. Mudali, "Temperature dependency studies on volumetric change and structural interaction in aqueous rare earth nitrate solution" *J. Soln. Chem.* (Under review)
5. **Debasmita Dash**, S. Kumar, C. Mallika, U. K. Mudali, "Structural interaction leading to volumetric changes in aqueous solutions of nitrates of rubidium, cesium, strontium, yttrium and gallium at different temperatures", *J. Radioanal. Nucl. Chem.*(Under review)
6. **Debasmita Dash**, S. Kumar, C. Mallika, U. K. Mudali, "Theoretical estimation of isobaric thermal expansivity of binary mixture of low molecular weight polyethylene glycol and water from density data over a temperature range of

293.15 K to 343.15 K and 0.1 MPa pressure”, *e-Polymers (To be communicated)*

CONFERENCE PROCEEDINGS:

1. **Debasmita Dash**, S. Kumar, C. Mallika, U.K. Mudali, “Thermo physical properties of aqueous solutions of 1-hexyl 3-methyl imidazolium bromide at 298.15 K and 0.1 MPa”, Proc. *13th CRSI-NSC symposium*, NISER, Bhubaneswar (2011) Paper 49
2. **Debasmita Dash**, S. Kumar, C. Mallika, U.K. Mudali, “Volumetric properties of aqueous solutions of rubidium, strontium, samarium, yttrium, lanthanum, europium, praseodymium, and gallium nitrate at 298.15 K”, *Chemistry Research Scholar Meet (CRSM-2011)*, Kalpakkam
3. **Debasmita Dash**, S. Kumar, C. Mallika, U.K. Mudali, “Temperature dependence of densities and volumetric properties of aqueous solution of nitrates of Rb, Sr, Sm, Y, La, Eu, Pr, and Ga at 298.15 K and 0.1 MPa”, Proc. *DAE – BRNS Biennial Symposium on Emerging Trends in Separation Science and Technology (SESTEC – 2012)*, Mumbai (2012) pp. 99
4. **Debasmita Dash,** S. Kumar, C. Mallika, U.K. Mudali, “An attempt to study the individual ion activity coefficients of Na^+ and Cl^- ions in aqueous NaCl solution at 298.15K”, *Theme meeting in recent advances in analytical chemistry (TRAC-2012)*, Madras University, Chennai